Spacetime Algebra and Electron Physics

AUTHORS
Chris Doran
Anthony Lasenby
Stephen Gull
Shyamal Somaroo
Anthony Challinor

In P. W. Hawkes, editor
Advances in Imaging and Electron Physics
Vol. **95**, p. 271-386 (Academic Press, 1996)

Contents

1 Introduction

This paper surveys the application of 'geometric algebra' to the physics of electrons. The mathematical ideas underlying geometric algebra were discovered jointly by Clifford [1] and Grassmann [2] in the late 19th century. Their discoveries were made during a period in which mathematicians were uncovering many new algebraic structures (quaternions, matrices, groups, *etc.*) and the full potential of Clifford and Grassmann's work was lost as mathematicians concentrated on its algebraic properties. This problem was exacerbated by Clifford's early death and Grassmann's lack of recognition during his lifetime. This paper is part of a concerted effort to repair the damage caused by this historical accident. We firmly believe that geometric algebra is the simplest and most coherent language available for mathematical physics, and deserves to be understood and used by the physics and engineering communities. Geometric algebra provides a single, unified approach to a vast range of mathematical physics, and formulating and solving a problem in geometric algebra invariably leeds to new physical insights. In the series of papers [3]–[6] geometric algebra techniques were applied to number of areas of physics, including relativistic electrodynamics and Dirac theory. In this paper we extend aspects of that work to encompass a wider range of topics relevant to electron physics. We hope that the work presented here makes a convincing case for the use of geometric algebra in electron physics.

The idea that Clifford algebra provides the framework for a unified language for physics has been advocated most strongly by Hestenes, who is largely responsible for shaping the modern form of the subject. His contribution should be evident from the number and range of citations to his work that punctuate this paper. One of Hestenes' crucial insights is the role of geometric algebra in the design of mathematical physics [7]. Modern physicists are expected to command an understanding of a vast range of algebraic systems and techniques — a problem that gets progressively worst if one is interested in the theoretical side of the subject. A list of the some of the algebraic systems and techniques employed in modern theoretical physics (and especially particle physics) is given in Table 1. Hestenes' point is that every one of the mathematical tools contained in Table 1 can be expressed within geometric algebra, but the converse is not true. One would be hard-pressed to prove that two of the angles in an isosceles triangle are equal using spinor techniques, for example, but the proof is simple in geometric algebra because it encompasses vector geometry. The work of physicists would be considerably simplified if, instead of being separately introduced to the techniques

coordinate geometry	spinor calculus
complex analysis	Grassmann algebra
vector analysis	Berezin calculus
tensor analysis	differential forms
Lie algebras	twistors
Clifford algebra	algebraic topology

Table 1: *Some algebraic systems employed in modern physics*

listed in Table 1, they were first given a firm basis in geometric algebra. Then, when a new technique is needed, physicists can simply slot this into their existing knowledge of geometric algebra, rather than each new technique sitting on its own, unincorporated into a wider framework. This way, physicists are relieved of the burden of independently discovering the deeper organisational principle underlying our mathematics. Geometric algebra fulfills this task for them.

In the course of this paper we will discuss a number of the algebraic systems listed in Table 1, and demonstrate precisely how they fit into the geometric algebra framework. However, the principle aim here is to discuss the application of geometric algebra to electron physics. These applications are limited essentially to physics in Minkowski spacetime, so we restrict our attention to the geometric algebra of spacetime — the *spacetime algebra* [8]. Our aim is twofold: to show that spacetime algebra simplifies the study of the Dirac theory, and to show that the Dirac theory, once formulated in the spacetime algebra, is a powerful and flexible tool for the analysis of all aspects of electron physics — not just relativistic theory. Accordingly, this paper contains a mixture of formalism and applications. We begin with an introduction to the spacetime algebra (henceforth the STA), concentrating on how the algebra of the STA is used to encode geometric ideas such as lines, planes and rotations. The introduction is designed to be self-contained for the purposes of this paper, and its length has been kept to a minimum. A list of references and further reading is given at the end of the introduction.

In Sections 3 and 4 Pauli and Dirac column spinors, and the operators that act on them, are formulated and manipulated in the STA. Once the STA formulation is achieved, matrices are eliminated from Dirac theory, and the Dirac equation can be studied and solved entirely within the real STA. A significant result of this work is that the unit imaginary of quantum mechanics is eliminated and replaced by a directed plane segment — a bivector. That it is possible to do this has many implications for the interpretation of quantum mechanics [9].

In Sections 5, 6 and 7 we turn to issues related to the propagation, scattering and tunnelling of Dirac waves. Once the STA form is available, studying the properties of electrons via the Dirac theory is no more complicated than using the non-relativistic Pauli theory. Indeed, the first-order form of the Dirac theory makes some of the calculations easier than their non-relativistic counterparts. After establishing various results for the behaviour of Dirac waves at potential steps, we study the tunnelling of a wavepacket through a potential step. Indirect timing measurements for quantum-mechanical tunnelling are now available from photon experiments, so it is important to have a solid theoretical understanding of the process. We argue that standard quantum theory has so far failed to provide such an understanding, as it misses two crucial features underlying the tunnelling process.

In Section 8 we give a relativistic treatment of a measurement made with a Stern-Gerlach apparatus on a fermion with zero charge and an anomalous magnetic moment. As with tunnelling, it is shown that a disjoint set of outcomes is consistent with the causal evolution of a wavepacket implied by the Dirac equation. Wavepacket collapse is therefore not required to explain the results of experiment, as the uncertainty in the final result derives from the uncertainty present in the initial wavepacket. It is also argued that the standard quantum theory interpretation of the measurement performed by a Stern-Gerlach apparatus is unsatisfactory. In the STA, the anticommutation of the Pauli operators merely expresses the fact that they represent orthonormal vectors, so cannot have any dynamical content. Accordingly, it should be possible to have simultaneous knowledge of all three components of the spin vector, and we argue that a Stern-Gerlach apparatus is precisely what is needed to achieve this knowledge!

Multiparticle quantum theory is considered in Section 9. We introduce a new device for analysing multiparticle states — the multiparticle STA. This is constructed from a copy of the STA for each particle of interest. The resulting algebraic structure is enormously rich in its properties, and offers the possibility of a geometric understanding of relativistic multiparticle quantum physics. Some applications of the multiparticle STA are given here, including a relativistic treatment of the Pauli exclusion principle. The paper ends with a brief survey of some other applications of the STA to electron physics, followed by a summary of the main conclusions drawn from this paper.

Summation convention and natural units ($\hbar = c = \epsilon_0 = 1$) are employed throughout, except where explicitly stated.

2 Spacetime Algebra

'Spacetime algebra' is the name given to the geometric (Clifford) algebra generated by Minkowski spacetime. In geometric algebra, vectors are equipped with a product that is associative and distributive over addition. This product has the distinguishing feature that the square of any vector in the algebra is a scalar. A simple re-arrangement of the expansion

$$(a+b)^2 = (a+b)(a+b) = a^2 + (ab+ba) + b^2 \tag{2.1}$$

yields

$$ab + ba = (a+b)^2 - a^2 - b^2, \tag{2.2}$$

from which it follows that the symmetrised product of any two vectors is also a scalar. We call this the *inner* product $a\cdot b$, where

$$a\cdot b \equiv \tfrac{1}{2}(ab+ba). \tag{2.3}$$

The remaining, antisymmetric part of the geometric product is called the *outer* product $a\wedge b$, where

$$a\wedge b \equiv \tfrac{1}{2}(ab-ba). \tag{2.4}$$

The result of the outer product of two vectors is a *bivector* — a grade-2 object representing a segment of the plane swept out by the vectors a and b.

On combining equations (2.3) and (2.4) we see that the full geometric product of two vectors decomposes as

$$ab = a\cdot b + a\wedge b. \tag{2.5}$$

The essential feature of this product is that it mixes two different types of object: scalars and bivectors. One might now ask how the right-hand side of (2.5) is to be interpreted. The answer is that the addition implied by (2.5) is that used when, for example, a real number is added to an imaginary number to form a complex number. We are all happy with the rules for manipulating complex numbers, and the rules for manipulating mixed-grade combinations are much the same [3]. But why should one be interested in the sum of a scalar and a bivector? The reason is again the same as for complex numbers: algebraic manipulations are simplified considerably by working with general mixed-grade elements (multivectors) instead of working independently with pure-grade elements (scalars, vectors *etc.*).

An example of how the geometric product of two vectors (2.5) is employed directly is in the description of rotations using geometric algebra. Suppose initially that the vector a is reflected in the hyperplane perpendicular to the unit vector n ($n^2 = 1$). The result of this reflection is the vector

$$a - 2a\cdot nn = a - (an + na)n = -nan. \tag{2.6}$$

The form on the right-hand side is unique to geometric algebra, and is already an improvement on the usual formula on the left-hand side. If one now applies a second reflection in the hyperplane perpendicular to a second unit vector m the result is the vector

$$-m(-nan)m = mna(mn)\tilde{}. \tag{2.7}$$

The tilde on the right-hand side denotes the operation of *reversion*, which simply reverses the order of the vectors in any geometric product,

$$(ab\ldots c)\tilde{} \equiv c\ldots ba. \tag{2.8}$$

The combination of two reflections is a rotation in the plane specified by the two reflection axes. We therefore see that a rotation is performed by

$$a \mapsto Ra\tilde{R} \tag{2.9}$$

where

$$R = mn. \tag{2.10}$$

The object R is called a *rotor*. It has the fundamental property that

$$R\tilde{R} = mnnm = 1. \tag{2.11}$$

Equation (2.9) provides a remarkably compact and efficient formulation for encoding rotations. The formula for R (2.10) shows that a rotor is formed from the geometric product of two unit vectors, so does indeed consist of the sum of a scalar and a bivector. A rotor can furthermore be written as the exponential of a bivector, $R = \pm\exp(B/2)$, where the bivector encodes the plane in which the rotation is performed. This naturally generalises the complex representation of rotations frequently used in two dimensions. Rotors illustrate how mixed-grade objects are frequently employed as *operators* which act on other quantities in the algebra. The fact that both geometric objects and the operators that act on them are handled

in a single unified framework is a central feature of geometric algebra.

The above discussion applies to vector spaces of any dimension. We now turn to the case of specific interest, that of Minkowski spacetime. To make the discussion more concrete, we introduce a set of four basis vectors $\{\gamma_\mu\}$, $\mu = 0 \ldots 3$, satisfying

$$\gamma_\mu \cdot \gamma_\nu = \eta_{\mu\nu} = \mathrm{diag}(+ - - -). \tag{2.12}$$

The vectors $\{\gamma_\mu\}$ satisfy the same algebraic relations as Dirac's γ-matrices, but they now form a set of four independent basis vectors for spacetime, not four components of a single vector in an internal 'spin space'. When manipulating (geometric) products of these vectors, one simply uses the rule that parallel vectors commute and orthogonal vectors anticommute. This result is clear immediately from equation (2.5). From the four vectors $\{\gamma_\mu\}$ we can construct a set of six basis elements for the space of bivectors:

$$\{\gamma_1\gamma_0, \gamma_2\gamma_0, \gamma_3\gamma_0, \gamma_3\gamma_2, \gamma_1\gamma_3, \gamma_2\gamma_1\}. \tag{2.13}$$

After the bivectors comes the space of grade-3 objects or trivectors. This space is four-dimensional and is spanned by the basis

$$\{\gamma_3\gamma_2\gamma_1, \gamma_0\gamma_3\gamma_2, \gamma_0\gamma_1\gamma_3, \gamma_0\gamma_2\gamma_1\}. \tag{2.14}$$

Finally, there is a single grade-4 element. This is called the *pseudoscalar* and is given the symbol i, so that

$$i \equiv \gamma_0\gamma_1\gamma_2\gamma_3. \tag{2.15}$$

The symbol i is used because the square of i is -1, but the pseudoscalar must not be confused with the unit scalar imaginary employed in quantum mechanics. The pseudoscalar i is a geometrically-significant entity and is responsible for the duality operation in the algebra. Furthermore, i *anti*commutes with odd-grade elements (vectors and trivectors), and commutes only with even-grade elements.

The full STA is spanned by the basis

$$1, \qquad \{\gamma_\mu\}, \qquad \{\sigma_k,\ i\sigma_k\}, \qquad \{i\gamma_\mu\}, \qquad i, \tag{2.16}$$

where

$$\sigma_k \equiv \gamma_k\gamma_0, \qquad k = 1, 2, 3. \tag{2.17}$$

An arbitrary element of this algebra is called a *multivector* and, if desired, can

be expanded in terms of the basis (2.16). Multivectors in which all elements have the same grade are usually written as A_r to show that A contains only grade-r components. Multivectors inherit an associative product from the geometric product of vectors, and the geometric product of a grade-r multivector A_r with a grade-s multivector B_s decomposes into

$$A_r B_s = \langle AB \rangle_{r+s} + \langle AB \rangle_{r+s-2} \ldots + \langle AB \rangle_{|r-s|}. \tag{2.18}$$

The symbol $\langle M \rangle_r$ denotes the projection onto the grade-r component of M. The projection onto the grade-0 (scalar) component of M is written as $\langle M \rangle$. The scalar part of a product of multivectors satisfies the cyclic reordering property

$$\langle A \ldots BC \rangle = \langle CA \ldots B \rangle. \tag{2.19}$$

The '$\cdot$' and '$\wedge$' symbols are retained for the lowest-grade and highest-grade terms of the series (2.18), so that

$$A_r \cdot B_s \equiv \langle AB \rangle_{|r-s|} \tag{2.20}$$

$$A_r \wedge B_s \equiv \langle AB \rangle_{s+r}, \tag{2.21}$$

which are called the inner and outer (or exterior) products respectively. We also make use of the scalar product, defined by

$$A * B \equiv \langle AB \rangle, \tag{2.22}$$

and the commutator product, defined by

$$A \times B \equiv \tfrac{1}{2}(AB - BA). \tag{2.23}$$

The associativity of the geometric product ensures that the commutator product satisfies the Jacobi identity

$$A \times (B \times C) + B \times (C \times A) + C \times (A \times B) = 0. \tag{2.24}$$

When manipulating chains of products we employ the operator ordering convention that, in the absence of brackets, *inner, outer and scalar products take precedence over geometric products.*

As an illustration of the working of these definitions, consider the inner product

of a vector a with a bivector $b \wedge c$:

$$\begin{aligned} a\cdot(b\wedge c) &= \langle ab\wedge c\rangle_1 \\ &= \tfrac{1}{2}\langle abc - acb\rangle_1 \\ &= a\cdot bc - a\cdot cb - \tfrac{1}{2}\langle bac - cab\rangle_1. \end{aligned} \tag{2.25}$$

The quantity $bac - cab$ reverses to give minus itself, so cannot contain a vector part. We therefore obtain the result

$$a\cdot(b\wedge c) = a\cdot bc - a\cdot cb, \tag{2.26}$$

which is useful in many applications.

2.1 The Spacetime Split

The three bivectors $\{\sigma_k\}$, where $\sigma_k \equiv \gamma_k\gamma_0$ (2.17) satisfy

$$\tfrac{1}{2}(\sigma_j\sigma_k + \sigma_k\sigma_j) = -\tfrac{1}{2}(\gamma_j\gamma_k + \gamma_k\gamma_j) = \delta_{jk} \tag{2.27}$$

and therefore generate the geometric algebra of three-dimensional Euclidean space [3, 10]. This is identified as the algebra for the rest-space relative to the timelike vector γ_0. The full algebra for this space is spanned by the set

$$1, \qquad \{\sigma_k\}, \qquad \{i\sigma_k\}, \qquad i, \tag{2.28}$$

which is identifiable as the even subalgebra of the full STA (2.16). The identification of the algebra of relative space with the even subalgebra of the STA simplifies the transition from relativistic quantities to observables in a given frame. It is apparent from (2.27) that the algebra of the $\{\sigma_k\}$ is isomorphic to the algebra of the Pauli matrices. As with the $\{\gamma_\mu\}$, the $\{\sigma_k\}$ are to be interpreted geometrically as spatial vectors (spacetime bivectors) and not as operators in an abstract spin space. It should be noted that the pseudoscalar employed in (2.28) is the same as that employed in spacetime, since

$$\sigma_1\sigma_2\sigma_3 = \gamma_1\gamma_0\gamma_2\gamma_0\gamma_3\gamma_0 = \gamma_0\gamma_1\gamma_2\gamma_3 = i. \tag{2.29}$$

The split of the six spacetime bivectors into relative vectors $\{\sigma_k\}$ and relative bivectors $\{i\sigma_k\}$ is a frame-dependent operation — different observers determine

different relative spaces. This fact is clearly illustrated using the Faraday bivector F. The 'spacetime split' [8, 11] of F into the γ_0-system is made by separating F into parts which anticommute and commute with γ_0. Thus

$$F = \boldsymbol{E} + i\boldsymbol{B} \tag{2.30}$$

where

$$\boldsymbol{E} = \tfrac{1}{2}(F - \gamma_0 F \gamma_0) \tag{2.31}$$

$$i\boldsymbol{B} = \tfrac{1}{2}(F + \gamma_0 F \gamma_0). \tag{2.32}$$

Both $\boldsymbol{E}$ and $\boldsymbol{B}$ are spatial vectors in the γ_0-frame, and $i\boldsymbol{B}$ is a spatial bivector. Equation (2.30) decomposes F into separate electric and magnetic fields, and the explicit appearance of γ_0 in the formulae for $\boldsymbol{E}$ and $\boldsymbol{B}$ shows how this split is observer-dependent. Where required, relative (or spatial) vectors in the γ_0-system are written in bold type to record the fact that in the STA they are actually bivectors. This distinguishes them from spacetime vectors, which are left in normal type. No problems arise for the $\{\sigma_k\}$, which are unambiguously spacetime bivectors, and so are left in normal type.

When dealing with spatial problems it is useful to define an operation which distinguishes between spatial vectors (such as $\boldsymbol{E}$) and spatial bivectors (such as $i\boldsymbol{B}$). (Since both the $\{\sigma_k\}$ and $\{i\sigma_k\}$ are spacetime bivectors, they behave the same under Lorentz-covariant operations.) The required operation is that of spatial reversion which, as it coincides with Hermitian conjugation for matrices, we denote with a dagger. We therefore define

$$M^\dagger \equiv \gamma_0 \tilde{M} \gamma_0, \tag{2.33}$$

so that, for example,

$$F^\dagger = \boldsymbol{E} - i\boldsymbol{B}. \tag{2.34}$$

The explicit appearance of γ_0 in the definition (2.33) shows that spatial reversion is not a Lorentz-covariant operation.

When working with purely spatial quantities, we often require that the dot and wedge operations drop down to their three-dimensional definitions. For example, given two spatial vectors $\boldsymbol{a}$ and $\boldsymbol{b}$, we would like $\boldsymbol{a}\wedge\boldsymbol{b}$ to denote the spatial bivector swept out by $\boldsymbol{a}$ and $\boldsymbol{b}$. Accordingly we adopt the convention that, *in expressions where both vectors are in bold type, the dot and wedge operations take their three-*

dimensional meaning. Whilst this convention may look clumsy, it is simple to use in practice and rarely causes any confusion.

Spacetime vectors can also be decomposed by a spacetime split, this time resulting in a scalar and a relative vector. The spacetime split of the vector a is achieved via

$$a\gamma_0 = a\cdot\gamma_0 + a\wedge\gamma_0 \equiv a_0 + \boldsymbol{a}, \tag{2.35}$$

so that a_0 is a scalar (the γ_0-time component of a) and $\boldsymbol{a}$ is the relative spatial vector. For example, the 4-momentum p splits into

$$p\gamma_0 = E + \boldsymbol{p} \tag{2.36}$$

where E is the energy in the γ_0 frame, and $\boldsymbol{p}$ is the 3-momentum. The definition of the relative vector (2.35) ensures that

$$\begin{aligned} a\cdot b &= \langle a\gamma_0\gamma_0 b\rangle \\ &= \langle (a_0 + \boldsymbol{a})(b_0 - \boldsymbol{b})\rangle \\ &= a_0 b_0 - \boldsymbol{a}\cdot\boldsymbol{b}, \end{aligned} \tag{2.37}$$

as required for the inner product in Minkowski spacetime.

2.2 Spacetime Calculus

The fundamental differential operator on spacetime is the derivative with respect to the position vector x. This is known as the *vector derivative* and is given the symbol ∇. The vector derivative is defined in terms of its directional derivatives, with the derivative in the a direction of a general multivector M defined by

$$a\cdot\nabla M(x) \equiv \lim_{\epsilon\to 0}\frac{M(x+\epsilon a) - M(x)}{\epsilon}. \tag{2.38}$$

If we now introduce a set of four arbitrary basis vectors $\{e_j\}$, with reciprocal vectors $\{e^k\}$ defined by the equation $e_j\cdot e^k = \delta^k_j$, then the vector derivative assembles from the separate directional derivatives as

$$\nabla \equiv e^j e_j\cdot\nabla. \tag{2.39}$$

This definition shows how ∇ acts algebraically as a vector, as well as inheriting a calculus from its directional derivatives.

As an explicit example, consider the $\{\gamma_\mu\}$ frame introduced above. In terms of this frame we can write the position vector x as $x^\mu\gamma_\mu$, with $x^0 = t$, $x^1 = \mathsf{x}$ *etc.* and $\{\mathsf{x}, \mathsf{y}, \mathsf{z}\}$ a usual set of Cartesian components for the rest-frame of the γ_0 vector. From the definition (2.38) it is clear that

$$\gamma_\mu \cdot \nabla = \frac{\partial}{\partial x^\mu} \tag{2.40}$$

which we abbreviate to ∂_μ. From the definition (2.39) we can now write

$$\nabla = \gamma^\mu \partial_\mu = \gamma^0 \partial_t + \gamma^1 \partial_{\mathsf{x}} + \gamma^2 \partial_{\mathsf{y}} + \gamma^3 \partial_{\mathsf{z}} \tag{2.41}$$

which, in the standard matrix language of Dirac theory, is the operator that acts on Dirac spinors. It is not surprising, therefore, that the ∇ operator should play a fundamental role in the STA formulation of the Dirac theory. What is less obvious is that the same operator should also play a fundamental role in the STA formulation of the Maxwell equations [8]. In tensor notation, the Maxwell equations take the form

$$\partial_\mu F^{\mu\nu} = J^\nu, \qquad \partial_{[\alpha} F_{\mu\nu]} = 0, \tag{2.42}$$

where $[\ldots]$ denotes total antisymmetrisation of the indices inside the bracket. On defining the bivector

$$F \equiv \tfrac{1}{2} F^{\mu\nu} \gamma_\mu \wedge \gamma_\nu \tag{2.43}$$

and the vector $J \equiv J^\mu \gamma_\mu$ the equations (2.42) become

$$\nabla \cdot F = J \tag{2.44}$$

and

$$\nabla \wedge F = 0. \tag{2.45}$$

But we can now utilise the geometric product to combine these separate equations into the single equation

$$\nabla F = J \tag{2.46}$$

which contains all of the Maxwell equations. We see from (2.46) that the vector derivative plays a central role in Maxwell theory, as well as Dirac theory. The observation that the vector derivative is the sole differential operator required to formulate both Maxwell and Dirac theories is a fundamental insight afforded by the STA. Some consequences of this observation for propagator theory are discussed in [6].

The vector derivative acts on the object to its immediate right unless brackets are present, when it acts on everything in the brackets. Since the vector derivative does not commute with multivectors, it is useful to have a notation for when the derivative acts on a multivector to which it is not adjacent. We use overdots for this, so that in the expression $\dot{\nabla}A\dot{B}$ the ∇ operator acts only on B. In terms of a frame of vectors we can write

$$\dot{\nabla}A\dot{B} = e^j A e_j \cdot \nabla B. \tag{2.47}$$

The overdot notation provides a useful means for expressing Leibniz' rule via

$$\nabla(AB) = \dot{\nabla}\dot{A}B + \dot{\nabla}A\dot{B}. \tag{2.48}$$

The spacetime split of the vector derivative requires some care. We wish to retain the symbol $\boldsymbol{\nabla}$ for the spatial vector derivative, so that

$$\boldsymbol{\nabla} = \sigma_k \partial_k, \qquad k = 1 \ldots 3. \tag{2.49}$$

This definition of $\boldsymbol{\nabla}$ is inconsistent with the definition (2.35), so for the vector derivative we have to remember that

$$\nabla\gamma_0 = \partial_t - \boldsymbol{\nabla}. \tag{2.50}$$

We conclude this introduction with some useful results concerning the vector derivative. We let the dimension of the space of interest be n, so that the results are applicable to both space and spacetime. The most basic results are that

$$\nabla x = n \tag{2.51}$$

and that

$$\nabla \wedge \nabla\psi = 0 \tag{2.52}$$

where ψ is an arbitrary multivector field. The latter result follows from the fact that partial derivatives commute. For a grade-r multivector A_r the following results are also useful:

$$\dot{\nabla}\dot{x}\cdot A_r = rA_r \tag{2.53}$$

$$\dot{\nabla}\dot{x}\wedge A_r = (n-r)A_r \tag{2.54}$$

$$\dot{\nabla}A_r\dot{x} = (-1)^r(n-2r)A_r. \tag{2.55}$$

More complicated results can be built up with the aid of Leibniz' rule, for example

$$\nabla x^2 = \dot{\nabla}\dot{x}\cdot x + \dot{\nabla}x\cdot\dot{x} = 2x. \tag{2.56}$$

This concludes our introduction to the spacetime algebra. Further details can be found in '*Space-Time Algebra*' by Hestenes [8] and '*Clifford Algebra to Geometric Calculus*' by Hestenes and Sobczyk [12]. The latter is a technical exposition of geometric algebra in general and does not deal directly with spacetime physics. A number of papers contain useful introductory material including those by Hestenes [13, 11, 7] and the series of papers [3, 4, 5, 6] written by three of the present authors. Baylis *et al.* [14] and Vold [15, 16] have also written good introductory pieces, and the books *'New Foundations for Classical Mechanics'* by Hestenes [10] and *'Multivectors and Clifford Algebras in Electrodynamics'* by Jancewicz [17] provide useful background material. Further work can be found in the three conference proceedings [18, 19, 20], though only a handful of papers are directly relevant to the work reviewed in this paper. Of greater interest are the proceedings of the conference entitled '*The Electron*' [21], which contains a number of papers dealing with the application of the STA to electron physics.

3 Spinors and the Dirac Equation

In this section we review how both the quantum states and matrix operators of the Pauli and Dirac theories can be formulated within the real STA. This approach to electron theory was initiated by Hestenes [22, 23] and has grown steadily in popularity ever since. We start with a review of the single-electron Pauli theory and then proceed to the Dirac theory. Multiparticle states are considered in Section 9.

Before proceeding, it is necessary to explain what we mean by a *spinor*. The literature is replete with discussions about different types of spinors and their interrelationships and transformation laws. This literature is highly mathematical, and is of very little relevance to electron physics. For our purposes, we define a spinor to be an element of a linear space which is closed under left-sided multiplication by a rotor. Thus spinors are acted on by rotor representations of the rotation group. With this in mind, we can proceed directly to study the spinors of relevance to physics. Further work relating to the material in this section is contained in [4].

3.1 Pauli Spinors

We saw in Section 2.1 that the algebra of the Pauli matrices is precisely that of a set of three orthonormal vectors in space under the geometric product. So the Pauli matrices are simply a matrix representation of the geometric algebra of space. This observation opens up the possibility of eliminating matrices from the Pauli theory in favour of geometrically-significant quantities. But what of the operator action of the Pauli matrices on spinors? This too needs to be represented with the geometric algebra of space. To achieve this aim, we recall the standard representation for the Pauli matrices

$$\hat{\sigma}_1 = \begin{pmatrix} 0 & 1 \\ 1 & 0 \end{pmatrix}, \quad \hat{\sigma}_2 = \begin{pmatrix} 0 & -j \\ j & 0 \end{pmatrix}, \quad \hat{\sigma}_3 = \begin{pmatrix} 1 & 0 \\ 0 & -1 \end{pmatrix}. \tag{3.1}$$

The overhats distinguish these matrix operators from the $\{\sigma_k\}$ vectors whose algebra they represent. The symbol i is reserved for the pseudoscalar, so the symbol j is used for the scalar unit imaginary employed in quantum theory. The $\{\hat{\sigma}_k\}$ operators act on 2-component complex spinors

$$|\psi\rangle = \begin{pmatrix} \psi_1 \\ \psi_2 \end{pmatrix}, \tag{3.2}$$

where ψ_1 and ψ_2 are complex numbers. Quantum states are written with bras and kets to distinguish them from STA multivectors. The set of $|\psi\rangle$'s form a two-dimensional complex vector space. To represent these states as multivectors in the STA we therefore need to find a four-dimensional (real) space on which the action of the $\{\hat{\sigma}_k\}$ operators can be replaced by operations involving the $\{\sigma_k\}$ vectors. There are many ways to achieve this goal, but the simplest is to represent a spinor $|\psi\rangle$ by an element of the even subalgebra of (2.28). This space is spanned by the set $\{1, i\sigma_k\}$ and the column spinor $|\psi\rangle$ is placed in one-to-one correspondence with the (Pauli)-even multivector $\psi = \gamma_0\psi\gamma_0$ through the identification [4, 24]

$$|\psi\rangle = \begin{pmatrix} a^0 + ja^3 \\ -a^2 + ja^1 \end{pmatrix} \leftrightarrow \psi = a^0 + a^k i\sigma_k. \tag{3.3}$$

In particular, the spin-up and spin-down basis states become

$$\begin{pmatrix} 1 \\ 0 \end{pmatrix} \leftrightarrow 1 \tag{3.4}$$

and

$$\begin{pmatrix} 0 \\ 1 \end{pmatrix} \leftrightarrow -i\sigma_2. \tag{3.5}$$

The action of the quantum operators $\{\hat{\sigma}_k\}$ and j is now replaced by the operations

$$\hat{\sigma}_k|\psi\rangle \leftrightarrow \sigma_k\psi\sigma_3 \qquad (k=1,2,3) \tag{3.6}$$

$$\text{and} \quad j|\psi\rangle \leftrightarrow \psi i\sigma_3. \tag{3.7}$$

Verifying these relations is a matter of routine computation; for example

$$\hat{\sigma}_1|\psi\rangle = \begin{pmatrix} -a^2 + ja^1 \\ a^0 + ja^3 \end{pmatrix} \leftrightarrow -a^2 + a^1 i\sigma_3 - a^0 i\sigma_2 + a^3 i\sigma_1 = \sigma_1\psi\sigma_3. \tag{3.8}$$

We have now achieved our aim. Every expression involving Pauli operators and spinors has an equivalent form in the STA and all manipulations can be carried out using the properties of the $\{\sigma_k\}$ vectors alone, with no need to introduce an explicit matrix representation. This is far more than just a theoretical nicety. Not only is there considerable advantage in being able to perform the computations required in the Pauli theory without multiplying matrices together, but abstract matrix algebraic manipulations are replaced by relations of clear geometric significance.

Pauli Observables

We now turn to a discussion of the observables associated with Pauli spinors. These show how the STA formulation requires a shift in our understanding of what constitutes scalar and vector observables at the quantum level. We first need to construct the STA form of the spinor inner product $\langle\psi|\phi\rangle$. It is sufficient just to consider the real part of the inner product, which is given by

$$\Re\langle\psi|\phi\rangle \leftrightarrow \langle\psi^\dagger\phi\rangle, \tag{3.9}$$

so that, for example,

$$\begin{aligned} \langle\psi|\psi\rangle \leftrightarrow \langle\psi^\dagger\psi\rangle &= \langle(a^0 - ia^j\sigma_j)(a^0 + ia^k\sigma_k)\rangle \\ &= (a^0)^2 + a^k a^k. \end{aligned} \tag{3.10}$$

(Note that no spatial integral is implied in our use of the bra-ket notation.) Since

$$\langle\psi|\phi\rangle = \Re\langle\psi|\phi\rangle - j\Re\langle\psi|j\phi\rangle, \tag{3.11}$$

the full inner product becomes

$$\langle\psi|\phi\rangle \;\leftrightarrow\; (\psi,\phi)_S \equiv \langle\psi^\dagger\phi\rangle - \langle\psi^\dagger\phi i\sigma_3\rangle i\sigma_3. \tag{3.12}$$

The right hand side projects out the $\{1, i\sigma_3\}$ components from the geometric product $\psi^\dagger\phi$. The result of this projection on a multivector A is written $\langle A\rangle_S$. For Pauli-even multivectors this projection has the simple form

$$\langle A\rangle_S = \tfrac{1}{2}(A - i\sigma_3 A i\sigma_3). \tag{3.13}$$

As an application of (3.12), consider the expectation value of the spin in the k-direction,

$$\langle\psi|\hat{\sigma}_k|\psi\rangle \;\leftrightarrow\; \langle\psi^\dagger\sigma_k\psi\sigma_3\rangle - \langle\psi^\dagger\sigma_k\psi i\rangle i\sigma_3. \tag{3.14}$$

Since $\psi^\dagger i\sigma_k\psi$ reverses to give minus itself, it has zero scalar part. The right-hand side of (3.14) therefore reduces to

$$\langle\sigma_k\psi\sigma_3\psi^\dagger\rangle = \sigma_k\cdot\langle\psi\sigma_3\psi^\dagger\rangle_v, \tag{3.15}$$

where $\langle\ldots\rangle_v$ denotes the relative vector component of the term in brackets. (This notation is required because $\langle\ldots\rangle_1$ would denote the spacetime vector part of the term in brackets.) The expression (3.15) has a rather different interpretation in the STA to standard quantum mechanics — it is the σ_k-component of the vector part of $\psi\sigma_3\psi^\dagger$. As $\psi\sigma_3\psi^\dagger$ is both Pauli-odd and Hermitian-symmetric it can contain only a relative vector part, so we define the spin-vector $\boldsymbol{s}$ by

$$\boldsymbol{s} \equiv \psi\sigma_3\psi^\dagger. \tag{3.16}$$

(In fact, both spin and angular momentum are better viewed as spatial bivector quantities, so it is usually more convenient to work with $i\boldsymbol{s}$ instead of $\boldsymbol{s}$.) The STA approach thus enables us to work with a single vector $\boldsymbol{s}$, whereas the operator/matrix theory treats only its individual components. We can apply a similar analysis to the momentum operator. The momentum density in the k-direction is given by

$$\langle\psi| - j\partial_k|\psi\rangle \;\leftrightarrow\; -\langle\psi^\dagger\sigma_k\cdot\boldsymbol{\nabla}\psi i\sigma_3\rangle - \langle\psi^\dagger\sigma_k\cdot\boldsymbol{\nabla}\psi\rangle i\sigma_3, \tag{3.17}$$

in which the final term is a total divergence and so is ignored. Recombining with

the $\{\sigma_k\}$ vectors, we find that the momentum vector field is given by

$$\boldsymbol{p} = -\dot{\boldsymbol{\nabla}}\langle\dot{\psi}i\sigma_3\psi^\dagger\rangle. \tag{3.18}$$

It might appear that we have just played a harmless game by redefining various observables, but in fact something remarkable has happened. The spin-vector $\boldsymbol{s}$ and the momentum $\boldsymbol{p}$ are both legitimate (*i.e.* gauge-invariant) quantities constructed from the spinor ψ. But standard quantum theory dictates that we cannot simultaneously measure all three components of $\boldsymbol{s}$, whereas we can for $\boldsymbol{p}$. The 'proof' of this result is based on the non-commutativity of the $\{\hat{\sigma}_k\}$ operators. But, in the STA formulation, this lack of commutativity merely expresses the fact that the $\{\sigma_k\}$ vectors are orthogonal — a fact of geometry, not of dynamics! Furthermore, given a spinor ψ there is certainly no difficulty in finding the vector $\boldsymbol{s}$. So how then are we to interpret a spin measurement, as performed by a Stern-Gerlach apparatus for example? This problem will be treated in detail in Section 8, but the conclusions are straightforward. A Stern-Gerlach apparatus is *not* a measuring device — it should really be viewed as a spin *polariser*. When a spinor wavepacket with arbitrary initial vector $\boldsymbol{s}$ enters a Stern-Gerlach apparatus, the wavepacket splits in two and the vector $\boldsymbol{s}$ rotates to align itself either parallel or anti-parallel to the $\boldsymbol{B}$ field. The two different alignments then separate into the two packets. Hence, in the final beams, the vector $\boldsymbol{s}$ has been polarised to point in a single direction. So, having passed through the apparatus, all three components of the spin-vector $\boldsymbol{s}$ are known - not just the component in the direction of the $\boldsymbol{B}$ field. This is a major conceptual shift, yet it is completely consistent with the standard predictions of quantum theory. Similar views have been expressed in the past by advocates of Bohm's 'causal' interpretation of quantum theory [25, 26, 27]. However, the shift in interpretation described here is due solely to the new understanding of the role of the Pauli matrices which the STA affords. It does not require any of the additional ideas associated with Bohm's interpretation, such as quantum forces and quantum torques.

Spinors and Rotations

Further insights into the role of spinors in the Pauli theory are obtained by defining a scalar

$$\rho \equiv \psi\psi^\dagger, \tag{3.19}$$

so that the spinor ψ can be decomposed into

$$\psi = \rho^{1/2} R. \tag{3.20}$$

Here R is defined as

$$R = \rho^{-1/2} \psi \tag{3.21}$$

and satisfies

$$R R^{\dagger} = 1. \tag{3.22}$$

In Section 2 we saw that rotors, which act double-sidedly to generate rotations, satisfy equation (3.22). It is not hard to show that, in three dimensions, all even quantities satisfying (3.22) are rotors. It follows from (3.20) that the spin-vector $\boldsymbol{s}$ can now be written as

$$\boldsymbol{s} = \rho R \sigma_3 R^{\dagger}, \tag{3.23}$$

which demonstrates that the double-sided construction of the expectation value (3.15) contains an instruction to rotate the fixed σ_3 axis into the spin direction and dilate it. The decomposition of the spinor ψ into a density term ρ and a rotor R suggests that a deeper substructure underlies the Pauli theory. This is a subject which has been frequently discussed by Hestenes [23, 28, 29, 9]. As an example of the insights afforded by this decomposition, one can now 'explain' why spinors transform single-sidedly under rotations. If the vector $\boldsymbol{s}$ is to be rotated to a new vector $R_0 \boldsymbol{s} R_0^{\dagger}$ then, according to the rotor group combination law, R must transform to $R_0 R$. This induces the spinor transformation law

$$\psi \mapsto R_0 \psi \tag{3.24}$$

which is the STA equivalent of the quantum transformation law

$$|\psi\rangle \mapsto \exp\{\frac{j}{2} \theta n_k \hat{\sigma}_k\} |\psi\rangle \tag{3.25}$$

where $\{n_k\}$ are the components of a unit vector.

We can also now see why the presence of the σ_3 vector on the right-hand side of the spinor ψ does not break rotational invariance. All rotations are performed by left-multiplication by a rotor, so the spinor ψ effectively shields the σ_3 on the right from the transformation. There is a strong analogy with rigid-body mechanics in this observation, which has been discussed by Hestenes [9, 30]. Similar ideas have also been pursued by Dewdney, Holland and Kyprianidis [31, 32]. We shall see in

Pauli Matrices	$\hat{\sigma}_1 = \begin{pmatrix} 0 & 1 \\ 1 & 0 \end{pmatrix} \quad \hat{\sigma}_2 = \begin{pmatrix} 0 & -j \\ j & 0 \end{pmatrix} \quad \hat{\sigma}_3 = \begin{pmatrix} 1 & 0 \\ 0 & -1 \end{pmatrix}$
Spinor Equivalence	$\lvert\psi\rangle = \begin{pmatrix} a^0 + ja^3 \\ -a^2 + ja^1 \end{pmatrix} \leftrightarrow \psi = a^0 + a^k i\sigma_k$
Operator Equivalences	$\begin{aligned} \hat{\sigma}_k\lvert\psi\rangle &\leftrightarrow \sigma_k\psi\sigma_3 \\ j\lvert\psi\rangle &\leftrightarrow \psi i\sigma_3 \\ \langle\psi\lvert\psi'\rangle &\leftrightarrow \langle\psi^\dagger\psi'\rangle_S \end{aligned}$
Observables	$\begin{aligned} \rho &= \psi\psi^\dagger \\ \boldsymbol{s} &= \psi\sigma_3\psi^\dagger \end{aligned}$

Table 2: *Summary of the main results for the STA representation of Pauli spinors*

the next section that this analogy extends to the Dirac theory. The main results of this section are summarised in Table 2.

3.2 Dirac Spinors

The procedures developed for Pauli spinors extend simply to Dirac spinors. Again, we seek to represent complex column spinors, and the matrix operators acting on them, by multivectors and functions in the STA. Dirac spinors are four-component complex entities, so must be represented by objects containing 8 real degrees of freedom. The representation that turns out to be most convenient for applications is via the 8-dimensional even subalgebra of the STA [23, 33]. If one recalls from Section 2.1 that the even subalgebra of the STA is isomorphic to the Pauli algebra, we see that what is required is a map between column spinors and elements of the Pauli algebra. To construct such a map we begin with the γ-matrices in the standard Dirac-Pauli representation [34],

$$\hat{\gamma}_0 = \begin{pmatrix} I & 0 \\ 0 & -I \end{pmatrix}, \quad \hat{\gamma}_k = \begin{pmatrix} 0 & -\hat{\sigma}_k \\ \hat{\sigma}_k & 0 \end{pmatrix} \quad \text{and} \quad \hat{\gamma}_5 = \begin{pmatrix} 0 & I \\ I & 0 \end{pmatrix}, \tag{3.26}$$

where $\hat{\gamma}_5 = \hat{\gamma}^5 \equiv -j\hat{\gamma}_0\hat{\gamma}_1\hat{\gamma}_2\hat{\gamma}_3$ and I is the 2×2 identity matrix. A Dirac column spinor $|\psi\rangle$ is placed in one-to-one correspondence with an 8-component even element of the STA via [24, 35]

$$|\psi\rangle = \begin{pmatrix} a^0 + ja^3 \\ -a^2 + ja^1 \\ b^0 + jb^3 \\ -b^2 + jb^1 \end{pmatrix} \leftrightarrow \psi = a^0 + a^k i\sigma_k + (b^0 + b^k i\sigma_k)\sigma_3. \tag{3.27}$$

With the spinor $|\psi\rangle$ now replaced by an even multivector, the action of the operators $\{\hat{\gamma}_\mu, \hat{\gamma}_5, j\}$ becomes

$$\begin{array}{rcll} \hat{\gamma}_\mu|\psi\rangle & \leftrightarrow & \gamma_\mu\psi\gamma_0 & (\mu = 0, \ldots, 3) \\ j|\psi\rangle & \leftrightarrow & \psi\, i\sigma_3 & \\ \hat{\gamma}_5|\psi\rangle & \leftrightarrow & \psi\sigma_3. & \end{array} \tag{3.28}$$

To verify these relations, we note that the map (3.27) can be written more concisely as

$$|\psi\rangle = \begin{pmatrix} |\phi\rangle \\ |\eta\rangle \end{pmatrix} \leftrightarrow \psi = \phi + \eta\sigma_3, \tag{3.29}$$

where $|\phi\rangle$ and $|\eta\rangle$ are two-component spinors, and ϕ and η are their Pauli-even equivalents, as defined by the map (3.3). We can now see, for example, that

$$\hat{\gamma}_k|\psi\rangle = \begin{pmatrix} -\hat{\sigma}_k|\eta\rangle \\ \hat{\sigma}_k|\phi\rangle \end{pmatrix} \leftrightarrow -\sigma_k\eta\sigma_3 + \sigma_k\phi = \gamma_k(\phi + \eta\sigma_3)\gamma_0, \tag{3.30}$$

as required. The map (3.29) shows that the split between the 'large' and 'small' components of the column spinor $|\psi\rangle$ is equivalent to splitting ψ into Pauli-even and Pauli-odd terms in the STA.

Alternative Representations

All algebraic manipulations can be performed in the STA without ever introducing a matrix representation, so equations (3.27) and (3.28) achieve a map to a representation-free language. However, the explicit map (3.27) between the components of a Dirac spinor and the multivector ψ is only relevant to the Dirac-Pauli matrix representation. A different matrix representation requires a different map so that that the effect of the matrix operators is still given by (3.28). The relevant map is easy to construct given the unitary matrix $\hat{S}$ which transforms between the

matrix representations via

$$\hat{\gamma}'_\mu = \hat{S}\hat{\gamma}_\mu\hat{S}^{-1}. \tag{3.31}$$

The corresponding spinor transformation is $|\psi\rangle \mapsto \hat{S}|\psi\rangle$, and the map is constructed by transforming the column spinor $|\psi\rangle'$ in the new representation back to a Dirac-Pauli spinor $\hat{S}^\dagger|\psi\rangle'$. The spinor $\hat{S}^\dagger|\psi\rangle'$ is then mapped into the STA in the usual way (3.27). As an example, consider the Weyl representation defined by the matrices [36]

$$\hat{\gamma}'_0 = \begin{pmatrix} 0 & -I \\ -I & 0 \end{pmatrix} \quad \text{and} \quad \hat{\gamma}'_k = \begin{pmatrix} 0 & -\hat{\sigma}_k \\ \hat{\sigma}_k & 0 \end{pmatrix}. \tag{3.32}$$

The Weyl representation is obtained from the Dirac-Pauli representation by the unitary matrix

$$\hat{U} = \frac{1}{\sqrt{2}}\begin{pmatrix} I & I \\ -I & I \end{pmatrix}. \tag{3.33}$$

A spinor in the Weyl representation is written as

$$|\psi\rangle' = \begin{pmatrix} |\chi\rangle \\ |\bar{\eta}\rangle \end{pmatrix}, \tag{3.34}$$

where $|\chi\rangle$ and $|\bar{\eta}\rangle$ are 2-component spinors. Acting on $|\psi\rangle'$ with $\hat{U}^\dagger$ gives

$$\hat{U}^\dagger|\psi\rangle' = \tfrac{1}{\sqrt{2}}\begin{pmatrix} |\chi\rangle - |\bar{\eta}\rangle \\ |\chi\rangle + |\bar{\eta}\rangle \end{pmatrix}. \tag{3.35}$$

Using equation (3.27), this spinor is mapped onto the even element

$$\hat{U}^\dagger|\psi\rangle' = \tfrac{1}{\sqrt{2}}\begin{pmatrix} |\chi\rangle - |\bar{\eta}\rangle \\ |\chi\rangle + |\bar{\eta}\rangle \end{pmatrix} \leftrightarrow \psi = \chi\tfrac{1}{\sqrt{2}}(1+\sigma_3) - \bar{\eta}\tfrac{1}{\sqrt{2}}(1-\sigma_3), \tag{3.36}$$

where χ and $\bar{\eta}$ are the Pauli-even equivalents of the 2-component complex spinors $|\chi\rangle$ and $|\bar{\eta}\rangle$, as defined by equation (3.3). The even multivector

$$\psi = \chi\tfrac{1}{\sqrt{2}}(1+\sigma_3) - \bar{\eta}\tfrac{1}{\sqrt{2}}(1-\sigma_3) \tag{3.37}$$

is therefore our STA version of the column spinor

$$|\psi\rangle' = \begin{pmatrix} |\chi\rangle \\ |\bar{\eta}\rangle \end{pmatrix}, \tag{3.38}$$

where $|\psi\rangle'$ is acted on by matrices in the Weyl representation. As a check, we observe that

$$\hat{\gamma}_0'|\psi\rangle' = \begin{pmatrix} -|\bar{\eta}\rangle \\ -|\chi\rangle \end{pmatrix} \leftrightarrow -\bar{\eta}\tfrac{1}{\sqrt{2}}(1+\sigma_3) + \chi\tfrac{1}{\sqrt{2}}(1-\sigma_3) = \gamma_0\psi\gamma_0 \tag{3.39}$$

and

$$\hat{\gamma}_k|\psi\rangle = \begin{pmatrix} -\hat{\sigma}_k|\bar{\eta}\rangle \\ \hat{\sigma}_k|\chi\rangle \end{pmatrix} \leftrightarrow -\sigma_k\bar{\eta}\sigma_3\tfrac{1}{\sqrt{2}}(1+\sigma_3) - \sigma_k\chi\sigma_3\tfrac{1}{\sqrt{2}}(1-\sigma_3) = \gamma_k\psi\gamma_0. \tag{3.40}$$

(Here we have used equation (3.7) and the fact that γ_0 commutes with all Pauli-even elements.) The map (3.36) does indeed have the required properties.

While our procedure ensures that the action of the $\{\hat{\gamma}_\mu, \hat{\gamma}_5\}$ matrix operators is always given by (3.28), the same is not true of the operation of complex conjugation. Complex conjugation is a representation-dependent operation, so the STA versions can be different for different representations. For example, complex conjugation in the Dirac-Pauli and Weyl representations is given by

$$|\psi\rangle^* \leftrightarrow -\gamma_2\psi\gamma_2, \tag{3.41}$$

whereas in the Majorana representation complex conjugation leads to the STA operation [4]

$$|\psi\rangle^*_{\text{Maj}} \leftrightarrow \psi\sigma_2. \tag{3.42}$$

Rather than think of (3.41) and (3.42) as different representations of the same operation, however, it is simpler to view them as distinct STA operations that can be performed on the multivector ψ.

3.3 The Dirac Equation and Observables

As a simple application of (3.27) and (3.28), consider the Dirac equation

$$\hat{\gamma}^\mu(j\partial_\mu - eA_\mu)|\psi\rangle = m|\psi\rangle. \tag{3.43}$$

The STA version of this equation is, after postmultiplication by γ_0,

$$\nabla\psi i\sigma_3 - eA\psi = m\psi\gamma_0, \tag{3.44}$$

where $\nabla = \gamma^\mu \partial_\mu$ is the spacetime vector derivative (2.41). The STA form of the Dirac equation (3.44) was first discovered by Hestenes [8], and has been discussed by many authors since; see, for example, references [35, 37, 38, 39, 40]. The translation scheme described here is direct and unambiguous and the resulting equation is both coordinate-free and representation-free. In manipulating equation (3.44) one needs only the algebraic rules for multiplying spacetime multivectors, and the equation can be solved completely without ever introducing a matrix representation. Stripped of the dependence on a matrix representation, equation (3.44) expresses the intrinsic geometric content of the Dirac equation.

In order to discuss the observables of the Dirac theory, we must first consider the spinor inner product. It is necessary at this point to distinguish between the Hermitian and Dirac adjoint. These are written as

$$\begin{array}{lcl} \langle \bar{\psi}| & - & \text{Dirac adjoint} \\ \langle \psi| & - & \text{Hermitian adjoint,} \end{array} \tag{3.45}$$

which are represented in the STA as follows,

$$\begin{array}{lcl} \langle \bar{\psi}| & \leftrightarrow & \tilde{\psi} \\ \langle \psi| & \leftrightarrow & \psi^\dagger = \gamma_0 \tilde{\psi} \gamma_0. \end{array} \tag{3.46}$$

One can see clearly from these definitions that the Dirac adjoint is Lorentz-invariant, whereas the Hermitian adjoint requires singling out a preferred timelike vector.

The inner product is handled as in equation (3.12), so that

$$\langle \bar{\psi} | \phi \rangle \;\leftrightarrow\; \langle \tilde{\psi} \phi \rangle - \langle \tilde{\psi} \phi i \sigma_3 \rangle i \sigma_3 = \langle \tilde{\psi} \phi \rangle_S, \tag{3.47}$$

which is also easily verified by direct calculation. By utilising (3.47) the STA forms of the Dirac spinor bilinear covariants [36] are readily found. For example,

$$\langle \bar{\psi} | \hat{\gamma}_\mu | \psi \rangle \;\leftrightarrow\; \langle \tilde{\psi} \gamma_\mu \psi \gamma_0 \rangle - \langle \tilde{\psi} \gamma_\mu \psi i \gamma_3 \rangle i \sigma_3 = \gamma_\mu \cdot \langle \psi \gamma_0 \tilde{\psi} \rangle_1 \tag{3.48}$$

identifies the 'observable' as the γ_μ-component of the vector $\langle \psi \gamma_0 \tilde{\psi} \rangle_1$. Since the quantity $\psi \gamma_0 \tilde{\psi}$ is odd and reverse-symmetric it can only contain a vector part, so we can define the frame-free vector J by

$$J \equiv \psi \gamma_0 \tilde{\psi}. \tag{3.49}$$

The spinor ψ has a Lorentz-invariant decomposition which generalises the

Bilinear Covariant	Standard Form	STA Equivalent	Frame-Free Form
Scalar	$\langle\bar{\psi}\vert\psi\rangle$	$\langle\psi\tilde{\psi}\rangle$	$\rho\cos\beta$
Vector	$\langle\bar{\psi}\vert\hat{\gamma}_\mu\vert\psi\rangle$	$\gamma_\mu\cdot(\psi\gamma_0\tilde{\psi})$	$\psi\gamma_0\tilde{\psi}=J$
Bivector	$\langle\bar{\psi}\vert j\hat{\gamma}_{\mu\nu}\vert\psi\rangle$	$(\gamma_\mu\wedge\gamma_\nu)\cdot(\psi i\sigma_3\tilde{\psi})$	$\psi i\sigma_3\tilde{\psi}=S$
Pseudovector	$\langle\bar{\psi}\vert\hat{\gamma}_\mu\hat{\gamma}_5\vert\psi\rangle$	$\gamma_\mu\cdot(\psi\gamma_3\tilde{\psi})$	$\psi\gamma_3\tilde{\psi}=s$
Pseudoscalar	$\langle\bar{\psi}\vert j\hat{\gamma}_5\vert\psi\rangle$	$\langle\psi\tilde{\psi}i\rangle$	$-\rho\sin\beta$

Table 3: *Bilinear covariants in the Dirac theory.*

decomposition of Pauli spinors into a rotation and a density factor (3.20). Since $\psi\tilde{\psi}$ is even and reverses to give itself, it contains only scalar and pseudoscalar terms. We can therefore define

$$\rho e^{i\beta}\equiv\psi\tilde{\psi}, \tag{3.50}$$

where both ρ and β are scalars. Assuming that $\rho\neq 0$, ψ can now be written as

$$\psi=\rho^{1/2}e^{i\beta/2}R \tag{3.51}$$

where

$$R=(\rho e^{i\beta})^{-1/2}\psi. \tag{3.52}$$

The even multivector R satisfies $R\tilde{R}=1$ and therefore defines a spacetime rotor. The current J (3.49) can now be written as

$$J=\rho v \tag{3.53}$$

where

$$v\equiv R\gamma_0\tilde{R}. \tag{3.54}$$

The remaining bilinear covariants can be analysed likewise, and the results are summarised in Table 3. The final column of this Table employs the quantities

$$s\equiv\psi\gamma_3\tilde{\psi},\quad\text{and}\quad S\equiv\psi i\sigma_3\tilde{\psi}. \tag{3.55}$$

Double-sided application of R on a vector a produces a Lorentz transformation [3]. The full Dirac spinor ψ therefore contains an instruction to rotate the fixed $\{\gamma_\mu\}$ frame into the frame of observables. The analogy with rigid-body dynamics first encountered in Section 3.1 with Pauli spinors therefore extends to the

relativistic theory. In particular, the unit vector v (3.54) is both future-pointing and timelike and has been interpreted as defining an electron velocity [23, 9] (see also the critical discussion in [6]). The 'β-factor' appearing in the decomposition of ψ (3.50) has also been the subject of much discussion [6, 9, 38, 39] since, for free-particle states, β determines the ratio of particle to anti-particle solutions. It remains unclear whether this idea extends usefully to interacting systems.

In Section 3.1 we argued that, for Pauli spinors, any dynamical consequences derived from the algebraic properties of the Pauli matrices were questionable, since the algebra of the Pauli matrices merely expresses the geometrical relations between a set of orthonormal vectors in space. Precisely the same is true of any consequences inferred from the properties of the Dirac matrices. This observation has the happy consequence of removing one particularly prevalent piece of nonsense — that the observed velocity of an electron must be the speed of light [41, 42]. The 'proof' of this result is based on the idea that the velocity operator in the k-direction is the $\hat{\gamma}_k\hat{\gamma}_0$ matrix. Since the square of this matrix is 1, its eigenvalues must be ± 1. But in the STA the fact that the square of the $\{\gamma_\mu\}$ matrices is ± 1 merely expresses the fact that they form an orthonormal basis. This cannot possibly have any observational consequences. To the extent that one can talk about a velocity in the Dirac theory, the relevant observable must be defined in terms of the current J. The $\{\gamma_\mu\}$ vectors play no other role than to pick out the components of this current in a particular frame. The shift from viewing the $\{\gamma_\mu\}$ as operators to viewing them as an arbitrary, fixed frame is seen clearly in the definition of the current J (3.49). In this expression it is now the ψ that 'operates' to align the γ_0 vector with the observable current. Since ψ transforms single-sidedly under rotations, the fixed initial γ_0-vector is never affected by the rotor and its presence does not violate Lorentz invariance [4].

We end this subsection by briefly listing how the C, P and T symmetries are handled in the STA. Following the conventions of Bjorken & Drell [34] we find that

$$\begin{array}{lcl} \hat{P}|\psi\rangle & \leftrightarrow & \gamma_0\psi(\bar{x})\gamma_0 \\ \hat{C}|\psi\rangle & \leftrightarrow & \psi\sigma_1 \\ \hat{T}|\psi\rangle & \leftrightarrow & i\gamma_0\psi(-\bar{x})\gamma_1, \end{array} \tag{3.56}$$

where $\bar{x} \equiv \gamma_0 x \gamma_0$ is (minus) a reflection of x in the timelike γ_0 axis. The combined CPT symmetry corresponds to

$$\psi \mapsto -i\psi(-x) \tag{3.57}$$

so that CPT symmetry does not require singling out a preferred timelike vector. A more complete discussion of the symmetries and conserved quantities of the Dirac theory from the STA viewpoint is given in [5]. There the 'multivector derivative' was advocated as a valuable tool for extracting conserved quantities from Lagrangians.

Plane-Wave States

In most applications of the Dirac theory, the external fields applied to the electron define a rest-frame, which is taken to be the γ_0-frame. The rotor R then decomposes relative to the γ_0 vector into a boost L and a rotation Φ,

$$R = L\Phi, \tag{3.58}$$

where

$$L^\dagger = L \tag{3.59}$$
$$\Phi^\dagger = \tilde{\Phi} \tag{3.60}$$

and $L\tilde{L} = \Phi\tilde{\Phi} = 1$. A positive-energy plane-wave state is defined by

$$\psi = \psi_0 e^{-i\sigma_3 p\cdot x} \tag{3.61}$$

where ψ_0 is a constant spinor. From the Dirac equation (3.44) with $A = 0$, it follows that ψ_0 satisfies

$$p\psi_0 = m\psi_0\gamma_0. \tag{3.62}$$

Postmultiplying by $\tilde{\psi}_0$ we see that

$$p\psi\tilde{\psi} = mJ \tag{3.63}$$

from which it follows that $\exp(i\beta) = \pm 1$. Since p has positive energy we must take the positive solution ($\beta = 0$). It follows that ψ_0 is just a rotor with a normalisation constant. The boost L determines the momentum by

$$p = mL\gamma_0\tilde{L} = mL^2\gamma_0, \tag{3.64}$$

which is solved by

$$L = \sqrt{p\gamma_0/m} = \frac{E + m + \boldsymbol{p}}{\sqrt{2m(E+m)}}, \tag{3.65}$$

where

$$p\gamma_0 = E + \boldsymbol{p}. \tag{3.66}$$

The Pauli rotor Φ determines the 'comoving' spin bivector $\Phi i\sigma_3\tilde{\Phi}$. This is boosted by L to give the spin S as seen in the laboratory frame. A $\Phi\sigma_3\tilde{\Phi}$ gives the relative spin in the rest-frame of the particle, we refer to this as the 'rest-spin'. In Section 6.3 we show that the rest-spin is equivalent to the 'polarisation' vector defined in the traditional matrix formulation.

Negative energy solutions are constructed in a similar manner, but with an additional factor of i or σ_3 on the right (the choice of which to use is simply a choice of phase). The usual positive- and negative-energy basis states employed in scattering theory are (following the conventions of Itzykson & Zuber [36, Section 2-2])

$$\text{positive energy} \qquad \psi^{(+)}(x) = u_r(p)e^{-i\sigma_3 p\cdot x} \tag{3.67}$$

$$\text{negative energy} \qquad \psi^{(-)}(x) = v_r(p)e^{i\sigma_3 p\cdot x} \tag{3.68}$$

with

$$u_r(p) = L(p)\chi_r \tag{3.69}$$

$$v_r(p) = L(p)\chi_r\sigma_3. \tag{3.70}$$

Here $L(p)$ is given by equation (3.65) and $\chi_r = \{1, -i\sigma_2\}$ are spin basis states. The decomposition into a boost and a rotor turns out to be very useful in scattering theory, as is demonstrated in Section 5.

The main results for Dirac operators and spinors are summarised in Table 4.

4 Operators, Monogenics and the Hydrogen Atom

So far, we have seen how the STA enables us to formulate the Dirac equation entirely in the real geometric algebra of spacetime. In so doing, one might worry that contact has been lost with traditional, operator-based techniques, but in fact this is not the case. Operator techniques are easily handled within the STA, and the use of a coordinate-free language greatly simplifies manipulations. The STA furthermore provides a sharper distinction between the roles of scalar and vector operators.

Dirac Matrices

$$\hat{\gamma}_0 = \begin{pmatrix} I & 0 \\ 0 & -I \end{pmatrix} \quad \hat{\gamma}_k = \begin{pmatrix} 0 & -\hat{\sigma}_k \\ \hat{\sigma}_k & 0 \end{pmatrix} \quad \hat{\gamma}_5 = \begin{pmatrix} 0 & I \\ I & 0 \end{pmatrix}$$

Spinor Equivalence

$$|\psi\rangle = \begin{pmatrix} a^0 + ja^3 \\ -a^2 + ja^1 \\ b^0 + jb^3 \\ -b^2 + jb^1 \end{pmatrix} \leftrightarrow \psi = \begin{matrix} a^0 + a^k i\sigma_k + \\ (b^0 + b^k i\sigma_k)\sigma_3 \end{matrix}$$

Operator Equivalences

$$\begin{aligned} \hat{\gamma}_\mu|\psi\rangle &\leftrightarrow \gamma_\mu \psi \gamma_0 \\ j|\psi\rangle &\leftrightarrow \psi i\sigma_3 \\ \hat{\gamma}_5|\psi\rangle &\leftrightarrow \psi\sigma_3 \\ \langle\bar{\psi}|\psi'\rangle &\leftrightarrow \langle\tilde{\psi}\psi'\rangle_S \end{aligned}$$

Dirac Equation

$$\nabla\psi i\sigma_3 - eA\psi = m\psi\gamma_0$$

Observables

$$\begin{aligned} \rho e^{i\beta} &= \psi\tilde{\psi} \quad & J &= \psi\gamma_0\tilde{\psi} \\ S &= \psi i\sigma_3\tilde{\psi} \quad & s &= \psi\gamma_3\tilde{\psi} \end{aligned}$$

Plane-Wave States

$$\begin{aligned} &\psi^{(+)}(x) = L(p)\Phi e^{-i\sigma_3 p\cdot x} \\ &\psi^{(-)}(x) = L(p)\Phi\sigma_3 e^{i\sigma_3 p\cdot x} \\ &L(p) = (p\gamma_0 + m)/\sqrt{2m(E+m)} \end{aligned}$$

Table 4: *Summary of the main results for the STA representation of Dirac spinors. The matrices and spinor equivalence are for the Dirac-Pauli representation. The spinor equivalences for other representations are constructed via the method outlined in the text.*

This section begins by constructing a Hamiltonian form of the Dirac equation. The standard split into even and odd operators then enables a smooth transition to the non-relativistic Pauli theory. We next study central fields and construct angular-momentum operators that commute with the Hamiltonian. These lead naturally to the construction of the spherical *monogenics*, a basis set of orthogonal eigenfunctions of the angular-momentum operators. We finally apply these techniques to two problems — the Hydrogen atom, and the Dirac 'oscillator'.

4.1 Hamiltonian Form and the Non-Relativistic Reduction

The problem of how to best formulate operator techniques within the STA is really little more than a question of finding a good notation. We could of course borrow the traditional Dirac 'bra-ket' notation, but we have already seen that the bilinear covariants are better handled without it. It is easier instead to just juxtapose the operator and the wavefunction on which it acts. But we saw in Section 3 that the STA operators often act double-sidedly on the spinor ψ. This is not a problem, as the only permitted right-sided operations are multiplication by γ_0 or $i\sigma_3$, and these operations commute. Our notation can therefore safely suppress these right-sided multiplications and lump all operations on the left. The overhat notation is useful to achieve this and we define

$$\hat{\gamma}_\mu \psi \equiv \gamma_\mu \psi \gamma_0. \tag{4.1}$$

It should be borne in mind that all operations are now defined in the STA, so the $\hat{\gamma}_\mu$ are not intended to be matrix operators, as they were in Section 3.2.

It is also useful to have a symbol for the operation of right-sided multiplication by $i\sigma_3$. The symbol j carries the correct connotations of an operator that commutes with all others and squares to -1, and we define

$$j\psi \equiv \psi i\sigma_3. \tag{4.2}$$

The Dirac equation (3.44) can now be written in the 'operator' form

$$j\hat{\nabla}\psi - e\hat{A}\psi = m\psi. \tag{4.3}$$

where

$$\hat{\nabla}\psi \equiv \nabla\psi\gamma_0, \quad \text{and} \quad \hat{A}\psi \equiv A\psi\gamma_0. \tag{4.4}$$

Writing the Dirac equation in the form (4.3) does not add anything new, but does confirm that we have an efficient notation for handling operators in the STA.

In many applications we require a Hamiltonian form of the Dirac equation. To express the Dirac equation (3.44) in Hamiltonian form we simply multiply from the left by γ_0. The resulting equation, with the dimensional constants temporarily put back in, is

$$j\hbar\partial_t\psi = c\hat{\boldsymbol{p}}\psi + eV\psi - ce\boldsymbol{A}\psi + mc^2\bar{\psi} \tag{4.5}$$

where

$$\begin{aligned} \hat{\boldsymbol{p}}\psi &\equiv -j\hbar\boldsymbol{\nabla}\psi & (4.6)\\ \bar{\psi} &\equiv \gamma_0\psi\gamma_0 & (4.7)\\ \text{and} \qquad \gamma_0 A &= V - c\boldsymbol{A}. & (4.8) \end{aligned}$$

Choosing a Hamiltonian is a non-covariant operation, since it picks out a preferred timelike direction. The Hamiltonian relative to the γ_0 direction is the operator on the right-hand side of equation (4.5). We write this operator with the symbol $\mathcal{H}$.

The Pauli Equation

As a first application, we consider the non-relativistic reduction of the Dirac equation. In most modern texts, the non-relativistic approximation is carried out via the Foldy-Wouthuysen transformation [34, 36]. Whilst the theoretical motivation for this transformation is clear, it has the defect that the wavefunction is transformed by a unitary operator which is very hard to calculate in all but the simplest cases. A simpler approach, dating back to Feynman [41], is to separate out the fast-oscillating component of the waves and then split into separate equations for the Pauli-even and Pauli-odd components of ψ. Thus we write (with $\hbar = 1$ and the factors of c kept in)

$$\psi = (\phi + \eta)e^{-i\sigma_3 mc^2 t} \tag{4.9}$$

where $\bar{\phi} = \phi$ and $\bar{\eta} = -\eta$. The Dirac equation (4.5) now splits into the two equations

$$\begin{aligned} \mathcal{E}\phi - c\mathcal{O}\eta &= 0 & (4.10)\\ (\mathcal{E} + 2mc^2)\eta - c\mathcal{O}\phi &= 0, & (4.11) \end{aligned}$$

where

$$\mathcal{E}\phi \equiv (j\partial_t - eV)\phi \tag{4.12}$$
$$\mathcal{O}\phi \equiv (\hat{\boldsymbol{p}} - e\boldsymbol{A})\phi. \tag{4.13}$$

The formal solution to the second equation (4.11) is

$$\eta = \frac{1}{2mc}\left(1 + \frac{\mathcal{E}}{2mc^2}\right)^{-1}\mathcal{O}\phi, \tag{4.14}$$

where the inverse on the right-hand side is understood to denote a power series. The power series is well-defined in the non-relativistic limit as the $\mathcal{E}$ operator is of the order of the non-relativistic energy. The remaining equation for ϕ is

$$\mathcal{E}\phi - \frac{\mathcal{O}}{2m}\left(1 - \frac{\mathcal{E}}{2mc^2} + \cdots\right)\mathcal{O}\phi = 0, \tag{4.15}$$

which can be expanded out to the desired order of magnitude. There is little point in going beyond the first relativistic correction, so we approximate (4.15) by

$$\mathcal{E}\phi + \frac{\mathcal{O}\mathcal{E}\mathcal{O}}{4m^2c^2}\phi = \frac{\mathcal{O}^2}{2m}\phi. \tag{4.16}$$

We seek an equation of the form $\mathcal{E}\phi = \mathcal{H}\phi$, where $\mathcal{H}$ is the non-relativistic Hamiltonian. We therefore need to replace the $\mathcal{O}\mathcal{E}\mathcal{O}$ term in equation (4.16) by a term that does not involve $\mathcal{E}$. To do so we would like to utilise the approximate result that

$$\mathcal{E}\phi \approx \frac{\mathcal{O}^2}{2m}\phi, \tag{4.17}$$

but we cannot use this result directly in the $\mathcal{O}\mathcal{E}\mathcal{O}$ term since the $\mathcal{E}$ does not operate directly on ϕ. Instead we employ the operator rearrangement

$$2\mathcal{O}\mathcal{E}\mathcal{O} = [\mathcal{O}, [\mathcal{E}, \mathcal{O}]] + \mathcal{E}\mathcal{O}^2 + \mathcal{O}^2\mathcal{E} \tag{4.18}$$

to write equation (4.16) in the form

$$\mathcal{E}\phi = \frac{\mathcal{O}^2}{2m}\phi - \frac{\mathcal{E}\mathcal{O}^2 + \mathcal{O}^2\mathcal{E}}{8m^2c^2}\phi - \frac{1}{8m^2c^2}[\mathcal{O}, [\mathcal{E}, \mathcal{O}]]\phi. \tag{4.19}$$

We can now make use of (4.17) to write

$$\mathcal{E}\mathcal{O}^2\phi \approx \mathcal{O}^2\mathcal{E}\phi \approx \frac{\mathcal{O}^4}{2m} + \mathrm{O}(c^{-2}) \tag{4.20}$$

and so approximate (4.16) by

$$\mathcal{E}\phi = \frac{\mathcal{O}^2}{2m}\phi - \frac{1}{8m^2c^2}[\mathcal{O},[\mathcal{E},\mathcal{O}]]\phi - \frac{\mathcal{O}^4}{8m^3c^2}\phi, \tag{4.21}$$

which is valid to order c^{-2}. The commutators are easily evaluated, for example

$$[\mathcal{E},\mathcal{O}] = -je(\partial_t \boldsymbol{A} + \boldsymbol{\nabla}V) = je\boldsymbol{E}. \tag{4.22}$$

There are no time derivatives left in this commutator, so we do achieve a sensible non-relativistic Hamiltonian. The full commutator required in equation (4.21) is

$$\begin{aligned}[\mathcal{O},[\mathcal{E},\mathcal{O}]] &= [-j\boldsymbol{\nabla} - e\boldsymbol{A}, je\boldsymbol{E}] \\ &= (e\boldsymbol{\nabla}\boldsymbol{E}) - 2e\boldsymbol{E}\wedge\boldsymbol{\nabla} - 2je^2\boldsymbol{A}\wedge\boldsymbol{E}\end{aligned} \tag{4.23}$$

in which the STA formulation ensures that we are manipulating spatial vectors, rather than performing abstract matrix manipulations.

The various operators (4.12), (4.13) and (4.23) can now be fed into equation (4.21) to yield the STA form of the Pauli equation

$$\begin{aligned}\partial_t\phi i\sigma_3 &= \frac{1}{2m}(\hat{\boldsymbol{p}} - e\boldsymbol{A})^2\phi + eV\phi - \frac{\hat{\boldsymbol{p}}^4}{8m^3c^2}\phi \\ &\quad -\frac{1}{8m^2c^2}[e(\boldsymbol{\nabla}\boldsymbol{E} - 2\boldsymbol{E}\wedge\boldsymbol{\nabla})\phi - 2e^2\boldsymbol{A}\wedge\boldsymbol{E}\phi i\sigma_3],\end{aligned} \tag{4.24}$$

which is valid to $\mathrm{O}(c^{-2})$. (We have assumed that $|\boldsymbol{A}| \sim c^{-1}$ to replace the $\mathcal{O}^4$ term by $\hat{\boldsymbol{p}}^4$.) Using the translation scheme of Table 2 it is straightforward to check that equation (4.24) is the same as that found in standard texts [34]. In the standard approach, the geometric product in the $\boldsymbol{\nabla}\boldsymbol{E}$ term (4.24) is split into a 'spin-orbit' term $\boldsymbol{\nabla}\wedge\boldsymbol{E}$ and the 'Darwin' term $\boldsymbol{\nabla}\cdot\boldsymbol{E}$. The STA approach reveals that these terms arise from a single source.

A similar approximation scheme can be adopted for the observables of the Dirac theory. For example the current, $\psi\gamma_0\tilde{\psi}$, has a three-vector part

$$\boldsymbol{J} = (\psi\gamma_0\tilde{\psi})\wedge\gamma_0 = \phi\eta^\dagger + \eta\phi^\dagger, \tag{4.25}$$

which is approximated to first-order by

$$\boldsymbol{J} \approx -\frac{1}{m}(\langle \boldsymbol{\nabla}\phi i\sigma_3\phi^\dagger\rangle_v - \boldsymbol{A}\phi\phi^\dagger). \tag{4.26}$$

Not all applications of the Pauli theory correctly identify (4.26) as the conserved current in the Pauli theory — an inconsistency first noted by Hestenes and Gurtler [13] (see also the discussion in [6]).

4.2 Angular Eigenstates and Monogenic Functions

Returning to the Hamiltonian of equation (4.5), let us now consider the problem of a central potential $V = V(r)$, $\boldsymbol{A} = 0$, where $r = |\boldsymbol{x}|$. We seek a set of angular-momentum operators which commute with this Hamiltonian. Starting with the scalar operator $B\cdot(\boldsymbol{x}\wedge\boldsymbol{\nabla})$, where B is a spatial bivector, we find that

$$\begin{aligned}[B\cdot(\boldsymbol{x}\wedge\boldsymbol{\nabla}), \mathcal{H}] &= [B\cdot(\boldsymbol{x}\wedge\boldsymbol{\nabla}), -j\boldsymbol{\nabla}] \\ &= j\dot{\boldsymbol{\nabla}}B\cdot(\dot{\boldsymbol{x}}\wedge\boldsymbol{\nabla}) \\ &= -jB\cdot\boldsymbol{\nabla}. \end{aligned} \tag{4.27}$$

But, since $B\cdot\boldsymbol{\nabla} = [B, \boldsymbol{\nabla}]/2$ and B commutes with the rest of $\mathcal{H}$, we can rearrange the commutator into

$$[B\cdot(\boldsymbol{x}\wedge\boldsymbol{\nabla}) - \tfrac{1}{2}B, \mathcal{H}] = 0, \tag{4.28}$$

which gives us the required operator. Since $B\cdot(\boldsymbol{x}\wedge\boldsymbol{\nabla}) - B/2$ is an anti-Hermitian operator, we define a set of Hermitian operators as

$$J_B \equiv j(B\cdot(\boldsymbol{x}\wedge\boldsymbol{\nabla}) - \tfrac{1}{2}B). \tag{4.29}$$

The extra term of $\frac{1}{2}B$ is the term that is conventionally viewed as defining 'spin-1/2'. However, the geometric algebra derivation shows that the result rests solely on the commutation properties of the $B\cdot(\boldsymbol{x}\wedge\boldsymbol{\nabla})$ and $\boldsymbol{\nabla}$ operators. Furthermore, the factor of one-half required in the J_B operators would be present in a space of any dimension. It follows that the factor of one-half in (4.29) cannot have anything to do with representations of the 3-D rotation group.

From the STA point of view, J_B is an operator-valued function of the bivector B. In conventional quantum theory, however, we would view the angular-momentum

operator as a vector with components

$$\hat{J}_i = \hat{L}_i + \tfrac{1}{2}\hat{\Sigma}_i \tag{4.30}$$

where $\hat{\Sigma}_i = (j/2)\epsilon_{ijk}\hat{\gamma}_j\hat{\gamma}_k$. The standard notation takes what should be viewed as the sum of a scalar operator and a bivector, and forces it to look like the sum of two vector operators! As well as being conceptually clearer, the STA approach is easier to compute with. For example, it is a simple matter to establish the commutation relation

$$[J_{B_1}, J_{B_2}] = -jJ_{B_1\times B_2}, \tag{4.31}$$

which forms the starting point for the representation theory of the angular-momentum operators.

The Spherical Monogenics

The key ingredients in the solution of the Dirac equation for problems with radial symmetry are the spherical monogenics. These are Pauli spinors (even elements of the Pauli algebra (2.28)) which satisfy the eigenvalue equation

$$-\boldsymbol{x}\wedge\boldsymbol{\nabla}\psi = l\psi. \tag{4.32}$$

Such functions are called spherical monogenics because they are obtained from the 'monogenic equation'

$$\boldsymbol{\nabla}\Psi = 0 \tag{4.33}$$

by separating Ψ into $r^l\psi(\theta,\phi)$. Equation (4.33) generalises the concept of an analytic function to higher dimensions [12, 7].

To analyse the properties of equation (4.32) we first note that

$$[J_B, \boldsymbol{x}\wedge\boldsymbol{\nabla}] = 0, \tag{4.34}$$

which is proved in the same manner as equation (4.28). It follows that ψ can simultaneously be an eigenstate of the $\boldsymbol{x}\wedge\boldsymbol{\nabla}$ operator and one of the J_B operators. To simplify the notation we now define

$$J_k\psi \equiv J_{i\sigma_k}\psi = (i\sigma_k\cdot(\boldsymbol{x}\wedge\boldsymbol{\nabla}) - \tfrac{1}{2}i\sigma_k)\psi i\sigma_3. \tag{4.35}$$

We choose ψ to be an eigenstate of J_3, and provisionally write

$$-\boldsymbol{x}\wedge\boldsymbol{\nabla}\psi = l\psi, \qquad J_3\psi = \mu\psi. \tag{4.36}$$

Before proceeding, we must introduce some notation for a spherical-polar coordinate system. We define the $\{r,\theta,\phi\}$ coordinates via

$$r \equiv \sqrt{\boldsymbol{x}^2}, \qquad \cos\theta \equiv \sigma_3\cdot\boldsymbol{x}/r, \qquad \tan\phi \equiv \sigma_2\cdot\boldsymbol{x}/\sigma_1\cdot\boldsymbol{x}. \tag{4.37}$$

The associated coordinate frame is

$$\begin{aligned} \boldsymbol{e}_r &= \sin\theta(\cos\phi\,\sigma_1 + \sin\phi\,\sigma_2) + \cos\theta\,\sigma_3 \\ \boldsymbol{e}_\theta &= r\cos\theta(\cos\phi\,\sigma_1 + \sin\phi\,\sigma_2) - r\sin\theta\,\sigma_3 \\ \boldsymbol{e}_\phi &\equiv r\sin\theta(-\sin\phi\,\sigma_1 + \cos\phi\,\sigma_2). \end{aligned} \tag{4.38}$$

From these we define the orthonormal vectors $\{\sigma_r,\sigma_\theta,\sigma_\phi\}$ by

$$\begin{aligned} \sigma_r &\equiv \boldsymbol{e}_r \\ \sigma_\theta &\equiv \boldsymbol{e}_\theta/r \\ \sigma_\phi &\equiv \boldsymbol{e}_\phi/(r\sin\theta). \end{aligned} \tag{4.39}$$

The $\{\sigma_r,\sigma_\theta,\sigma_\phi\}$ form a right-handed set, since

$$\sigma_r\sigma_\theta\sigma_\phi = i. \tag{4.40}$$

The vector σ_r satisfies

$$\boldsymbol{x}\wedge\boldsymbol{\nabla}\sigma_r = 2\sigma_r. \tag{4.41}$$

It follows that

$$-\boldsymbol{x}\wedge\boldsymbol{\nabla}(\sigma_r\psi\sigma_3) = -(l+2)\sigma_r\psi\sigma_3 \tag{4.42}$$

so, without loss of generality, we can choose l to be positive and recover the negative-l states through multiplying by σ_r. In addition, since

$$\boldsymbol{x}\wedge\boldsymbol{\nabla}(\boldsymbol{x}\wedge\boldsymbol{\nabla}\psi) = l^2\psi \tag{4.43}$$

we find that

$$\frac{1}{\sin\theta}\frac{\partial}{\partial\theta}\left(\sin\theta\frac{\partial\psi}{\partial\theta}\right) + \frac{1}{\sin^2\theta}\frac{\partial^2\psi}{\partial\phi^2} = -l(l+1)\psi. \tag{4.44}$$

Hence, with respect to a constant basis for the STA, the components of ψ are spherical harmonics and l must be an integer for any physical solution.

The next step is to introduce ladder operators to move between different J_3 eigenstates. The required analysis is standard, and has been relegated to Appendix A. The conclusions are that, for each value of l, the allowed values of the eigenvalues of J_3 range from $(l + 1/2)$ to $-(l + 1/2)$. The total degeneracy is therefore $2(l + 1)$. The states can therefore be labeled by two *integers* l and m such that

$$-\boldsymbol{x}\wedge\boldsymbol{\nabla}\psi_l^m = l\psi_l^m \qquad l \geq 0 \tag{4.45}$$

$$J_3\psi_l^m = (m + \tfrac{1}{2})\psi_l^m \qquad -1 - l \leq m \leq l. \tag{4.46}$$

Labelling the states in this manner is unconventional, but provides for many simplifications in describing the properties of the ψ_l^m.

To find an explicit expression for the ψ_l^m we start from the highest-m eigenstate, which is given by

$$\psi_l^l = \sin^l\theta\, e^{l\phi i\sigma_3}, \tag{4.47}$$

and act on this with the lowering operator J_-. This procedure is described in detail in Appendix A. The result is the following, remarkably compact formula:

$$\psi_l^m = [(l + m + 1)P_l^m(\cos\theta) - P_l^{m+1}(\cos\theta)i\sigma_\phi]e^{m\phi i\sigma_3}, \tag{4.48}$$

where the associated Legendre polynomials follow the conventions of Gradshteyn & Ryzhik [43]. The expression (4.48) offers a considerable improvement over formulae found elsewhere in terms of both compactness and ease of use. The formula (4.48) is valid for non-negative l and both signs of m. The positive and negative m-states are related by

$$\psi_l^m(-i\sigma_2) = (-1)^m\frac{(l + m + 1)!}{(l - m)!}\psi_l^{-(m+1)}. \tag{4.49}$$

The negative-l states are constructed using (4.42) and the J_3 eigenvalues are unchanged by this construction. The possible eigenvalues and degeneracies are summarised in Table 5. One curious feature of this table is that we appear to be missing a line for the eigenvalue $l = -1$. In fact solutions for this case do exist, but they contain singularities which render them unnormalisable. For example, the functions

$$\frac{i\sigma_\phi}{\sin\theta}, \qquad \text{and} \qquad \frac{e^{-i\sigma_3\phi}}{\sin\theta} \tag{4.50}$$

l	Eigenvalues of J_3	Degeneracy
$\vdots$	$\vdots$	$\vdots$
2	$5/2 \cdots -5/2$	6
1	$3/2 \cdots -3/2$	4
0	$1/2 \cdots -1/2$	2
(-1)	?	?
-2	$1/2 \cdots -1/2$	2
$\vdots$	$\vdots$	$\vdots$

Table 5: *Eigenvalues and degeneracies for the ψ_l^m monogenics.*

have $l = -1$ and J_3 eigenvalues $+1/2$ and $-1/2$ respectively. Both solutions are singular along the z-axis, however, so are of limited physical interest.

4.3 Applications

Having established the properties of the spherical monogenics, we can proceed quickly to the solution of various problems. We have chosen to consider two — the standard case of the Hydrogen atom, and the 'Dirac Oscillator' [44].

The Coulomb Problem

The Hamiltonian for this problem is

$$\mathcal{H}\psi = \hat{\boldsymbol{p}}\psi - \frac{Z\alpha}{r}\psi + m\bar{\psi}, \tag{4.51}$$

where $\alpha = e^2/4\pi$ is the fine-structure constant and Z is the atomic charge. Since the J_B operators commute with $\mathcal{H}$, ψ can be placed in an eigenstate of J_3. The operator J_iJ_i must also commute with $\mathcal{H}$, but $\boldsymbol{x}\wedge\boldsymbol{\nabla}$ does not, so both the ψ_l^m and $\sigma_r\psi_l^m\sigma_3$ monogenics are needed in the solution.

Though $\boldsymbol{x}\wedge\boldsymbol{\nabla}$ does not commute with $\mathcal{H}$, the operator

$$K = \hat{\gamma}_0(1 - \boldsymbol{x}\wedge\boldsymbol{\nabla}) \tag{4.52}$$

does, as follows from

$$\begin{aligned}[\hat{\gamma}_0(1-\boldsymbol{x}\wedge\boldsymbol{\nabla}),\boldsymbol{\nabla}] &= 2\hat{\gamma}_0\boldsymbol{\nabla}-\hat{\gamma}_0\dot{\boldsymbol{\nabla}}\dot{\boldsymbol{x}}\wedge\boldsymbol{\nabla}\\ &= 0. \end{aligned} \tag{4.53}$$

We can therefore work with eigenstates of the K operator, which means that the spatial part of ψ goes either as

$$\psi(\boldsymbol{x},l+1)=\psi_l^m u(r)+\sigma_r\psi_l^m v(r)i\sigma_3 \tag{4.54}$$

or as

$$\psi(\boldsymbol{x},-(l+1))=\sigma_r\psi_l^m\sigma_3 u(r)+\psi_l^m iv(r). \tag{4.55}$$

In both cases the second label in $\psi(\boldsymbol{x},l+1)$ specifies the eigenvalue of K. The functions $u(r)$ and $v(r)$ are initially 'complex' superpositions of a scalar and an $i\sigma_3$ term. It turns out, however, that the scalar and $i\sigma_3$ equations decouple, and it is sufficient to treat $u(r)$ and $v(r)$ as scalars.

We now insert the trial functions (4.54) and (4.55) into the Hamiltonian (4.51). Using the results that

$$-\boldsymbol{\nabla}\psi_l^m=l/r\,\sigma_r\psi_l^m,\qquad -\boldsymbol{\nabla}\sigma_r\psi_l^m=-(l+2)/r\,\psi_l^m, \tag{4.56}$$

and looking for stationary-state solutions of energy E, the radial equations reduce to

$$\begin{pmatrix} u' \\ v' \end{pmatrix}=\begin{pmatrix} (\kappa-1)/r & -(E+Z\alpha/r+m) \\ E+Z\alpha/r-m & (-\kappa-1)/r \end{pmatrix}\begin{pmatrix} u \\ v \end{pmatrix}, \tag{4.57}$$

where κ is the eigenvalue of K. (κ is a non-zero positive or negative integer.) The solution of these radial equations can be found in many textbooks (see, for example, [34, 36, 45]). The solutions can be given in terms of confluent hypergeometric functions, and the energy spectrum is obtained from the equation

$$E^2=m^2\left[1-\frac{(Z\alpha)^2}{n^2+2n\nu+(l+1)^2}\right], \tag{4.58}$$

where n is a positive integer and

$$\nu=[(l+1)^2+(Z\alpha)^2]^{1/2}. \tag{4.59}$$

Whilst this analysis does not offer any new results, it should demonstrate how

easy it is to manipulate expressions involving the spherical monogenics.

The Dirac 'Oscillator'

The equation describing a Dirac 'oscillator' was introduced as recently as 1989 [44]. The equation is one for a chargeless particle with an anomalous magnetic moment [34] which, in the STA, takes the form

$$\nabla\psi i\sigma_3 - i\mu F\psi\gamma_3 = m\psi\gamma_0. \tag{4.60}$$

This equation will be met again in Section 8, where it is used to analyse the effects of a Stern-Gerlach apparatus. The situation describing the Dirac oscillator is one where the F field exerts a linear, confining force described by

$$F = \frac{m\omega}{\mu}\boldsymbol{x}. \tag{4.61}$$

The Hamiltonian in this case is

$$\mathcal{H}\psi = \hat{\boldsymbol{p}}\psi - jm\omega\boldsymbol{x}\bar{\psi} + m\bar{\psi}. \tag{4.62}$$

It is a simple matter to verify that this Hamiltonian commutes with both the J_B and K operators defined above, so we can again take the wavefunction to be of the form of equations (4.54) and (4.55). The resulting equations in this case are

$$\begin{pmatrix} u' \\ v' \end{pmatrix} = \begin{pmatrix} (\kappa-1)/r - m\omega r & -(E+m) \\ E-m & (-\kappa-1)/r + m\omega r \end{pmatrix} \begin{pmatrix} u \\ v \end{pmatrix}. \tag{4.63}$$

The equations are simplified by transforming to the dimensionless variable ρ,

$$\rho \equiv (m\omega)^{1/2} r, \tag{4.64}$$

and removing the asymptotic behaviour via

$$u = \rho^l e^{-\rho^2/2} u_1 \tag{4.65}$$

$$v = \rho^l e^{-\rho^2/2} u_2. \tag{4.66}$$

The analysis is now slightly different for the positive- and negative-κ equations, which we consider in turn.

Positive-κ. The equations reduce to

$$\frac{d}{d\rho}\begin{pmatrix} u_1 \\ u_2 \end{pmatrix} = \begin{pmatrix} 0 & -(E+m)/\sqrt{m\omega} \\ (E-m)/\sqrt{m\omega} & -2(l+1)/\rho + 2\rho \end{pmatrix}\begin{pmatrix} u_1 \\ u_2 \end{pmatrix}, \tag{4.67}$$

which are solved with the power series

$$u_1 = \sum_{n=0} A_n \rho^{2n} \tag{4.68}$$

$$u_2 = \sum_{n=0} B_n \rho^{2n+1}. \tag{4.69}$$

The recursion relations are

$$2nA_n = -\frac{E+m}{\sqrt{m\omega}} B_{n-1} \tag{4.70}$$

$$(2n+2l+3)B_n = \frac{E-m}{\sqrt{m\omega}} A_n + 2B_{n-1}, \tag{4.71}$$

and the requirement that the series terminate produces the eigenvalue spectrum

$$E^2 - m^2 = 4nm\omega \qquad n = 1, 2 \ldots \tag{4.72}$$

Remarkably, the energy levels do not depend on l, so are infinitely degenerate!

Negative-κ. In this case the equations reduce to

$$\frac{d}{d\rho}\begin{pmatrix} u_1 \\ u_2 \end{pmatrix} = \begin{pmatrix} -2(l+1)/\rho & -(E+m)/\sqrt{m\omega} \\ (E-m)/\sqrt{m\omega} & 2\rho \end{pmatrix}\begin{pmatrix} u_1 \\ u_2 \end{pmatrix}, \tag{4.73}$$

and are solved with the power series

$$u_1 = \sum_{n=0} A_n \rho^{2n+1} \tag{4.74}$$

$$u_2 = \sum_{n=0} B_n \rho^{2n}. \tag{4.75}$$

The recursion relations become

$$(2n+2l+3)A_n = -\frac{E+m}{\sqrt{m\omega}} B_n \tag{4.76}$$

$$2nB_n = \frac{E-m}{\sqrt{m\omega}} A_{n-1} + 2B_{n-1}, \tag{4.77}$$

and this time the eigenvalues are given by the formula

$$E^2 - m^2 = 2(2n + 2l + 1)m\omega \qquad n = 1, 2 \ldots . \tag{4.78}$$

The energy spectrum only contains E through equations for E^2. It follows that both positive and negative energies are allowed. The lowest positive-energy state (the ground state) has $E^2 = m^2 + 4m\omega$, leading to a non-relativistic energy of $\sim 2\hbar\omega$. The groundstate is infinitely degenerate, whereas the first excited state has a degeneracy of two. The energy spectrum is clearly quite bizarre and does not correspond to any sensible physical system. In particular, this system does not reduce to a simple harmonic oscillator in the non-relativistic limit. The simple, if bizarre, nature of the energy spectrum is obscured in other approaches [44, 46], which choose a less clear labeling system for the eigenstates.

5 Propagators and Scattering Theory

In this section we give a brief review of how problems requiring propagators are formulated and solved in the STA. The STA permits a first-order form of both Maxwell and Dirac theories involving the same differential operator — the vector derivative ∇. The key problem is to find Green's functions for the vector derivative that allow us to propagate initial data off some surface. We therefore start by studying the characteristic surfaces of the vector derivative. We then turn to the use of spinor potentials, which were dealt with in greater detail in [6]. The section concludes with a look at single-particle scattering theory. Using the mappings established in Sections 3 and 4 it is a simple matter to reformulate in the STA the standard matrix approach to scattering problems as described in [34, 36]. The STA approach allows for a number of improvements, however, particularly in the treatment of spin. This is a subject which was first addressed by Hestenes [47], and our presentation closely follows his work.

5.1 Propagation and Characteristic Surfaces

One of the simplest demonstrations of the insights provided by the STA formulation of both Maxwell and Dirac theories is in the treatment of characteristic surfaces. In the second-order theory, characteristic surfaces are usually found by algebraic methods. Here we show how the same results can be found using a simple geometric argument applied to first-order equations. Suppose, initially, that we have a generic

equation of the type

$$\nabla\psi = f(\psi, x), \tag{5.1}$$

where $\psi(x)$ is any multivector field (not necessarily a spinor field) and $f(\psi, x)$ is some arbitrary, known function. If we are given initial data over some 3-D surface are there any obstructions to us propagating this information off the surface? If so, the surface is a characteristic surface. We start at a point on the surface and pick three independent vectors $\{a, b, c\}$ tangent to the surface at the chosen point. Knowledge of ψ on the surface enables us to calculate

$$a\cdot\nabla\psi, \quad b\cdot\nabla\psi \quad \text{and} \quad c\cdot\nabla\psi. \tag{5.2}$$

We next form the trivector $a\wedge b\wedge c$ and dualise to define

$$n \equiv ia\wedge b\wedge c. \tag{5.3}$$

We can now multiply equation (5.1) by n and use

$$\begin{aligned} n\nabla\psi &= n\cdot\nabla\psi + n\wedge\nabla\psi \\ &= n\cdot\nabla\psi + i(a\wedge b\wedge c)\cdot\nabla\psi \qquad (5.4)\\ &= n\cdot\nabla\psi + i(a\wedge b\,c\cdot\nabla\psi - a\wedge c\,b\cdot\nabla\psi + b\wedge c\,a\cdot\nabla\psi), \qquad (5.5)\end{aligned}$$

to obtain

$$n\cdot\nabla\psi = nf(\psi, x) - i(a\wedge b\,c\cdot\nabla\psi - a\wedge c\,b\cdot\nabla\psi + b\wedge c\,a\cdot\nabla\psi). \tag{5.6}$$

All of the terms on the right-hand side of equation (5.6) are known, so we can find $n\cdot\nabla\psi$ and use this to propagate ψ in the n direction (*i.e.* off the surface). The only situation in which we fail to propagate, therefore, is when n remains in the surface. This occurs when

$$\begin{aligned} n\wedge(a\wedge b\wedge c) &= 0 \\ \Longrightarrow \quad n\wedge(ni) &= 0 \\ \Longrightarrow \quad n\cdot n &= 0. \end{aligned} \tag{5.7}$$

Hence we only fail to propagate when $n^2 = 0$, and it follows immediately that the characteristic surfaces of equation (5.1) are *null* surfaces. This result applies to any first-order equation based on the vector derivative ∇, including the Maxwell and

Dirac equations. The fundamental significance of null directions in these theories is transparent in their STA form. Furthermore, the technique extends immediately to a gravitational background, as described in [48].

5.2 Spinor Potentials and Propagators

A simple method to generate propagators for the Dirac theory is to introduce a spinor potential satisfying a scalar second-order equation. Suppose that ψ satisfies the Dirac equation

$$\nabla\psi i\sigma_3 - m\psi\gamma_0 = 0. \tag{5.8}$$

ψ can be generated from the (odd multivector) potential ϕ via

$$\psi = \nabla\phi i\sigma_3 + m\phi\gamma_0 \tag{5.9}$$

provided that

$$(\nabla^2 + m^2)\phi = 0. \tag{5.10}$$

The standard second-order theory can then be applied to ϕ, and then used to recover ψ. In [6] this technique was applied to constant-energy waves

$$\psi = \psi(\boldsymbol{x})e^{-i\sigma_3 Et}. \tag{5.11}$$

The Dirac equation then becomes

$$\boldsymbol{\nabla}\psi i\sigma_3 + E\psi - m\bar{\psi} = 0 \tag{5.12}$$

which is solved by

$$\psi = -\boldsymbol{\nabla}\phi i\sigma_3 + E\phi + m\bar{\phi} \tag{5.13}$$

where

$$\phi(\boldsymbol{x}) = -\frac{1}{4\pi}\oint |dS'|\, \boldsymbol{n}'\psi(\boldsymbol{x}')\frac{e^{i\sigma_3 pr}}{r}. \tag{5.14}$$

In this integral the initial data $\psi(\boldsymbol{x}')$ is given over some closed spatial surface with normal $\boldsymbol{n}' = \boldsymbol{n}(\boldsymbol{x}')$, and p and r are defined by

$$p \equiv \sqrt{E^2 + m^2} \quad \text{and} \quad r \equiv |\boldsymbol{x} - \boldsymbol{x}'|. \tag{5.15}$$

Similar techniques can be applied to the propagation of electromagnetic waves (see [6] for details).

5.3 Scattering Theory

We finish this short section with a brief look at how the matrix approach to scattering theory is handled in the STA, closely following the work of Hestenes [47]. We continue to employ the symbol j for $i\sigma_3$ in places where it simplifies the notation. In particular, we employ the j symbol in the exponential terms introduced by Fourier transforming to momentum space. Where the j's play a more significant geometric role they are left in the $i\sigma_3$ form.

We start by replacing the Dirac equation (3.44) with the integral equation

$$\psi(x) = \psi_i(x) + e \int d^4x' \, S_F(x - x') A(x') \psi(x') \tag{5.16}$$

where ψ_i is the asymptotic in-state which solves the free-particle equation, and $S_F(x - x')$ is the STA form of the Feynman propagator. Substituting (5.16) into the Dirac equation, we find that $S_F(x - x')$ must satisfy

$$\nabla_x S_F(x - x') M(x') i\sigma_3 - m S_F(x - x') M(x') \gamma_0 = \delta(x - x') M(x') \tag{5.17}$$

for an arbitrary multivector $M(x')$. The solution to this equation is

$$S_F(x - x') M(x') = \int \frac{d^4p}{(2\pi)^4} \frac{pM(x') + mM(x')\gamma_0}{p^2 - m^2} e^{-jp\cdot(x - x')} \tag{5.18}$$

where, for causal propagation, the dE integral must arrange that positive-frequency waves propagate into the future ($t > t'$) and negative-frequency waves propagate into the past ($t' > t$). The result of performing the dE integral is

$$\begin{aligned} S_F(x - x')M \;\; = \;\; & -\theta(t - t') \int \frac{d^3\boldsymbol{p}}{(2\pi)^3} \frac{1}{2E} (pM + mM\gamma_0) i\sigma_3 e^{-jp\cdot(x - x')} \\ & + \theta(t' - t) \int \frac{d^3\boldsymbol{p}}{(2\pi)^3} \frac{1}{2E} (pM - mM\gamma_0) i\sigma_3 e^{jp\cdot(x - x')} \end{aligned} \tag{5.19}$$

where $E = +\sqrt{\boldsymbol{p}^2 + m^2}$ and $M = M(x')$.

With $\psi_{\text{diff}}(x)$ defined by

$$\psi_{\text{diff}}(x) \equiv \psi(x) - \psi_i(x) \tag{5.20}$$

we find that, as t tends to $+\infty$, $\psi_{\text{diff}}(x)$ is given by

$$\psi_{\text{diff}}(x) = -e \int d^4x' \int \frac{d^3\boldsymbol{p}}{(2\pi)^3} \frac{1}{2E} [pA(x')\psi(x') + mA(x')\psi(x')\gamma_0] i\sigma_3 e^{-jp\cdot(x-x')}. \tag{5.21}$$

We therefore define a set of final states $\psi_f(x)$ by

$$\psi_f(x) \equiv -e \int \frac{d^4x'}{2E_f} [p_f A(x')\psi(x') + mA(x')\psi(x')\gamma_0] i\sigma_3 e^{-jp_f\cdot(x-x')}, \tag{5.22}$$

which are plane-wave solutions to the free-field equations with momentum p_f. $\psi_{\text{diff}}(x)$ can now be expressed as a superposition of these plane-wave states,

$$\psi_{\text{diff}}(x) = \int \frac{d^3\boldsymbol{p}_f}{(2\pi)^3} \psi_f(x). \tag{5.23}$$

The Born Approximation and Coulomb Scattering

In order to find $\psi_f(x)$ we must evaluate the integral (5.22). In the Born approximation, we simplify the problem by approximating $\psi(x')$ by $\psi_i(x')$. In this case, since

$$\psi_i(x') = \psi_i e^{-jp_i\cdot x'}, \quad \text{and} \quad m\psi_i\gamma_0 = p_i\psi_i, \tag{5.24}$$

we can write

$$\psi_f(x) = -e \int \frac{d^4x'}{2E_f} [p_f A(x') + A(x')p_i]\psi_i i\sigma_3 e^{jq\cdot x'} e^{-jp_f\cdot x}, \tag{5.25}$$

where

$$q \equiv p_f - p_i. \tag{5.26}$$

The integral in (5.25) can now be evaluated for any given A-field.

As a simple application consider Coulomb scattering, for which $A(x')$ is given by

$$A(x') = \frac{Ze}{4\pi|\boldsymbol{x}'|}\gamma_0. \tag{5.27}$$

Inserting this in (5.25) and carrying out the integrals, we obtain

$$\psi_f(x) = -S_{fi}\psi_i i\sigma_3 \frac{(2\pi)^2}{E_f}\delta(E_f - E_i) \tag{5.28}$$

where

$$\begin{aligned} S_{fi} &\equiv \frac{Z\alpha}{4\pi}[p_f\gamma_0 + \gamma_0 p_i]\int d^3x\,\frac{e^{-j\boldsymbol{q}\cdot\boldsymbol{r}}}{r} \\ &= \frac{Z\alpha}{\boldsymbol{q}^2}(2E + \boldsymbol{q}). \end{aligned} \tag{5.29}$$

Here $E = E_f = E_i$ and $\alpha = e^2/(4\pi)$ is the fine-structure constant. The quantity S_{fi} contains all the information about the scattering process. Its magnitude determines the cross-section via [47]

$$\frac{d\sigma}{d\Omega_f} = S_{fi}\tilde{S}_{fi} \tag{5.30}$$

and the remainder of S_{fi} determines the change of momentum and spin vectors. This is clear from (5.28), which shows that S_{fi} must contain the rotor $R_f\tilde{R}_i$, where R_i and R_f are the rotors for the initial and final plane-wave states.

Substituting (5.29) into (5.30) we immediately recover the Mott scattering cross-section

$$\frac{d\sigma}{d\Omega_f} = \frac{Z^2\alpha^2}{\boldsymbol{q}^4}(4E^2 - \boldsymbol{q}^2) = \frac{Z^2\alpha^2}{4\boldsymbol{p}^2\beta^2\sin^4(\theta/2)}\left(1 - \beta^2\sin^2(\theta/2)\right), \tag{5.31}$$

where

$$\boldsymbol{q}^2 = (\boldsymbol{p}_f - \boldsymbol{p}_i)^2 = 2\boldsymbol{p}^2(1 - \cos\theta) \quad \text{and} \quad \beta = |\boldsymbol{p}|/E. \tag{5.32}$$

The notable feature of this derivation is that no spin sums are required. Instead, all the spin dependence is contained in the directional information in S_{fi}. As well as being computationally more efficient, the STA method for organising cross-section calculations offers deeper insights into the structure of the theory. For example, for Mott-scattering the directional information is contained entirely in the quantity [47]

$$S'_{fi} = \frac{1}{m}[p_f\gamma_0 + \gamma_0 p_i] = L_f^2 + \tilde{L}_i^2 \tag{5.33}$$

where L_f and L_i are the boosts contained in R_f and R_i respectively. The algebraic structure

$$S_{fi} = p_f M + M p_i, \tag{5.34}$$

where M is some odd multivector, is common to many scattering problems.

Since S_{fi} contains the quantity $R_f\tilde{R}_i$, we obtain a spatial rotor by removing

the two boost terms. We therefore define the (unnormalised) rotor

$$U'_{fi} \equiv \tilde{L}_f(L_f^2 + \tilde{L}_i^2)L_i = L_f L_i + \tilde{L}_f \tilde{L}_i, \tag{5.35}$$

so that $U_{fi} = U'_{fi}/|U_{fi}|$ determines the rotation from initial to final rest-spins. A simple calculation gives

$$U'_{fi} = 2[(E+m)^2 + \boldsymbol{p}_f \boldsymbol{p}_i], \tag{5.36}$$

hence the rest-spin vector precesses in the $\boldsymbol{p}_f \wedge \boldsymbol{p}_i$ plane through an angle δ, where

$$\tan(\delta/2) = \frac{\sin\theta}{(E+m)/(E-m) + \cos\theta}. \tag{5.37}$$

Whilst the derivations of the Mott scattering formula and the polarisation precession angle are only presented in outline here (further details are contained in [47]) it should be clear that they offer many advantages over the usual derivations [34, 36]. All the features of the scattering are contained in the single multivector S_{fi}, algebraic form of which is very simple. Much work remains, however, if these techniques are to be extended to the whole of QED.

6 Plane Waves at Potential Steps

We now turn to a discussion of the matching of Dirac plane waves at a potential step. The case of perpendicular incidence is a standard problem and is treated in most texts [34, 36, 42]. In order to demonstrate the power of the STA approach we treat the more general case of oblique incidence, adapting an approach used in electrical engineering to analyse the propagation of electromagnetic waves. A number of applications are given as illustrations, including the tunnelling of monochromatic waves and spin precession on total reflection at a barrier. We conclude the section with a discussion of the Klein paradox.

The problem of interest is that of plane waves incident on a succession of potential steps. The steps are taken as lying along the x direction, with infinite extent in the y and z directions. Since the spatial components of the incoming and outgoing wavevectors lie in a single plane, the matching problem can be reduced to one in two dimensions. The analysis is simplified further if the wavevectors are taken to lie in the $i\sigma_3$ plane. (Other configurations can always be obtained by applying a rotation.) The arrangement is illustrated in Figure 6. The waves all

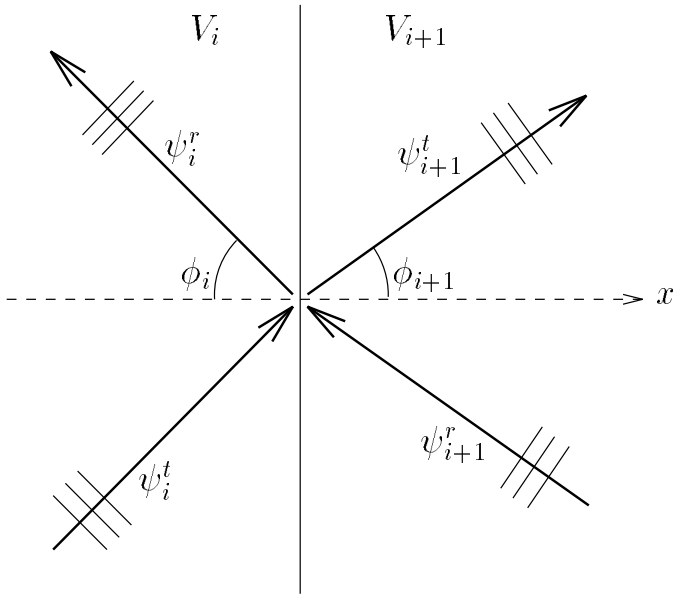

Figure 1: Plane waves at a potential step. The spatial component of the wavevector lies in the x–y plane and the step lies in the y–z plane.

oscillate at a single frequency E, and the Dirac equation in the ith region is

$$(E - eV_i)\psi = -\boldsymbol{\nabla}\psi i\sigma_3 + m\gamma_0\psi\gamma_0. \tag{6.1}$$

By continuity of ψ at each boundary, the y component of the wavevector, p_y, must be the same in all regions. For the ith region we define

$$E_i' \equiv E - eV_i \tag{6.2}$$

and, depending on the magnitude of V_i, the waves in the this region will be either travelling or evanescent. For travelling waves we define (dropping the subscripts)

$$p_x^2 \equiv E'^2 - p_y^2 - m^2 \qquad |E - eV| > \sqrt{p_y^2 + m^2}. \tag{6.3}$$

In terms of the angle of incidence ϕ we also have

$$p_x = p\cos\phi, \qquad p_y = p\sin\phi, \qquad E'^2 = p^2 + m^2. \tag{6.4}$$

For evanescent waves we write

$$\kappa^2 \equiv -E'^2 + p_y^2 + m^2 \qquad |E - eV| < \sqrt{p_y^2 + m^2}. \tag{6.5}$$

In all the cases that we study, the incoming waves are assumed to be positive-energy travelling waves in a region where $eV < E - \sqrt{p_y^2 + m^2}$. Recalling the plane-wave solutions found in Section 3.3, the travelling waves are given by

$$\begin{aligned} \psi^t &= [\cosh(u/2) + \sinh(u/2)(\cos\phi\,\sigma_1 + \sin\phi\,\sigma_2)]\Phi e^{-i\sigma_3(Et - p_x x - p_y y)}T \\ \psi^r &= [\cosh(u/2) + \sinh(u/2)(-\cos\phi\,\sigma_1 + \sin\phi\,\sigma_2)]\Phi e^{-i\sigma_3(Et + p_x x - p_y y)}R, \end{aligned} \tag{6.6}$$

where

$$\tanh(u/2) = p/(E' + m) \tag{6.7}$$

so that

$$\sinh u = p/m, \qquad \cosh u = E'/m. \tag{6.8}$$

The transmission and reflection coefficients T and R are scalar $+i\sigma_3$ combinations, always appearing on the right-hand side of the spinor. The fact that p_y is the same in all regions gives the electron equivalent of Snell's law,

$$\sinh u \,\sin\phi = \text{constant}. \tag{6.9}$$

The Pauli spinor Φ describes the rest-spin of the particle, with $\Phi = 1$ giving spin-up and $\Phi = -i\sigma_2$ spin down. Other situations are, of course, built from superpositions of these basis states. For these two spin basis states the spin vector is $\pm\sigma_3$, which lies in the plane of the barrier and is perpendicular to the plane of motion. Choosing the states so that the spin is aligned in this manner simplifies the analysis, as the two spin states completely decouple. Many treatments (including one published by some of the present authors [6]) miss this simplification.

There are three matching situations to consider, depending on whether the transmitted waves are travelling, evanescent or in the Klein region ($eV > E + \sqrt{p_y^2 + m^2}$). We consider each of these in turn.

6.1 Matching Conditions for Travelling Waves

The situation of interest here is when there are waves of type (6.6) in both regions. The matching condition in all of these problems is simply that ψ is continuous at the boundary. The work involved is therefore, in principle, less than for the

equivalent non-relativistic problem. The matching is slightly different for the two spins, so we consider each in turn.

Spin-Up ($\Phi = 1$)

We simplify the problem initially by taking the boundary at $x = 0$. Steps at other values of x are then dealt with by inserting suitable phase factors. The matching condition at $x = 0$ reduces to

$$\begin{aligned}
&[\cosh(u_i/2) + \sinh(u_i/2)\sigma_1 e^{\phi_i i\sigma_3}]T_i^{\uparrow} \\
&+ [\cosh(u_i/2) - \sinh(u_i/2)\sigma_1 e^{-\phi_i i\sigma_3}]R_i^{\uparrow} \\
&\qquad = [\cosh(u_{i+1}/2) + \sinh(u_{i+1}/2)\sigma_1 e^{\phi_{i+1} i\sigma_3}]T_{i+1}^{\uparrow} \\
&\qquad\quad + [\cosh(u_{i+1}/2) - \sinh(u_{i+1}/2)\sigma_1 e^{-\phi_{i+1} i\sigma_3}]R_{i+1}^{\uparrow}. \qquad (6.10)
\end{aligned}$$

Since the equations for the reflection and transmission coefficients involve only scalar and $i\sigma_3$ terms, it is again convenient to replace the $i\sigma_3$ bivector with the symbol j. If we now define the 2×2 matrix

$$\boldsymbol{A}_i \equiv \begin{pmatrix} \cosh(u_i/2) & \cosh(u_i/2) \\ \sinh(u_i/2)e^{j\phi_i} & -\sinh(u_i/2)e^{-j\phi_i} \end{pmatrix} \qquad (6.11)$$

we find that equation (6.10) can be written concisely as

$$\boldsymbol{A}_i \begin{pmatrix} T_i^{\uparrow} \\ R_i^{\uparrow} \end{pmatrix} = \boldsymbol{A}_{i+1} \begin{pmatrix} T_{i+1}^{\uparrow} \\ R_{i+1}^{\uparrow} \end{pmatrix}. \qquad (6.12)$$

The $\boldsymbol{A}_i$ matrix has a straightforward inverse, so equation (6.12) can be easily manipulated to describe various physical situations. For example, consider plane waves incident on a single step. The equation describing this configuration is simply

$$\boldsymbol{A}_1 \begin{pmatrix} T_1^{\uparrow} \\ R_1^{\uparrow} \end{pmatrix} = \boldsymbol{A}_2 \begin{pmatrix} T_2^{\uparrow} \\ 0 \end{pmatrix} \qquad (6.13)$$

so that

$$\begin{aligned}
\begin{pmatrix} T_1^{\uparrow} \\ R_1^{\uparrow} \end{pmatrix} =& \frac{T_2^{\uparrow}}{\sinh u_1 \cos\phi_1} \cdot \\
& \begin{pmatrix} \sinh(u_1/2)\cosh(u_2/2)e^{-j\phi_1} + \cosh(u_1/2)\sinh(u_2/2)e^{j\phi_2} \\ \sinh(u_1/2)\cosh(u_2/2)e^{j\phi_1} - \cosh(u_1/2)\sinh(u_2/2)e^{j\phi_2} \end{pmatrix} \qquad (6.14)
\end{aligned}$$

from which the reflection and transmission coefficients can be read off. The case of perpendicular incidence is particularly simple as equation (6.12) can be replaced by

$$\begin{pmatrix} T_{i+1} \\ R_{i+1} \end{pmatrix} = \frac{1}{\sinh u_{i+1}} \begin{pmatrix} \sinh\frac{1}{2}(u_{i+1}+u_i) & \sinh\frac{1}{2}(u_{i+1}-u_i) \\ \sinh\frac{1}{2}(u_{i+1}-u_i) & \sinh\frac{1}{2}(u_{i+1}+u_i) \end{pmatrix} \begin{pmatrix} T_i \\ R_i \end{pmatrix}, \quad (6.15)$$

which is valid for all spin orientations. So, for perpendicular incidence, the reflection coefficient $r = R_1/T_1$ and transmission coefficient $t = T_2/T_1$ at a single step are

$$r = \frac{\sinh\frac{1}{2}(u_1-u_2)}{\sinh\frac{1}{2}(u_1+u_2)}, \qquad t = \frac{\sinh u_1}{\sinh\frac{1}{2}(u_1+u_2)}, \quad (6.16)$$

which agree with the results given in standard texts (and also [35]).

Spin-Down ($\Phi = -i\sigma_2$)

The matching equations for the case of opposite spin are

$$\begin{aligned} &[\cosh(u_i/2) + \sinh(u_i/2)\sigma_1 e^{\phi_i i\sigma_3}](-i\sigma_2)T_i^{\downarrow} \\ &+ [\cosh(u_i/2) - \sinh(u_i/2)\sigma_1 e^{-\phi_i i\sigma_3}](-i\sigma_2)R_i^{\downarrow} \\ &\qquad = [\cosh(u_{i+1}/2) + \sinh(u_{i+1}/2)\sigma_1 e^{\phi_{i+1} i\sigma_3}](-i\sigma_2)T_{i+1}^{\downarrow} \\ &\qquad\quad + [\cosh(u_{i+1}/2) - \sinh(u_{i+1}/2)\sigma_1 e^{-\phi_{i+1} i\sigma_3}](-i\sigma_2)R_{i+1}^{\downarrow}. \end{aligned} \quad (6.17)$$

Pulling the $i\sigma_2$ out on the right-hand side just has the effect of complex-conjugating the reflection and transmission coefficients, so the matrix equation (6.10) is unchanged except that it now relates the complex conjugates of the reflection and transmission coefficients. The analog of equation (6.12) is therefore

$$\boldsymbol{A}_i^* \begin{pmatrix} T_i^{\downarrow} \\ R_i^{\downarrow} \end{pmatrix} = \boldsymbol{A}_{i+1}^* \begin{pmatrix} T_{i+1}^{\downarrow} \\ R_{i+1}^{\downarrow} \end{pmatrix}. \quad (6.18)$$

As mentioned earlier, the choice of alignment of spin basis states ensures that there is no coupling between them.

One can string together series of barriers by including suitable 'propagation' matrices. For example, consider the set-up described in Figure 6.1. The matching equations for spin-up are, at the first barrier,

$$\boldsymbol{A} \begin{pmatrix} T^{\uparrow} \\ R^{\uparrow} \end{pmatrix} = \boldsymbol{A}_1 \begin{pmatrix} T_1^{\uparrow} \\ R_1^{\uparrow} \end{pmatrix} \quad (6.19)$$

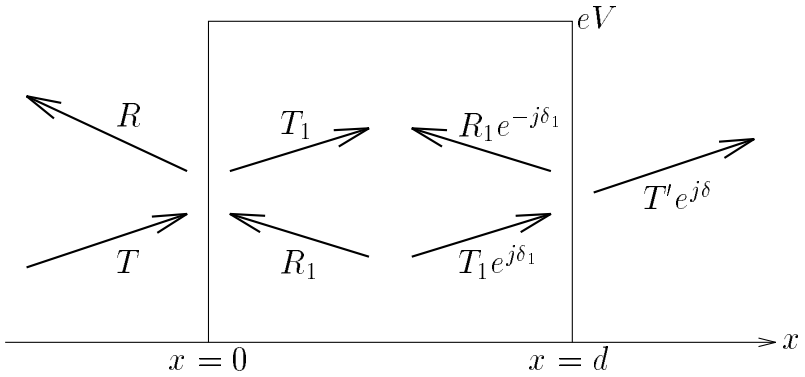

Figure 2: Plane waves scattering from a barrier. The barrier has height eV and width d. Quantities inside the barrier are labeled with a subscript 1, and the free quantities have no subscripts. The phases are given by $\delta_1 = md\sinh u_1 \cos\phi_1$ and $\delta = p_x d$.

and at the second barrier,

$$\boldsymbol{A}_1 \begin{pmatrix} e^{j\delta_1} & 0 \\ 0 & e^{-j\delta_1} \end{pmatrix} \begin{pmatrix} T_1^{\uparrow} \\ R_1^{\uparrow} \end{pmatrix} = \boldsymbol{A} \begin{pmatrix} e^{j\delta} & 0 \\ 0 & e^{-j\delta} \end{pmatrix} \begin{pmatrix} T^{\uparrow\prime} \\ 0 \end{pmatrix}. \tag{6.20}$$

Equation (6.20) demonstrates neatly how matrices of the type

$$\mathbf{P} = \begin{pmatrix} e^{j\delta} & 0 \\ 0 & e^{-j\delta} \end{pmatrix}, \tag{6.21}$$

where $\delta = p_x d$ and d is the distance between steps, can be used to propagate from one step to the next. In this case the problem is reduced to the equation

$$\begin{pmatrix} T^{\uparrow} \\ R^{\uparrow} \end{pmatrix} = \left[\cos\delta_1 \, \boldsymbol{I} - j \sin\delta_1 \, \boldsymbol{A}^{-1}\boldsymbol{A}_1 \begin{pmatrix} 1 & 0 \\ 0 & -1 \end{pmatrix} \boldsymbol{A}_1^{-1}\boldsymbol{A}\right] \begin{pmatrix} e^{j\delta}T^{\uparrow\prime} \\ 0 \end{pmatrix}, \tag{6.22}$$

which quickly yields the reflection and transmission coefficients.

6.2 Matching onto Evanescent Waves

Before studying matching onto evanescent waves, we must first solve the Dirac equation in the evanescent region. Again, the two spin orientations behave differently and are treated separately. Taking spin-up first and looking at the transmitted

(decaying) wave in the evanescent region, the solution takes the form

$$\psi^t = [\cosh(u/2) + \sinh(u/2)\sigma_2]e^{-\kappa x}e^{-i\sigma_3(Et - p_y y)}T. \tag{6.23}$$

Substituting this into the Dirac equation yields

$$(E'\gamma_0 + p_y\gamma_2)e^{u\sigma_2/2} = e^{u\sigma_2/2}(m\gamma_0 - \kappa\gamma_2) \tag{6.24}$$

which is consistent with the definition of κ (6.5). From equation (6.24) we find that

$$\tanh(u/2) = \frac{E' - m}{p_y - \kappa} = \frac{p_y + \kappa}{E' + m}, \tag{6.25}$$

which completes the solution. For the incoming (growing) wave we flip the sign of κ. We therefore define $u^{\pm}$ via

$$\tanh(u^{\pm}/2) = \frac{p_y \pm \kappa}{E' + m} \tag{6.26}$$

and write the outgoing and incoming spin-up waves in the evanescent region as

$$\begin{aligned} \psi^t &= [\cosh(u^+/2) + \sinh(u^+/2)\sigma_2]e^{-\kappa x}e^{-i\sigma_3(Et - p_y y)}T^{\uparrow} \\ \psi^r &= [\cosh(u^-/2) + \sinh(u^-/2)\sigma_2]e^{\kappa x}e^{-i\sigma_3(Et - p_y y)}R^{\uparrow}. \end{aligned} \tag{6.27}$$

If we now consider matching at $x = 0$, the continuity equation becomes

$$\begin{aligned} &[\cosh(u_i/2) + \sinh(u_i/2)\sigma_1 e^{\phi_i i\sigma_3}]T_i^{\uparrow} \\ &+ [\cosh(u_i/2) - \sinh(u_i/2)\sigma_1 e^{-\phi_i i\sigma_3}]R_i^{\uparrow} \\ &\qquad = [\cosh(u_{i+1}^+/2) + \sinh(u_{i+1}^+/2)\sigma_2]T_{i+1}^{\uparrow} \\ &\qquad\quad + [\cosh(u_{i+1}^-/2) + \sinh(u_{i+1}^-/2)\sigma_2)]R_{i+1}^{\uparrow}. \end{aligned} \tag{6.28}$$

On defining the matrix

$$\boldsymbol{B}_i^+ \equiv \begin{pmatrix} \cosh(u_i^+/2) & \cosh(u_i^-/2) \\ j\sinh(u_i^+/2) & +j\sinh(u_i^-/2) \end{pmatrix}, \tag{6.29}$$

we can write equation (6.28) compactly as

$$\boldsymbol{A}_i \begin{pmatrix} T_i^{\uparrow} \\ R_i^{\uparrow} \end{pmatrix} = \boldsymbol{B}_{i+1}^+ \begin{pmatrix} T_{i+1}^{\uparrow} \\ R_{i+1}^{\uparrow} \end{pmatrix}. \tag{6.30}$$

Again, either of the matrices can be inverted to analyse various physical situations. For example, the case of total reflection by a step is handled by

$$\boldsymbol{A}_1 \begin{pmatrix} T_1^{\uparrow} \\ R_1^{\uparrow} \end{pmatrix} = \boldsymbol{B}_2^{+} \begin{pmatrix} T_2^{\uparrow} \\ 0 \end{pmatrix}, \tag{6.31}$$

from which one finds the reflection coefficient

$$r^{\uparrow} = -\frac{\tanh(u^{+}/2) + \tanh(u/2) j e^{j\phi}}{\tanh(u^{+}/2) - \tanh(u/2) j e^{-j\phi}} \tag{6.32}$$

which has $|r^{\uparrow}| = 1$, as expected. The subscripts on u_1, $u_2^{\pm}$ and ϕ_1 are all obvious, and have been dropped.

The case of spin-down requires some sign changes. The spinors in the evanescent region are now given by

$$\begin{aligned} \psi^t &= [\cosh(u^{-}/2) + \sinh(u^{-}/2)\sigma_2](-i\sigma_2) e^{-\kappa x} e^{-i\sigma_3(Et - p_y y)} T^{\downarrow} \\ \psi^r &= [\cosh(u^{+}/2) + \sinh(u^{+}/2)\sigma_2](-i\sigma_2) e^{\kappa x} e^{-i\sigma_3(Et - p_y y)} R^{\downarrow} \end{aligned} \tag{6.33}$$

and, on defining

$$\boldsymbol{B}_i^{-} \equiv \begin{pmatrix} \cosh(u_i^{-}/2) & \cosh(u_i^{+}/2) \\ j\sinh(u_i^{-}/2) & -j\sinh(u_i^{+}/2) \end{pmatrix}, \tag{6.34}$$

the analog of equation (6.30) is

$$\boldsymbol{A}_i^{*} \begin{pmatrix} T_i^{\downarrow} \\ R_i^{\downarrow} \end{pmatrix} = \boldsymbol{B}_{i+1}^{-^{*}} \begin{pmatrix} T_{i+1}^{\downarrow} \\ R_{i+1}^{\downarrow} \end{pmatrix}. \tag{6.35}$$

These formulae are now applied to two situations of physical interest.

6.3 Spin Precession at a Barrier

When a monochromatic wave is incident on a single step of sufficient height that the wave cannot propagate there is total reflection. In the preceding section we found that the reflection coefficient for spin-up is given by equation (6.32), and the analogous calculation for spin-down yields

$$r^{\downarrow} = -\frac{\tanh(u^{-}/2) - \tanh(u/2) j e^{-j\phi}}{\tanh(u^{-}/2) + \tanh(u/2) j e^{j\phi}}. \tag{6.36}$$

Both $r^{\uparrow}$ and $r^{\downarrow}$ are pure phases, but there is an overall phase difference between the two. If the rest-spin vector $\boldsymbol{s} = \Phi\sigma_3\tilde{\Phi}$ is not perpendicular to the plane of incidence, then this phase difference produces a precession of the spin vector. To see how, suppose that the incident wave contains an arbitrary superposition of spin-up and spin-down states,

$$\Phi = \cos(\theta/2)e^{i\sigma_3\phi_1} - \sin(\theta/2)i\sigma_2 e^{i\sigma_3\phi_2} = e^{i\sigma_3\phi/2}e^{-i\sigma_2\theta/2}e^{-i\sigma_3\epsilon/2}, \qquad (6.37)$$

where

$$\phi = \phi_1 - \phi_2, \qquad \epsilon = \phi_1 + \phi_2, \qquad (6.38)$$

and the final pure-phase term is irrelevant. After reflection, suppose that the separate up and down states receive phase shifts of $\delta^{\uparrow}$ and $\delta^{\downarrow}$ respectively. The Pauli spinor in the reflected wave is therefore

$$\begin{aligned} \Phi^r &= \cos(\theta/2)e^{i\sigma_3(\phi_1+\delta^{\uparrow})} - \sin(\theta/2)i\sigma_2 e^{i\sigma_3(\phi_2+\delta^{\downarrow})} \\ &= e^{i\sigma_3\delta/2}e^{i\sigma_3\phi/2}e^{-i\sigma_2\theta/2}e^{-i\sigma_3\epsilon'/2}, \end{aligned} \qquad (6.39)$$

where

$$\delta = \delta^{\uparrow} - \delta^{\downarrow} \qquad (6.40)$$

and again there is an irrelevant overall phase. The rest-spin vector for the reflected wave is therefore

$$\boldsymbol{s}^r = \Phi^r\sigma_3\tilde{\Phi}^r = e^{i\sigma_3\delta/2}\boldsymbol{s}e^{-i\sigma_3\delta/2}, \qquad (6.41)$$

so the spin-vector precesses in the plane of incidence through an angle $\delta^{\uparrow} - \delta^{\downarrow}$. If $\delta^{\uparrow}$ and $\delta^{\downarrow}$ are defined for the asymptotic (free) states then this result for the spin precession is general.

To find the precession angle for the case of a single step we return to the formulae (6.32) and (6.36) and write

$$\begin{aligned} e^{j\delta} &= r^{\uparrow}r^{\downarrow *} \\ &= \frac{(\tanh(u^+/2) + \tanh(u/2)je^{j\phi})(\tanh(u^-/2) + \tanh(u/2)je^{j\phi})}{(\tanh(u^+/2) - \tanh(u/2)je^{-j\phi})(\tanh(u^-/2) - \tanh(u/2)je^{-j\phi})} \end{aligned} \qquad (6.42)$$

If we now recall that

$$\tanh(u/2) = p/(E+m), \qquad \tanh(\frac{u^{\pm}}{2}) = \frac{p_y \pm \kappa}{E - eV + m}, \qquad (6.43)$$

we find that

$$e^{j\delta} = e^{2j\phi}\frac{m\cos\phi - jE\sin\phi}{m\cos\phi + jE\sin\phi}. \tag{6.44}$$

The remarkable feature of this result is that all dependence on the height of the barrier has vanished, so that the precession angle is determined solely by the incident energy and direction. To proceed we write

$$m\cos\phi - jE\sin\phi = \rho e^{j\alpha} \tag{6.45}$$

so that

$$\tan\alpha = -\cosh u\tan\phi. \tag{6.46}$$

Equation (6.44) now yields

$$\tan(\delta/2 - \phi) = -\cosh u\tan\phi, \tag{6.47}$$

from which we obtain the final result that

$$\tan(\delta/2) = -\frac{(\cosh u - 1)\tan\phi}{1 + \cosh u\tan^2\phi}. \tag{6.48}$$

A similar result for the precession angle of the rest-spin vector was obtained by Fradkin & Kashuba [49] using standard techniques. Readers are invited to compare their derivation with the present approach. The formula (6.48) agrees with equation (5.37) from Section 5.3, since the angle θ employed there is related to the angle of incidence ϕ by

$$\theta = \pi - 2\phi. \tag{6.49}$$

Since the decomposition of the plane-wave spinor into a boost term and a Pauli spinor term is unique to the STA, it is not at all clear how the conventional approach can formulate the idea of the rest-spin. In fact, the rest-spin vector is contained in the standard approach in the form of the 'polarisation operator' [49, 50] which, in the STA, is given by

$$\hat{O}(\boldsymbol{n}) \equiv -\frac{j}{\hat{\boldsymbol{p}}^2}[i\hat{\boldsymbol{p}}\hat{\boldsymbol{p}}\cdot\boldsymbol{n} + \hat{\gamma}_0 i(\boldsymbol{n}\wedge\hat{\boldsymbol{p}})\cdot\hat{\boldsymbol{p}}] \tag{6.50}$$

where $\boldsymbol{n}$ is a unit spatial vector. This operator is Hermitian, squares to 1 and commutes with the free-field Hamiltonian. If we consider a free-particle plane-wave

state, then the expectation value of the $\hat{O}(\sigma_i)$ operator is

$$\begin{aligned}\frac{\langle\psi^\dagger\hat{O}(\sigma_i)\psi\rangle}{\langle\psi^\dagger\psi\rangle} &= \frac{m}{E\boldsymbol{p}^2}\langle\tilde{\Phi}L(\sigma_i\cdot\boldsymbol{p}\boldsymbol{p}L\Phi\sigma_3+\sigma_i\wedge\boldsymbol{p}\boldsymbol{p}\tilde{L}\Phi\sigma_3)\rangle \\ &= \frac{m}{E\boldsymbol{p}^2}[L(\sigma_i\cdot\boldsymbol{p}\boldsymbol{p}L+\sigma_i\wedge\boldsymbol{p}\boldsymbol{p}\tilde{L})]\cdot\boldsymbol{s} \qquad (6.51)\end{aligned}$$

where L is the boost

$$L(\boldsymbol{p})=\frac{E+m+\boldsymbol{p}}{\sqrt{2m(E+m)}} \qquad (6.52)$$

and $\hat{\boldsymbol{p}}$ is replaced by its eigenvalue $\boldsymbol{p}$. To manipulate equation (6.51) we use the facts that L commutes with $\boldsymbol{p}$ and satisfies

$$L^2=(E+\boldsymbol{p})/m \qquad (6.53)$$

to construct

$$\begin{aligned}\frac{m}{E\boldsymbol{p}^2}[L(\sigma_i\cdot\boldsymbol{p}\boldsymbol{p}L+\sigma_i\wedge\boldsymbol{p}\boldsymbol{p}\tilde{L})] &= \frac{m}{E\boldsymbol{p}^2}[\sigma_i\cdot\boldsymbol{p}\frac{(E+\boldsymbol{p})}{m}\boldsymbol{p}-\sigma_i\cdot\boldsymbol{p}\boldsymbol{p} \\ &\quad +\frac{E-m}{2m}(E+m+\boldsymbol{p})\sigma_i(E+m-\boldsymbol{p})] \qquad (6.54)\end{aligned}$$

Since only the relative vector part of this quantity is needed in equation (6.51) we are left with

$$\begin{aligned}\frac{E-m}{2E\boldsymbol{p}^2}(2\sigma_i\cdot\boldsymbol{p}\boldsymbol{p}+(E+m)^2\sigma_i-\boldsymbol{p}\sigma_i\boldsymbol{p}) &= \frac{1}{2E(E+m)}(\boldsymbol{p}^2\sigma_i+(E+m)^2\sigma_i) \\ &= \sigma_i. \qquad (6.55)\end{aligned}$$

The expectation value of the 'polarisation' operators is therefore simply

$$\frac{\langle\psi^\dagger\hat{O}(\sigma_i)\psi\rangle}{\langle\psi^\dagger\psi\rangle}=\sigma_i\cdot\boldsymbol{s}, \qquad (6.56)$$

which just picks out the components of the rest-spin vector, as claimed.

For the case of the potential step, $\hat{O}(\boldsymbol{n})$ still commutes with the full Hamiltonian when $\boldsymbol{n}$ is perpendicular to the plane of incidence. In their paper Fradkin & Kashuba decompose the incident and reflected waves into eigenstates of $\hat{O}(\boldsymbol{n})$, which is equivalent to aligning the spin in the manner adopted in this section. As we have stressed, removing the boost and working directly with Φ simplifies many

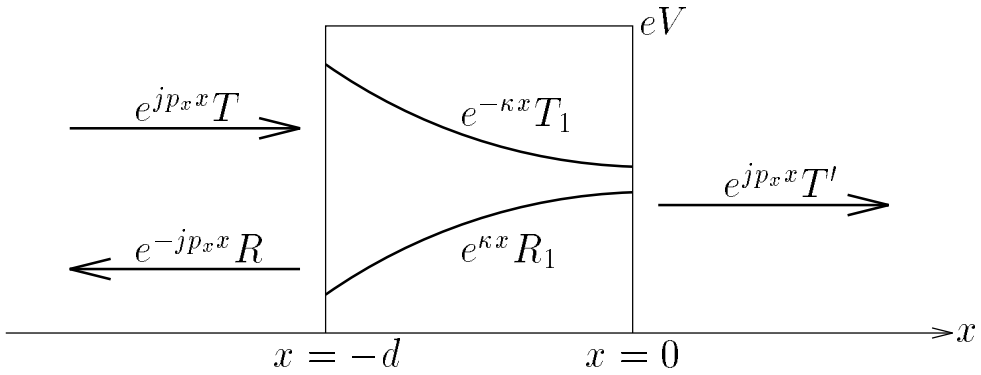

Figure 3: Schematic representation of plane-wave tunnelling.

.

of these manipulations, and removes any need for the polarisation operator.

6.4 Tunnelling of Plane Waves

Suppose now that a continuous beam of plane waves is incident on a potential barrier of finite width. We know that, quantum-mechanically, some fraction of the wave tunnels through to the other side. In Section 7 we address the question 'how long does the tunnelling process take?'. To answer this we will need to combine plane-wave solutions to construct a wavepacket, so here we give the results for plane waves. The physical set-up is illustrated in Figure 6.4.

The matching equation at the $x = 0$ boundary is, for spin-up,

$$\boldsymbol{B}^+ \begin{pmatrix} T_1^\uparrow \\ R_1^\uparrow \end{pmatrix} = \boldsymbol{A} \begin{pmatrix} T^{\uparrow\prime} \\ 0 \end{pmatrix}, \tag{6.57}$$

where the $\boldsymbol{A}$ and $\boldsymbol{B}^+$ matrices are as defined in (6.11) and (6.29) respectively. All subscripts can be dropped again as $\boldsymbol{A}$ always refers to free space and $\boldsymbol{B}^+$ to the barrier region. The matching conditions at $x = -d$ require the inclusion of suitable propagators and the resulting equation is

$$\boldsymbol{A} \begin{pmatrix} e^{-jdp_x} & 0 \\ 0 & e^{jdp_x} \end{pmatrix} \begin{pmatrix} T^\uparrow \\ R^\uparrow \end{pmatrix} = \boldsymbol{B}^+ \begin{pmatrix} e^{\kappa d} & 0 \\ 0 & e^{-\kappa d} \end{pmatrix} \begin{pmatrix} T_1^\uparrow \\ R_1^\uparrow \end{pmatrix}. \tag{6.58}$$

Equation (6.58) shows that the relevant propagator matrix for evanescent waves is

$$\boldsymbol{P} = \begin{pmatrix} e^{\kappa d} & 0 \\ 0 & e^{-\kappa d} \end{pmatrix}. \tag{6.59}$$

The problem now reduces to the matrix equation

$$\begin{pmatrix} e^{-jdp_x}T^{\uparrow} \\ e^{jdp_x}R^{\uparrow} \end{pmatrix} = \left[\cosh(\kappa d) + \sinh(\kappa d)\boldsymbol{A}^{-1}\boldsymbol{B}^{+}\begin{pmatrix} 1 & 0 \\ 0 & -1 \end{pmatrix}\boldsymbol{B}^{+-1}\boldsymbol{A}\right]\begin{pmatrix} T^{\uparrow\prime} \\ 0 \end{pmatrix}, \tag{6.60}$$

from which the reflection and transmission coefficients are easily obtained.

The applications to tunnelling discussed in Section 7 deal mainly with perpendicular incidence, so we now specialise to this situation. For perpendicular incidence we can set $u^{+} = -u^{-} = u'$, where

$$\tanh u' = \frac{\kappa}{E' + m}. \tag{6.61}$$

It follows that the equations for spin-up and spin-down are the same, and we can remove the up-arrows from the preceding equations. Equation (6.57) now yields

$$\begin{pmatrix} T_1 \\ R_1 \end{pmatrix} = \frac{T'}{\sinh u'}\begin{pmatrix} \sinh(u'/2)\cosh(u/2) - j\cosh(u'/2)\sinh(u/2) \\ \sinh(u'/2)\cosh(u/2) + j\cosh(u'/2)\sinh(u/2) \end{pmatrix} \tag{6.62}$$

and from T_1 and R_1 the current in the evanescent region can be constructed. The ratio J_1/J_0 may be interpreted as defining a 'velocity' inside the barrier. The consequences of this idea were discussed in [6] where it was concluded that the tunnelling times predicted by this velocity are not related to tunnelling times measured for individual particles. The reasons for this are discussed in Section 7.

Multiplying out the matrices in equation (6.60) is straightforward, and yields

$$\begin{pmatrix} e^{-jdp}T \\ e^{jdp}R \end{pmatrix} = T'\begin{pmatrix} \cosh(\kappa d) - j\sinh(\kappa d)(EE' - m^2)/(\kappa p) \\ -j\sinh(\kappa d)eVm/(\kappa p) \end{pmatrix}, \tag{6.63}$$

which solves the problem. The transmission coefficient is

$$t = \frac{\kappa p e^{-jdp}}{\kappa p\cosh(\kappa d) - j(p^2 - eVE)\sinh(\kappa d)} \tag{6.64}$$

which recovers the familiar non-relativistic formula in the limit $E \approx m$.

6.5 The Klein Paradox

In the Klein region, $eV - E > \sqrt{p_y^2 + m^2}$, travelling wave solutions exist again. To find these we observe that plane-wave solutions must now satisfy

$$(p - eV\gamma_0)\psi = m\psi\gamma_0 \tag{6.65}$$

and, as $p - eV\gamma_0$ has a negative time component, $\psi\tilde{\psi}$ must now be -1. We could achieve this flip by inserting a 'β-factor' of the type described in Section (3.3), but this would mix the rest-spin states. It is more convenient to work with solutions given by

$$\psi^t = [\cosh(u/2) + \sinh(u/2)(\cos\phi\sigma_1 - \sin\phi\sigma_2)]\sigma_1\Phi e^{-i\sigma_3(Et + p_x x - p_y y)}T \tag{6.66}$$

and

$$\psi^r = [\cosh(u/2) + \sinh(u/2)(-\cos\phi\sigma_1 - \sin\phi\sigma_2)]\sigma_1\Phi e^{-i\sigma_3(Et - p_x x - p_y y)}R, \tag{6.67}$$

where the choice of σ_1 or σ_2 on the right-hand side of the boost is merely a phase choice. To verify that ψ^t is a solution we write the Dirac equation as

$$\begin{aligned}[(E - eV)\gamma_0 - p_x\gamma_1 + p_y\gamma_2]e^{(\cos\phi\sigma_1 - \sin\phi\sigma_2)u/2}{}_{\sigma_1} \\ = me^{(\cos\phi\sigma_1 - \sin\phi\sigma_2)u/2}{}_{\sigma_1\gamma_0}\end{aligned} \tag{6.68}$$

which holds provided that

$$\tanh(u/2) = \frac{p}{m + eV - E}. \tag{6.69}$$

It follows that

$$m\cosh u = eV - E, \qquad m\sinh u = p. \tag{6.70}$$

The current obtained from ψ^t is found to be

$$\psi^t\gamma_0\tilde{\psi}^t = (eV - E)\gamma_0 + p_x\gamma_1 - p_y\gamma_2 \tag{6.71}$$

which is future pointing (as it must be) and points in the positive-x direction. It is in order to obtain the correct direction for the current that the sign of p_x is changed in (6.66) and (6.67). As has been pointed out by various authors [35, 51, 52], some texts on quantum theory miss this argument and match onto a solution inside the

barrier with an incoming group velocity [34, 36]. The result is a reflection coefficient greater than 1. This is interpreted as evidence for pair production, though in fact the effect is due to the choice of boundary conditions. To find the correct reflection and transmission coefficients for an outgoing current, we return to the matching equation which, for spin-up, gives

$$\begin{aligned}&[\cosh(u_i/2) + \sinh(u_i/2)\sigma_1 e^{\phi_i i\sigma_3}]T_i^{\uparrow} \\ &+ [\cosh(u_i/2) - \sinh(u_i/2)\sigma_1 e^{-\phi_i i\sigma_3}]R_i^{\uparrow} \\ &\qquad = [\cosh(u_{i+1}/2) + \sinh(u_{i+1}/2)\sigma_1 e^{-\phi_{i+1} i\sigma_3}]\sigma_1 T_{i+1}^{\uparrow} \\ &\qquad\quad + [\cosh(u_{i+1}/2) - \sinh(u_{i+1}/2)\sigma_1 e^{\phi_{i+1} i\sigma_3}]\sigma_1 R_{i+1}^{\uparrow}. \end{aligned} \tag{6.72}$$

This time we define the matrix

$$\boldsymbol{C}_i \equiv \begin{pmatrix} \sinh(u_i/2)e^{j\phi_i} & -\sinh(u_i/2)e^{-j\phi_i} \\ \cosh(u_i/2) & \cosh(u_i/2) \end{pmatrix} \tag{6.73}$$

so that equation (6.72) becomes

$$\boldsymbol{A}_i \begin{pmatrix} T_i^{\uparrow} \\ R_i^{\uparrow} \end{pmatrix} = \boldsymbol{C}_{i+1} \begin{pmatrix} T_{i+1}^{\uparrow} \\ R_{i+1}^{\uparrow} \end{pmatrix}. \tag{6.74}$$

It should be noted that

$$\boldsymbol{C}_i = \begin{pmatrix} 0 & 1 \\ 1 & 0 \end{pmatrix} \boldsymbol{A}_i. \tag{6.75}$$

The corresponding equation for spin-down is simply

$$\boldsymbol{A}_i^* \begin{pmatrix} T_i^{\downarrow} \\ R_i^{\downarrow} \end{pmatrix} = \boldsymbol{C}_{i+1}^* \begin{pmatrix} T_{i+1}^{\downarrow} \\ R_{i+1}^{\downarrow} \end{pmatrix}. \tag{6.76}$$

The Klein 'paradox' occurs at a single step, for which the matching equation is

$$\boldsymbol{A}_1 \begin{pmatrix} T_1^{\uparrow} \\ R_1^{\uparrow} \end{pmatrix} = \boldsymbol{C}_2 \begin{pmatrix} T_2^{\uparrow} \\ 0 \end{pmatrix}. \tag{6.77}$$

Inverting the $\boldsymbol{A}_1$ matrix yields

$$\begin{pmatrix} T_1^{\uparrow} \\ R_1^{\uparrow} \end{pmatrix} = \frac{T_2^{\uparrow}}{\sinh u \cos\phi} \begin{pmatrix} \cosh(u+u')/2 \\ \sinh(u/2)\sinh(u'/2)e^{2j\phi} - \cosh(u/2)\cosh(u'/2) \end{pmatrix} \tag{6.78}$$

from which the reflection and transmission coefficients can be read off. (The primed quantities relate to the barrier region, as usual.) In particular, for perpendicular incidence, we recover

$$r = -\frac{\cosh(u-u')/2}{\cosh(u+u')/2}, \qquad t = \frac{\sinh u}{\cosh(u+u')/2} \tag{6.79}$$

as found in [35]. The reflection coefficient is always ≤ 1, as it must be from current conservation with these boundary conditions. But, although a reflection coefficient ≤ 1 appears to ease the paradox, some difficulties remain. In particular, the momentum vector inside the barrier points in an opposite direction to the current.

A more complete understanding of the Klein barrier requires quantum field theory since, as the barrier height is $> 2m$, we expect pair creation to occur. An indication that this must be the case comes from an analysis of boson modes based on the Klein-Gordon equation. There one finds that superradiance ($r > 1$) does occur, which has to be interpreted in terms of particle production. For the fermion case the resulting picture is that electron-positron pairs are created and split apart, with the electrons travelling back out to the left and the positrons moving into the barrier region. If a single electron is incident on such a step then it is reflected and, according to the Pauli principle, the corresponding pair-production mode is suppressed.

A complete analysis of the Klein barrier has been given by Manogue [51] to which readers are referred for further details. Manogue concludes that the fermion pair-production rate is given by

$$\Gamma = \int \frac{d^2\boldsymbol{k}}{(2\pi)^2} \int \frac{d\omega}{2\pi} \frac{\sinh u'}{\sinh u} \sum_i |T^i|^2 \tag{6.80}$$

where the integrals run over the available modes in the Klein region, and the sum runs over the two spin states. This formula gives a production rate per unit time, per unit area, and applies to any shape of barrier. The integrals in (6.80) are not easy to evaluate, but a useful expression can be obtained by assuming that the barrier height is only slightly greater than $2m$,

$$eV = 2m(1+\epsilon). \tag{6.81}$$

Then, for the case of a single step, we obtain a pair-production rate of

$$\Gamma = \frac{\pi m^3 \epsilon^3}{32}, \tag{6.82}$$

to leading order in ϵ. The dimensional term is m^3 which, for electrons, corresponds to a rate of 10^{48} particles per second, per square meter. Such an enormous rate would clearly be difficult to sustain in any physically-realistic situation!

The results obtained in this section are summarised in Table 6.

7 Tunnelling Times

In this Section we study tunnelling phenomena. We do so by setting up a wavepacket and examining its evolution as it impinges on a potential barrier. The packet splits into reflected and transmitted parts, and the streamlines of the conserved current show which parts of the initial packet end up being transmitted. The analysis can be used to obtain a distribution of arrival times at some fixed point on the far side of the barrier, which can be compared directly with experiment. The bulk of this section is concerned with packets in one spatial dimension, and compares our approach to other studies of the tunnelling-time problem. The section ends with a discussion of the complications introduced in attempting 2- or 3-dimensional simulations.

The study of tunnelling neatly combines the solutions found in Section 6 with the views on operators and the interpretation of quantum mechanics expressed in Section 3. Tunnelling also provides a good illustration of how simple it is study electron physics via the Dirac theory once the STA is available.

7.1 Wavepacket Tunnelling

In Section 6.4 we studied tunnelling of a continuous plane wave through a potential barrier. It was found that the growing and decaying waves in the barrier region are given by equations (6.27) for spin-up and (6.33) for spin-down. Restricting to the case of perpendicular incidence, the amplitudes of the reflected and transmitted waves are given by equation (6.62). It follows that, for arbitrary spin, the wavefunction in the barrier region is

$$\begin{aligned} \psi_1 \;=\; & [\cosh(u'/2)\Phi + \sinh(u'/2)\sigma_2\sigma_3\Phi\sigma_3]e^{-\kappa x}e^{-i\sigma_3 Et}\alpha + \\ & [\cosh(u'/2)\Phi - \sinh(u'/2)\sigma_2\sigma_3\Phi\sigma_3]e^{\kappa x}e^{-i\sigma_3 Et}\alpha^* \end{aligned} \tag{7.1}$$

Travelling Waves

$$\psi^t = [\cosh(u/2) + \sinh(u/2)\sigma_1 e^{\phi i\sigma_3}]\Phi e^{-i\sigma_3(Et - p_x x - p_y y)}$$
$$\psi^r = [\cosh(u/2) - \sinh(u/2)\sigma_1 e^{-\phi i\sigma_3}]\Phi e^{-i\sigma_3(Et + p_x x - p_y y)}$$
$$\tanh(u/2) = p/(E - eV + m)$$

Evanescent Waves

$$\psi^t = [\cosh(u^{\pm}/2) + \sinh(u^{\pm}/2)\sigma_2]e^{-\kappa x}e^{-i\sigma_3(Et - p_y y)}T$$
$$\psi^r = [\cosh(u^{\mp}/2) + \sinh(u^{\mp}/2)\sigma_2]e^{\kappa x}e^{-i\sigma_3(Et - p_y y)}R$$
(upper/lower signs = spin up/down)
$$\tanh(u^{\pm}/2) = (p_y \pm \kappa)/(E - eV + m)$$

Klein Waves

$$\psi^t = [\cosh(u/2) + \sinh(u/2)\sigma_1 e^{-\phi i\sigma_3}]\sigma_1\Phi e^{-i\sigma_3(Et + p_x x - p_y y)}$$
$$\psi^r = [\cosh(u/2) - \sinh(u/2)\sigma_1 e^{\phi i\sigma_3}]\sigma_1\Phi e^{-i\sigma_3(Et - p_x x - p_y y)}$$
$$\tanh(u/2) = p/(m + eV - E)$$

Matching Matrices

$$\boldsymbol{A} = \begin{pmatrix} \cosh(u/2) & \cosh(u/2) \\ \sinh(u/2)e^{j\phi} & -\sinh(u/2)e^{-j\phi} \end{pmatrix}$$
$$\boldsymbol{B}^{+} = \begin{pmatrix} \cosh(u^{+}/2) & \cosh(u^{-}/2) \\ j\sinh(u^{+}/2) & +j\sinh(u^{-}/2) \end{pmatrix}$$
$$\boldsymbol{C} = \begin{pmatrix} \sinh(u/2)e^{j\phi} & -\sinh(u/2)e^{-j\phi} \\ \cosh(u/2) & \cosh(u/2) \end{pmatrix}$$
$\boldsymbol{A}^*$, $\boldsymbol{B}^{-^*}$, $\boldsymbol{C}^*$ for spin down.

Propagators

$$\begin{pmatrix} e^{jdp_x} & 0 \\ 0 & e^{-jdp_x} \end{pmatrix}, \quad \begin{pmatrix} e^{\kappa d} & 0 \\ 0 & e^{-\kappa d} \end{pmatrix}$$

Table 6: *Summary of results for plane waves incident on a potential step. The waves travel in the $x - y$ plane and the steps lie in the $y - z$ plane. The matching matrices relate T and R on either side of a step.*

where

$$\alpha \equiv \frac{T'}{\sinh u'}[\sinh(u'/2)\cosh(u/2) - i\sigma_3\cosh(u'/2)\sinh(u/2)] \tag{7.2}$$

and

$$\tanh(u'/2) = \frac{\kappa}{E'+m} = \frac{\kappa}{E-eV+m}, \qquad \kappa^2 = m^2 - E'^2. \tag{7.3}$$

The current in the barrier region is

$$\begin{aligned}\psi_1\gamma_0\tilde{\psi}_1 &= \frac{|T'|^2}{m\kappa^2}[m^2eV\cosh(2\kappa x) + E'(p^2 - Eev) \\ &\quad +p\kappa^2\sigma_1 - m\kappa eV\sinh(2\kappa x)(i\sigma_1)\cdot\boldsymbol{s}]\gamma_0\end{aligned} \tag{7.4}$$

from which we can define a 'velocity'

$$\frac{dx}{dt} \equiv \frac{J\cdot\gamma^1}{J\cdot\gamma_0} = \frac{p\kappa^2}{m^2eV\cosh(2\kappa x) + E'(p^2 - Eev)}. \tag{7.5}$$

In fact, the velocity (7.5) does not lead to a sensible definition of a tunnelling time for an individual particle [6]. As we shall see shortly, an additional phenomenon underlies wavepacket tunnelling, leading to much shorter times than those predicted from (7.5). To study wavepacket tunnelling it is useful, initially, to simplify to a one-dimensional problem. To achieve this we must eliminate the transverse current in (7.4) by setting $\boldsymbol{s} = \pm\sigma_1$. This is equivalent to aligning the spin vector to point in the direction of motion. (In this case there is no distinction between the laboratory and comoving spin.) With Φ chosen so that $\boldsymbol{s} = \sigma_1$ it is a now a simple matter to superpose solutions at $t = 0$ to construct a wavepacket centred to the left of the barrier and moving towards the barrier. The wavepacket at later times is then reassembled from the plane-wave states, whose time evolution is known. The density $J^0 = \gamma_0\cdot J$ can then be plotted as a function of time and the result of such a simulation is illustrated in Figure 7.1.

The Dirac current $J = \psi\gamma_0\tilde{\psi}$ is conserved even in the presence of an electromagnetic field. It follows that J defines a set of streamlines which never end or cross. Furthermore, the time-component of the current is positive-definite so the tangents to the streamlines are always future-pointing timelike vectors. According to the standard interpretation of quantum mechanics, $J^0(\boldsymbol{x}, t)$ gives the probability density of locating a particle at position $\boldsymbol{x}$ at time t. But, considering a flux tube defined by adjacent streamlines, we find that

$$\rho(t_0, x_0)dx_0 = \rho(t_1, x_1)dx_1 \tag{7.6}$$

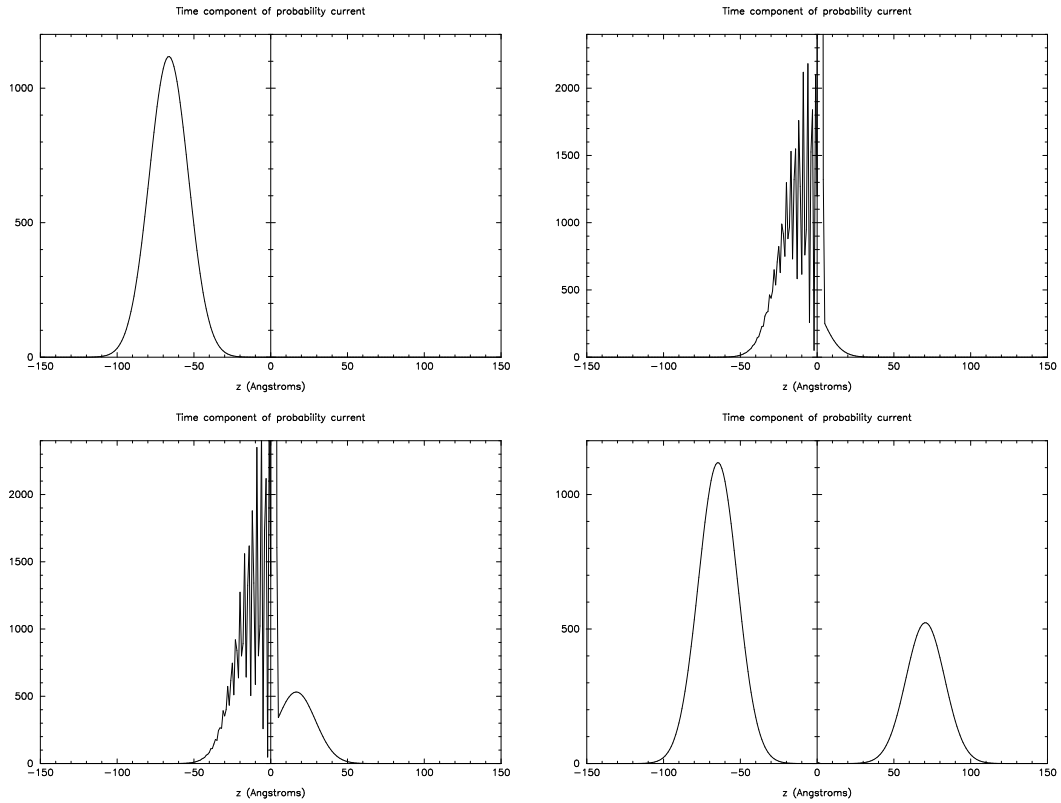

Figure 4: Evolution of the density J^0 as a function of time. The initial packet is a Gaussian of width $\Delta k = 0.04\mathring{A}^{-1}$ and energy 5eV. The barrier starts at the origin and has width $5\mathring{A}$ and height 10eV. The top line shows the density profile at times -0.5×10^{-14}s and -0.1×10^{-14}s, and the bottom line shows times 0.1×10^{-14}s and 0.5×10^{-14}s. In all plots the vertical scale to the right of the barrier is multiplied by 10^4 to enhance the features of the small, transmitted packet.

where (t_0, x_0) and (t_1, x_1) are connected by a streamline. It follows that the density J^0 flows along the streamlines without 'leaking' between them. So, in order to study the tunnelling process, we should follow the streamlines from the initial wavepacket through spacetime. A sample set of these streamlines is shown in Figure 7.1. A significant feature of this plot is that a continuously-distributed set of initial input conditions has given rise to a disjoint set of outcomes (whether or not a streamline passes through the barrier). Hence the deterministic evolution of the wavepacket alone is able to explain the discrete results expected in a quantum measurement, and all notions of wavefunction collapse are avoided. This is of fundamental significance to the interpretation of quantum mechanics. Some consequences of this view for other areas of quantum measurement have been explored by Dewdney *et al.* [27] and Vigier *et al.* [26], though their work was founded in the Bohmian interpretation of non-relativistic quantum mechanics. The results presented here are, of course, independent of any interpretation — we do not need the apparatus of Bohm/de Broglie theory in order to accept the validity of predictions obtained from the current streamlines.

The second key feature of the streamline plot in Figure 7.1 is that it is only the streamlines starting near the front of the initial wavepacket that pass through the barrier. Relative to the centre of the packet, they therefore have a 'head start' in their arrival time at some chosen point on the far side of the barrier. Over the front part of the barrier, however, the streamlines slow down considerably, as can be seen by the change in their slope. These two effects, of picking out the front end of the packet and then slowing it down, compete against each other and it is not immediately obvious which dominates. To establish this, we return to Figure 7.1 and look at the positions of the wavepacket peaks. At $t = 0.5 \times 10^{-14}$s, the peak of the transmitted packet lies at $x = 70\mathring{A}$, whereas the peak of the initial packet would have been at $x = 66\mathring{A}$ had the barrier not been present. In this case, therefore, the peak of the transmitted packet is slightly advanced, a phenomenon often interpreted as showing that tunnelling particles speed up, sometimes to velocities greater than c [53]. The plots presented here show that such an interpretation is completely mistaken. There is no speeding up, as all that happens is that it is only the streamlines from the front of the wavepacket that cross the barrier (slowing down in the process) and these reassemble to form a localised packet on the far side. The reason that tunnelling particles may be transmitted faster than free particles is due entirely to the spread of the initial wavepacket.

There is considerable interest in the theoretical description of tunnelling processes because it is now possible to obtain measurements of the times involved.

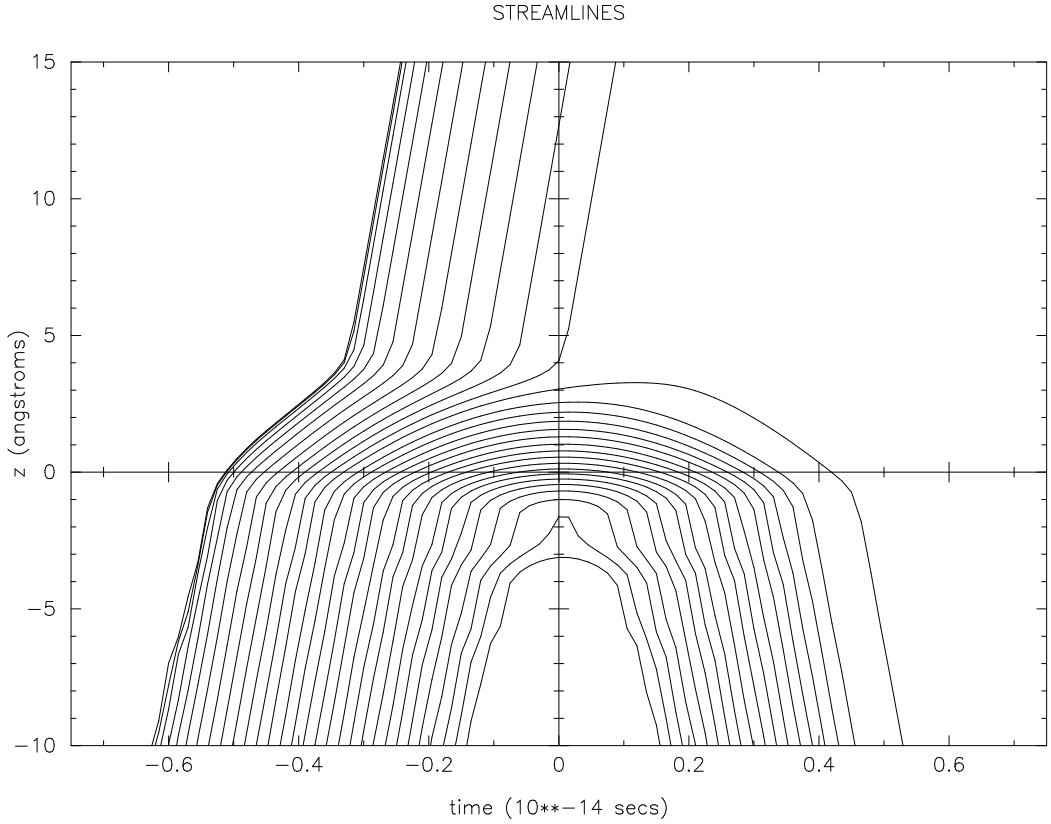

Figure 5: Particle streamlines for the packet evolution shown in Figure 7.1. Only the streamlines from the very front of the packet cross the barrier, with the individual streamlines slowing down as they pass through.

The clearest experiments conducted to date have concerned photon tunnelling [54], where an ingenious 2-photon interference technique is used to compare photons that pass through a barrier with photons that follow an unobstructed path. The discussion of the results of photon-tunnelling experiments usually emphasise packet reshaping, but miss the arguments about the streamlines. Thus many articles concentrate on a comparison of the peaks of the incident and transmitted wavepackets and discuss whether the experiments show particles travelling at speeds $> c$ [53, 55]. As we have seen, a full relativistic study of the streamlines followed by the electron probability density show clearly that no superluminal velocities are present. The same result is true for photons, as we will discuss elsewhere.

Ever since the possibility of tunnelling was revealed by quantum theory, people have attempted to define how long the process takes. Reviews of the various different approaches to this problem have been given by Hauge & Støvneng [56] and, more recently, by Landauer & Martin [57]. Most approaches attempt to define a single tunnelling time for the process, rather than a distribution of possible outcomes as is the case here. Quite why one should believe that it is possible to define a single time in a probabilistic process such as tunnelling is unclear, but the view is still regularly expressed in the modern literature. A further flaw in many other approaches is that they attempt to define how long the particle spent in the barrier region, with answers ranging from the implausible (zero time) to the utterly bizarre (imaginary time). From the streamline plot presented here, it is clearly possible to obtain a distribution of the times spent in the barrier for the tunnelling particles, and the answers will be relatively long as the particles slow down in the barrier. But such a distribution neglects the fact that the front of the packet is preferentially selected, and anyway does not appear to be accessible to direct experimental measurement. As the recent experiments show [54], it is the arrival time at a point on the far side of the barrier that is measurable, and not the time spent in the barrier.

7.2 2-Dimensional Simulations

In the preceding section we simplified the problem in two ways: by assuming perpendicular incidence, and by aligning the spin-vector in the direction of motion. For other configurations more complicated two-dimensional or three-dimensional simulations are required. As well as the obvious numerical complications introduced there are some further difficulties. For the 1-D plots just shown, there was no difficulty in deciding which part of the wavepacket was transmitted and which was

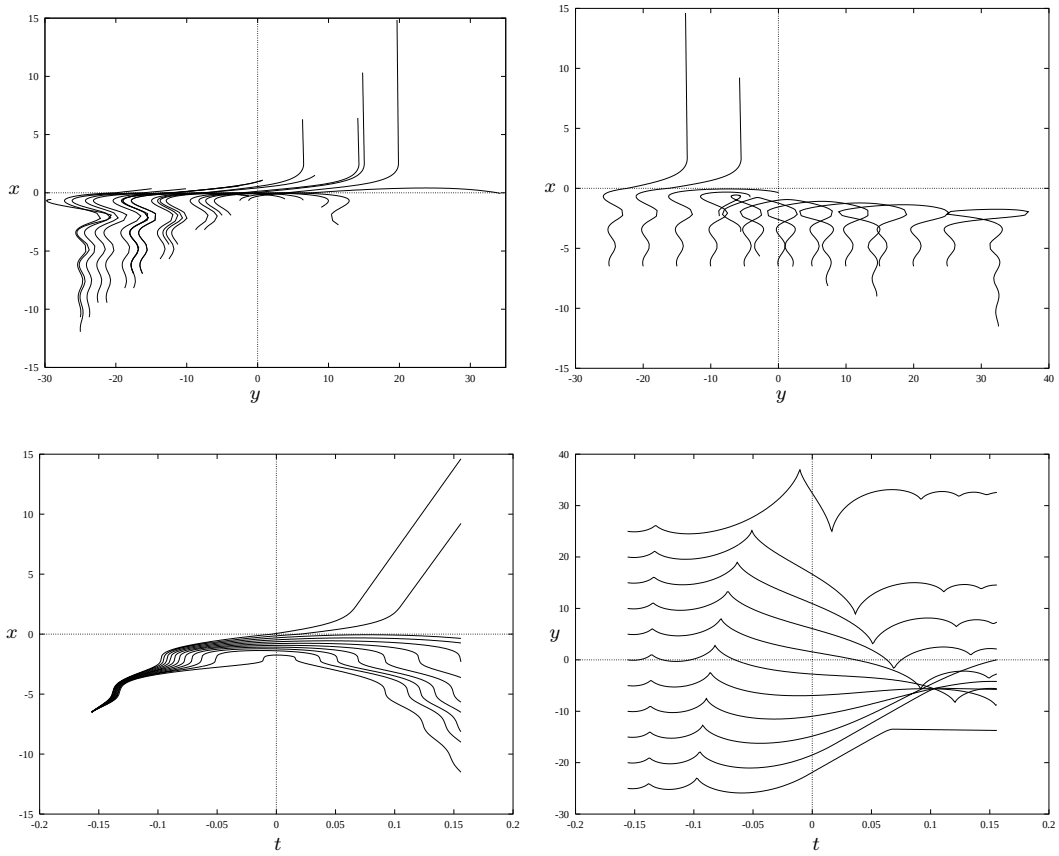

Figure 6: A 2-Dimensional simulation. The simulation uses a 2-D wavepacket in the x–y plane of width $\Delta k = 0.04\mathring{A}^{-1}$ and energy 5eV. The packet is incident perpendicular to the barrier, and the spin vector lies in the $+z$ direction. The barrier is at $x = 0$ and has width $2.5\mathring{A}$ and height 10eV. The top two plots show streamlines in the x–y plane. The top left plot shows streamlines about the bifurcation line, illustrating that the left side of the packet, which 'spins' into the barrier, is preferentially transmitted. The top right plot shows streamlines for a set of points near the front of the packet with the same x value. Again, it is the left side of the packet that is transmitted. The reflected trajectories show quite complex behaviour, and in both plots the effect of the transverse current in the barrier is clear. The t-dependence of the streamlines in the top right plot is shown in the bottom two plots. The left-hand plot shows the streamlines in t–x space. Since the streamlines were started from the same x position and different y positions, the streamlines start from the same point and then spread out as the individual lines evolve differently. Again, it is possible to infer that the streamlines slow down as they pass through the barrier. The right-hand plot shows the t–y evolution of the same streamlines. In all plots distance is measured in $\mathring{A}$ and time in units of 10^{-14}s.

reflected, since the bifurcation point occurred at some fixed value of x. For 2-D or 3-D simulations, however, the split of the initial packet into transmitted and reflected parts occurs along a line or over a 2-D surface. Furthermore, this split is spin-dependent — if one constructs a moving wavepacket, one finds that the streamlines circulate around the spin axis [29]. (A similar circulation phenomena is found in the ground state of the hydrogen atom [6].) The full picture of how the packet behaves is therefore quite complicated, though qualitatively it is still the front portion of the packet that is transmitted. The results of a 2-D simulation are shown in Figure 7.2, and show a number of interesting features. For example, it is the part of the wavepacket that 'spins' *into* the barrier that is predominantly responsible for the transmitted wavepacket. The significance of the spin in the barrier region was clear from equation (7.4), which showed that the spin vector generates a transverse current in the barrier region. These transverse currents are clearly displayed in Figure 7.2. The motion near the barrier is highly complex, with the appearance of current loops suggesting the formation of vortices. Similar effects have been described by Hirschfelder *et al.* [58] in the context of the Schrödinger theory. The streamline plots again show a slowing down in the barrier, which offsets the fact that it is the front of the packet that crosses the barrier.

8 Spin Measurements

We now turn to a second application of the local observables approach to quantum theory, namely to determine what happens to a wavepacket when a spin measurement is made. The first attempts to answer this question were made by Dewdney *et al.* [31, 27], who used the Pauli equation for a particle with zero charge and an anomalous magnetic moment to provide a model for a spin-1/2 particle in a Stern-Gerlach apparatus. Written in the STA, the relevant equation is

$$\partial_t \Phi i\sigma_3 = -\frac{1}{2m}\boldsymbol{\nabla}^2\Phi - \mu \boldsymbol{B}\Phi\sigma_3 \tag{8.1}$$

and the current employed by Dewdney *et al.* is

$$\boldsymbol{J} = -\frac{1}{m}\dot{\boldsymbol{\nabla}}\langle\dot{\Phi}i\sigma_3\Phi^\dagger\rangle. \tag{8.2}$$

Dewdney *et al.* parameterise the Pauli spinor Φ in terms of a density and three 'Euler angles'. In the STA, this parameterisation takes the transparent form

$$\Phi = \rho^{1/2} e^{i\sigma_3\phi/2} e^{i\sigma_1\theta/2} e^{i\sigma_3\psi/2}, \tag{8.3}$$

where the rotor term is precisely that needed to parameterise a rotation in terms of the Euler angles. With this parameterisation, it is a simple matter to show that the current becomes

$$\boldsymbol{J} = \frac{\rho}{2m}(\boldsymbol{\nabla}\psi + \cos\theta\boldsymbol{\nabla}\phi). \tag{8.4}$$

But, as was noted in Section 4.1, the current defined by equation (8.2) is not consistent with that obtained from the Dirac theory through a non-relativistic reduction. In fact, the two currents differ by a term in the curl of the spin vector [6, 28].

To obtain a fuller understanding of the spin measurement process, an analysis based on the Dirac theory is required. Such an analysis is presented here. As well as dealing with a well-defined current, basing the analysis in the Dirac theory is important if one intends to proceed to study correlated spin measurements performed over spacelike intervals (*i.e.* to model an EPR-type experiment). To study such systems it is surely essential that one employs relativistic equations so that causality and the structure of spacetime are correctly built in.

8.1 A Relativistic Model of a Spin Measurement

As is shown in Section 4.3, the modified Dirac equation for a neutral particle with an anomalous magnetic moment μ is

$$\nabla\psi i\sigma_3 - i\mu F\psi\gamma_3 = m\psi\gamma_0. \tag{8.5}$$

This is the equation we use to study the effects of a spin measurement, and it is not hard to show that equation (8.5) reduces to (8.1) in the non-relativistic limit. Following Dewdney *et al.* [31] we model the effect of a spin measurement by applying an impulsive magnetic field gradient,

$$F = Bz\delta(t)i\sigma_3. \tag{8.6}$$

The other components of $\boldsymbol{B}$ are ignored, as we are only modelling the behaviour of the packet in the z-direction. Around $t = 0$ equation (8.5) is approximated by

$$\partial_t \psi i\sigma_3 = \Delta p\, z\delta(t)\gamma_3\psi\gamma_3, \tag{8.7}$$

where

$$\Delta p \equiv \mu B. \tag{8.8}$$

To solve (8.7) we decompose the initial spinor ψ_0 into

$$\psi^{\uparrow} \equiv \tfrac{1}{2}(\psi_0 - \gamma_3\psi_0\gamma_3), \qquad \psi^{\downarrow} \equiv \tfrac{1}{2}(\psi_0 + \gamma_3\psi_0\gamma_3). \tag{8.9}$$

Equation (8.7) now becomes, for $\psi^{\uparrow}$

$$\partial_t \psi^{\uparrow} = \Delta p\, z\delta(t)\psi^{\uparrow} i\sigma_3 \tag{8.10}$$

with the opposite sign for $\psi^{\downarrow}$. The solution is now straightforward, as the impulse just serves to insert a phase factor into each of $\psi^{\uparrow}$ and $\psi^{\downarrow}$:

$$\psi^{\uparrow} \to \psi^{\uparrow} e^{i\sigma_3 \Delta p\, z}, \qquad \psi^{\downarrow} \to \psi^{\downarrow} e^{-i\sigma_3 \Delta p\, z}. \tag{8.11}$$

If we now suppose that the initial ψ consists of a positive-energy plane-wave

$$\psi_0 = L(\boldsymbol{p})\Phi e^{i\sigma_3(\boldsymbol{p}\cdot\boldsymbol{x} - Et)} \tag{8.12}$$

then, immediately after the shock, ψ is given by

$$\psi = \psi^{\uparrow} e^{i\sigma_3(\boldsymbol{p}\cdot\boldsymbol{x} + \Delta p\, z)} + \psi^{\downarrow} e^{i\sigma_3(\boldsymbol{p}\cdot\boldsymbol{x} - \Delta p\, z)}. \tag{8.13}$$

The spatial dependence of ψ is now appropriate to two different values of the 3-momentum, $\boldsymbol{p}^{\uparrow}$ and $\boldsymbol{p}^{\downarrow}$, where

$$\boldsymbol{p}^{\uparrow} \equiv \boldsymbol{p} + \Delta p\, \sigma_3, \qquad \boldsymbol{p}^{\downarrow} \equiv \boldsymbol{p} - \Delta p\, \sigma_3. \tag{8.14}$$

The boost term $L(\boldsymbol{p})$ corresponds to a different momentum, however, so both positive and negative frequency waves are required for the future evolution. After the shock, the wavefunction therefore propagates as

$$\psi = \psi^{\uparrow}_{+} e^{-i\sigma_3 p^{\uparrow}\cdot x} + \psi^{\uparrow}_{-} e^{i\sigma_3 \bar{p}^{\uparrow}\cdot x} + \psi^{\downarrow}_{+} e^{-i\sigma_3 p^{\downarrow}\cdot x} + \psi^{\downarrow}_{-} e^{i\sigma_3 \bar{p}^{\downarrow}\cdot x} \tag{8.15}$$

where

$$p^{\uparrow}\gamma_0 = E^{\uparrow} + \boldsymbol{p}^{\uparrow}, \tag{8.16}$$
$$\bar{p}^{\uparrow}\gamma_0 = E^{\uparrow} - \boldsymbol{p}^{\uparrow}, \tag{8.17}$$

and

$$E^{\uparrow} = (m^2 + \boldsymbol{p}^{\uparrow 2})^{1/2}. \tag{8.18}$$

Both $p^{\downarrow}$ and $E^{\downarrow}$ are defined similarly.

Each term in (8.15) must separately satisfy the free-particle Dirac equation, so it follows that

$$p^{\uparrow}\psi_+^{\uparrow} = m\psi_+^{\uparrow}\gamma_0, \tag{8.19}$$
$$-\bar{p}^{\uparrow}\psi_-^{\uparrow} = m\psi_-^{\uparrow}\gamma_0, \tag{8.20}$$

which are satisfied together with

$$\psi^{\uparrow} = \psi_+^{\uparrow} + \psi_-^{\uparrow}. \tag{8.21}$$

The same set of equations hold for $\psi^{\downarrow}$. Dropping the arrows, we find that

$$\psi_+ = \frac{1}{2E}(p\gamma_0\psi + m\bar{\psi}) \tag{8.22}$$
$$\psi_- = \frac{1}{2E}(\bar{p}\gamma_0\psi - m\bar{\psi}) \tag{8.23}$$

which hold for both $\psi^{\uparrow}$ and $\psi^{\downarrow}$.

The effect of the magnetic shock on a monochromatic wave is to split the wave into four components, each with a distinct momentum. The positive frequency waves are transmitted by the device and split into two waves, whereas the negative frequency states are reflected. The appearance of the antiparticle states must ultimately be attributed to pair production, and only becomes significant for large $\boldsymbol{B}$-fields. We examine this effect after looking at more physical situations.

8.2 Wavepacket Simulations

For computational simplicity we take the incident particle to be localised along the field direction only, with no momentum components transverse to the field. This reduces the dimensionality of the problem to one spatial coordinate and the time coordinate. This was the set-up considered by Dewdney *et al.* [31] and is sufficient

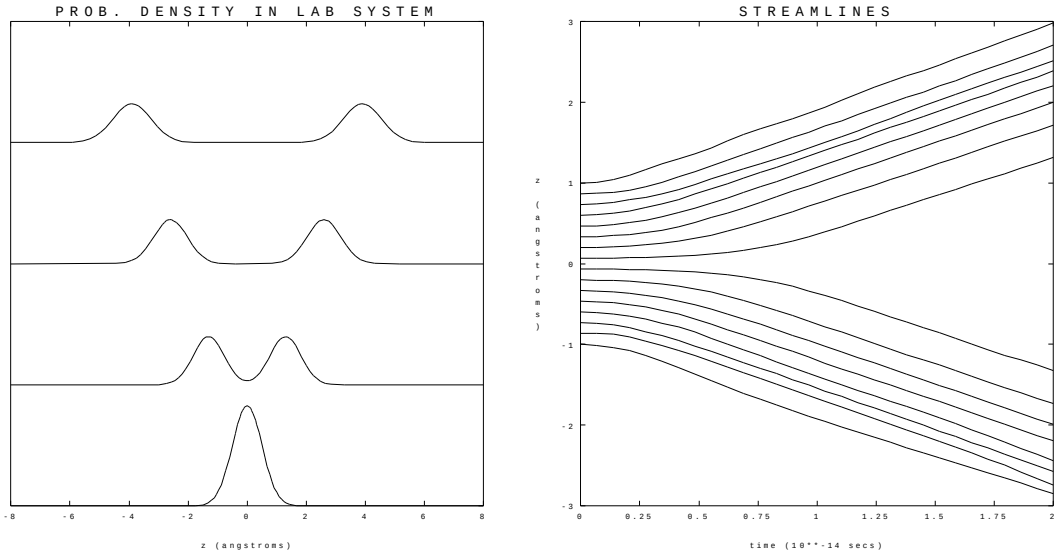

Figure 7: Splitting of a wavepacket caused by an impulsive $\boldsymbol{B}$-field. The initial packet has a width of $1 \times 10^{-24} kg\, m\, s^{-1}$ in momentum space, and receives an impulse of $\Delta p = 1 \times 10^{-23} kg\, m\, s^{-1}$. The figure on the left shows the probability density J_0 at $t = 0, 1.3, 2.6, 3.9 \times 10^{-14}$s, with t increasing up the figure. The figure on the right shows streamlines in the (t, z) plane.

to demonstrate the salient features of the measurement process. The most obvious difference between this model and a real experiment where the electron is moving is that, in our model, all four packets have group velocities along the field direction.

The initial packet is built up from plane-wave solutions of the form

$$\psi = e^{u\sigma_3/2} \Phi e^{i\sigma_3(pz - Et)} \tag{8.24}$$

which are superposed numerically to form a Gaussian packet. After the impulse, the future evolution is found from equation (8.15) and the behaviour of the spin vector and the streamlines can be found for various initial values of Φ. The results of these simulations are plotted on the next few pages.

In Figures 8.2 and 8.2 we plot the evolution of a packet whose initial spin vector points in the σ_1 direction ($\Phi = \exp\{-i\sigma_2\pi/4\}$). After the shock, the density splits neatly into two equal-sized packets, and the streamlines bifurcate at the origin. As with the tunnelling simulations, we see that disjoint quantum outcomes are entirely consistent with the causal wavepacket evolution defined by the Dirac equation. The plot of the spin vector $s \wedge \gamma_0$ shows that immediately after the shock the spins

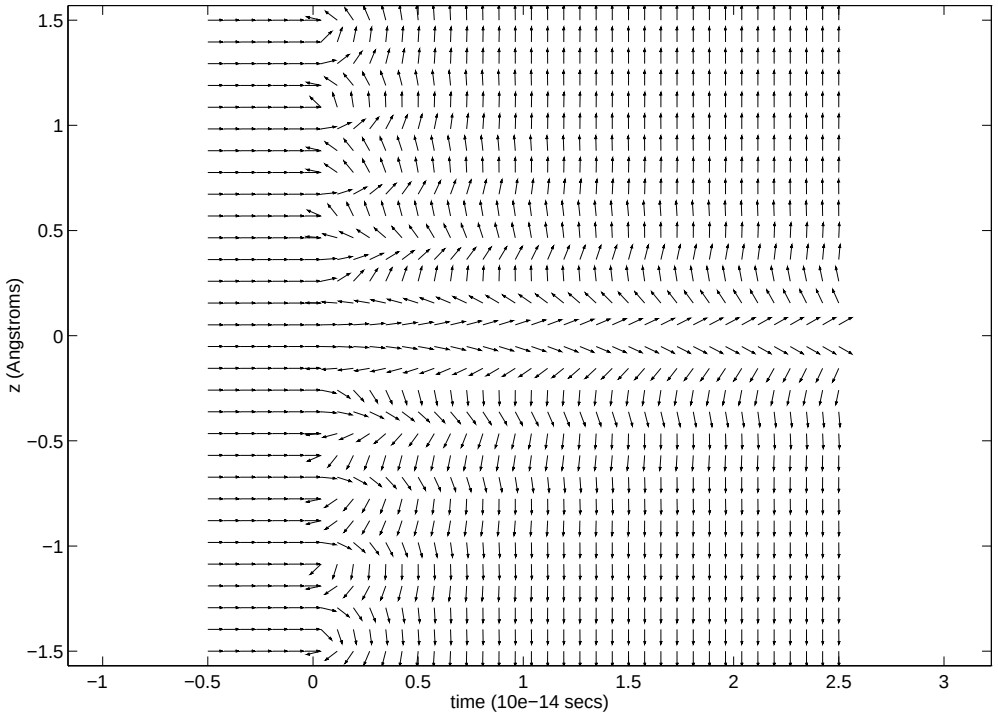

Figure 8: Evolution of the relative spin-vector $s \wedge \gamma_0$, in projection in the (x, z) plane. Immediately after the shock the spin-vectors point in all directions, but after about 2×10^{-14}s they sort themselves into the two packets, pointing in the $+z$ and $-z$ directions.

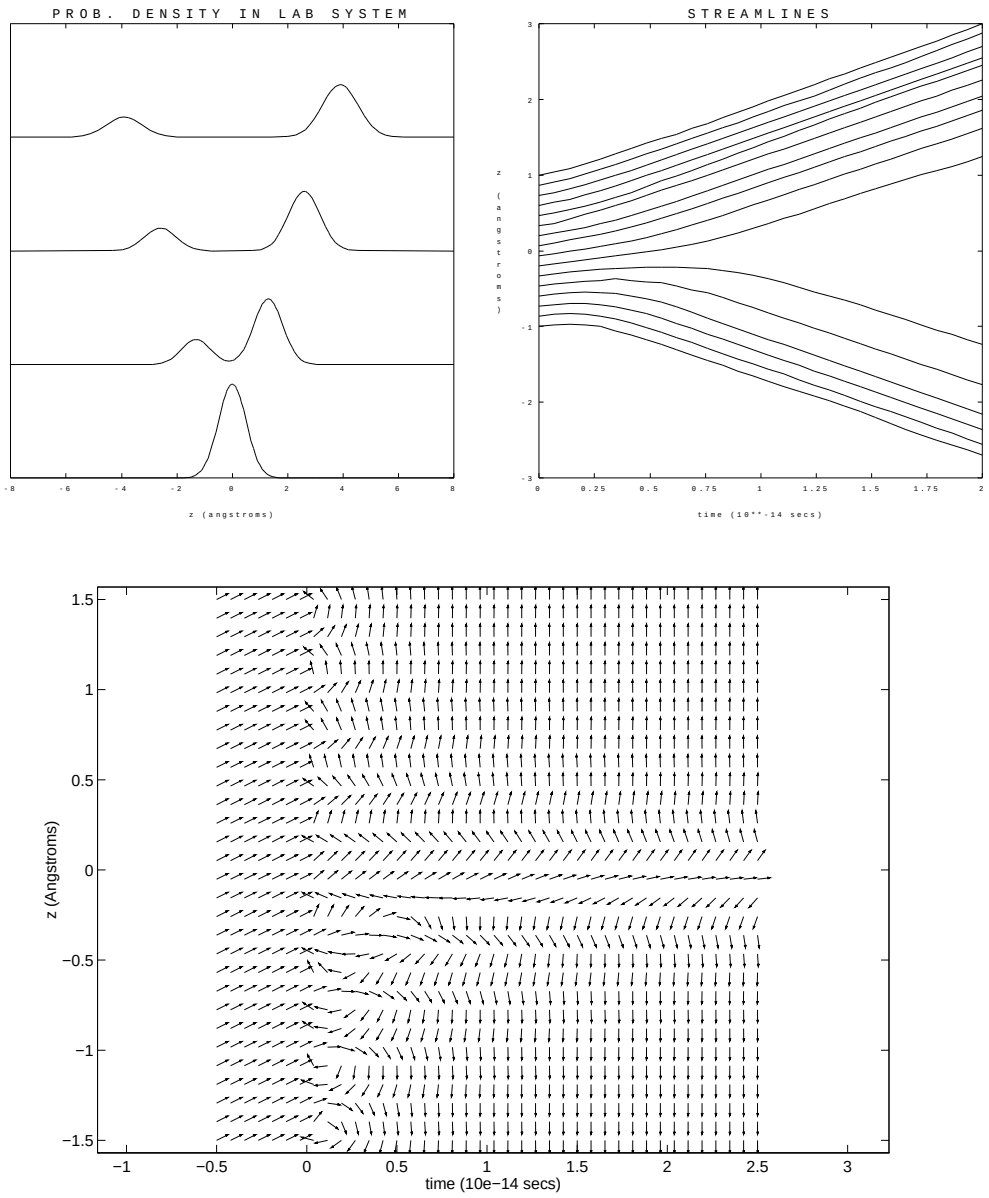

Figure 9: Splitting of a wavepacket with unequal mixtures of spin-up and spin-down components. The initial packet has $\Phi = 1.618 - i\sigma_2$, so more of the streamlines are deflected upwards, and the bifurcation point lies below the $z = 0$ plane. The evolution of the spin vector is shown in the bottom plot.

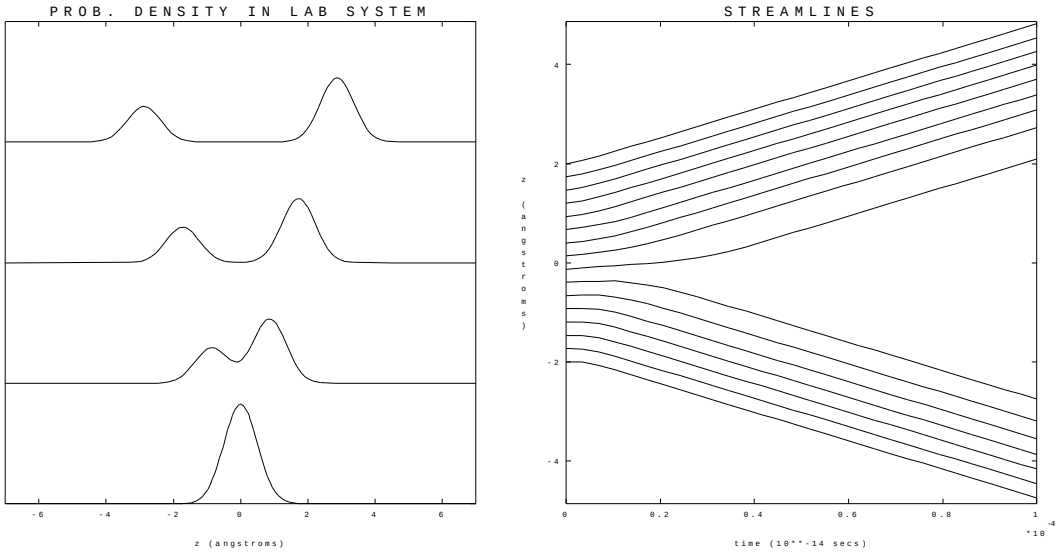

Figure 10: Creation of antiparticle states by a strong magnetic shock. The impulse used is $\Delta p = 1 \times 10^{-18} \mathrm{kg\,m\,s^{-1}}$ and the initial packet is entirely spin-up ($\Phi = 1$). The packet travelling to the left consists of negative energy (antiparticle) states.

are disordered, but that after a little time they sort themselves into one of the two packets, with the spin vector pointing in the direction of motion of the deflected packet. These plots are in good qualitative agreement with those obtained by Dewdney *et al.* [31], who also found that the choice of which packet a streamline enters is determined by its starting position in the incident wavepacket.

Figure 8.2 shows the results of a similar simulation, but with the initial spinor now containing unequal amounts of spin-up and spin-down components. This time we observe an asymmetry in the wavepacket split, with more of the density travelling in the spin-up packet. It is a simple matter to compute the ratio of the sizes of the two packets, and to verify that the ratio agrees with the prediction of standard quantum theory.

As a final, novel, illustration of our approach, we consider a strong shock applied to a packet which is already aligned in the spin-up direction. For a weak shock the entire packet is deflected but, if the shock is sufficiently strong that the antiparticle states have significant amplitude, we find that a second packet is created. The significant feature of Figure 8.2 is that the antiparticle states are deflected in the opposite direction, despite the fact that their spin is still oriented in the $+z$ direction. The antiparticle states thus behave as if they have a magnetic moment

to mass ratio of opposite sign. A more complete understanding of this phenomenon requires a field-theoretic treatment. The appearance of antiparticle states would then be attributed to pair production, with the antiparticle states having the same magnetic moment, but the opposite spin. (One of the crucial effects of the field quantisation of fermionic systems is to flip the signs of the charges and spins of antiparticle states.)

The conclusions reached in this section are in broad agreement with those of Dewdney *et al.*. From the viewpoint of the local observables of the Dirac wavefunction (the current and spin densities), a Stern-Gerlach apparatus does not fulfil the role of a classical measuring device. Instead, it behaves much more like a polariser, where the ratio of particles polarised up and down is dependent on the initial wavefunction. The $\boldsymbol{B}$-field dramatically alters the wavefunction and its observables, though in a causal manner that is entirely consistent with the predictions of standard quantum theory. The implications of these observations for the interpretation of quantum mechanics are profound, though they are only slowly being absorbed by the wider physics community. (Some of these issues are debated in the collection of essays entitled '*Quantum Implications*' [59] and in the recent book by Holland [32].)

9 The Multiparticle STA

So far we have dealt with the application of the STA to single-particle quantum theory. In this section we turn to multiparticle theory. The aim here is to develop the STA approach so that it is capable of encoding multiparticle wavefunctions, and describing the correlations between them. Given the advances in clarity and insight that the STA brings to single-particle quantum mechanics, we expect similar advances in the multiparticle case. This is indeed what we have found, although the field is relatively unexplored as yet. Here we highlight some areas where the multiparticle STA promises a new conceptual approach, rather than attempting to reproduce the calculational techniques employed in standard approaches to many-body or many-electron theory. In particular, we concentrate on the unique geometric insights that the multiparticle STA provides — insights that are lost in the matrix theory. A preliminary introduction to the ideas developed here was given in [4], though this is the first occasion that a full relativistic treatment has been presented.

The n-particle STA is created simply by taking n sets of basis vectors $\{\gamma_\mu^i\}$, where the superscript labels the particle space, and imposing the geometric algebra

relations

$$\begin{array}{ll} \gamma^i_\mu \gamma^j_\nu + \gamma^i_\nu \gamma^j_\mu = 0, & i \neq j \\ \gamma^i_\mu \gamma^j_\nu + \gamma^i_\nu \gamma^j_\mu = 2\eta_{\mu\nu} & i = j. \end{array} \tag{9.1}$$

These relations are summarised in the single formula

$$\gamma^i_\mu \cdot \gamma^j_\nu = \delta^{ij} \eta_{\mu\nu}. \tag{9.2}$$

The fact that the basis vectors from distinct particle spaces anticommute means that we have constructed a basis for the geometric algebra of a $4n$-dimensional configuration space. There is nothing uniquely quantum-mechanical in this idea — a system of three classical particles could be described by a set of three trajectories in a single space, or one path in a nine-dimensional space. The extra dimensions serve simply to label the properties of each individual particle, and should not be thought of as existing in anything other than a mathematical sense. This construction enables us, for example, to define a rotor which rotates one particle whilst leaving all the others fixed. The unique feature of the multiparticle STA is that it implies a separate copy of the time dimension for each particle, as well as the three spatial dimensions. To our knowledge, this is the first attempt to construct a solid conceptual framework for a multi-time approach to quantum theory. Clearly, if successful, such an approach will shed light on issues of locality and causality in quantum theory.

The $\{\gamma^i_\mu\}$ serve to generate a geometric algebra of enormously rich structure. Here we illustrate just a few of the more immediate features of this algebra. It is our belief that the multiparticle STA will prove rich enough to encode all aspects of multiparticle quantum field theory, including the algebra of the fermionic creation/annihilation operators.

Throughout, Roman superscripts are employed to label the particle space in which the object appears. So, for example, ψ^1 and ψ^2 refer to two copies of the same 1-particle object ψ, and not to separate, independent objects. Separate objects are given distinct symbols, or subscripts if they represent a quantity such as the current or spin-vector, which are vectors in configuration space with different projections into the separate copies of the STA. The absence of superscripts denotes that all objects have been collapsed into a single copy of the STA. As always, Roman and Greek subscripts are also used as frame indices, though this does not interfere with the occasional use of subscripts to determine separate projections.

9.1 2-Particle Pauli States and the Quantum Correlator

As an introduction to the properties of the multiparticle STA, we first consider the 2-particle Pauli algebra and the spin states of pairs of spin-1/2 particles. As in the single-particle case, the 2-particle Pauli algebra is just a subset of the full 2-particle STA. A set of basis vectors is defined by

$$\sigma_i^1 = \gamma_i^1\gamma_0^1 \tag{9.3}$$
$$\sigma_i^2 = \gamma_i^2\gamma_0^2 \tag{9.4}$$

which satisfy

$$\sigma_i^1\sigma_j^2 = \gamma_i^1\gamma_0^1\gamma_j^2\gamma_0^2 = \gamma_i^1\gamma_j^2\gamma_0^2\gamma_0^1 = \gamma_j^2\gamma_0^2\gamma_i^1\gamma_0^1 = \sigma_j^2\sigma_i^1. \tag{9.5}$$

So, in constructing multiparticle Pauli states, the basis vectors from different particle spaces commute rather than anticommute. Using the elements $\{1, i\sigma_k^1, i\sigma_k^2, i\sigma_j^1\, i\sigma_k^2\}$ as a basis, we can construct 2-particle states. Here we have introduced the abbreviation

$$i\sigma_i^1 \equiv i^1\sigma_i^1 \tag{9.6}$$

since, in most expressions, it is obvious which particle label should be attached to the i. In cases where there is potential for confusion, the particle label is put back on the i. The basis set $\{1, i\sigma_k^1, i\sigma_k^2, i\sigma_j^1\, i\sigma_k^2\}$ spans a 16-dimensional space, which is twice the dimension of the direct product space of two 2-component complex spinors. For example, the outer-product space of two spin-1/2 states can be built from complex superpositions of the set

$$\begin{pmatrix} 1 \\ 0 \end{pmatrix} \otimes \begin{pmatrix} 1 \\ 0 \end{pmatrix}, \quad \begin{pmatrix} 0 \\ 1 \end{pmatrix} \otimes \begin{pmatrix} 1 \\ 0 \end{pmatrix}, \quad \begin{pmatrix} 1 \\ 0 \end{pmatrix} \otimes \begin{pmatrix} 0 \\ 1 \end{pmatrix}, \quad \begin{pmatrix} 0 \\ 1 \end{pmatrix} \otimes \begin{pmatrix} 0 \\ 1 \end{pmatrix}, \tag{9.7}$$

which forms a 4-dimensional complex space (8 real dimensions). The dimensionality has doubled because we have not yet taken the complex structure of the spinors into account. While the role of j is played in the two single-particle spaces by right multiplication by $i\sigma_3^1$ and $i\sigma_3^2$ respectively, standard quantum mechanics does not distinguish between these operations. A projection operator must therefore be included to ensure that right multiplication by $i\sigma_3^1$ or $i\sigma_3^2$ reduces to the same operation. If a 2-particle spin state is represented by the multivector ψ, then ψ must satisfy

$$\psi i\sigma_3^1 = \psi i\sigma_3^2 \tag{9.8}$$

from which we find that

$$\begin{array}{rl} & \psi = -\psi i\sigma_3^1\, i\sigma_3^2 \\ \Longrightarrow & \psi = \psi\tfrac{1}{2}(1 - i\sigma_3^1\, i\sigma_3^2). \end{array} \tag{9.9}$$

On defining

$$E = \tfrac{1}{2}(1 - i\sigma_3^1\, i\sigma_3^2), \tag{9.10}$$

we find that

$$E^2 = E \tag{9.11}$$

so right multiplication by E is a projection operation. (The relation $E^2 = E$ means that E is technically referred to as an 'idempotent' element.) It follows that the 2-particle state ψ must contain a factor of E on its right-hand side. We can further define

$$J = Ei\sigma_3^1 = Ei\sigma_3^2 = \tfrac{1}{2}(i\sigma_3^1 + i\sigma_3^2) \tag{9.12}$$

so that

$$J^2 = -E. \tag{9.13}$$

Right-sided multiplication by J takes on the role of j for multiparticle states.

The STA representation of a direct-product 2-particle Pauli spinor is now given by $\psi^1\phi^2 E$, where ψ^1 and ϕ^2 are spinors (even multivectors) in their own spaces. A complete basis for 2-particle spin states is provided by

$$\begin{array}{rcl} \begin{pmatrix} 1 \\ 0 \end{pmatrix} \otimes \begin{pmatrix} 1 \\ 0 \end{pmatrix} & \leftrightarrow & E \\ \begin{pmatrix} 0 \\ 1 \end{pmatrix} \otimes \begin{pmatrix} 1 \\ 0 \end{pmatrix} & \leftrightarrow & -i\sigma_2^1 E \\ \begin{pmatrix} 1 \\ 0 \end{pmatrix} \otimes \begin{pmatrix} 0 \\ 1 \end{pmatrix} & \leftrightarrow & -i\sigma_2^2 E \\ \begin{pmatrix} 0 \\ 1 \end{pmatrix} \otimes \begin{pmatrix} 0 \\ 1 \end{pmatrix} & \leftrightarrow & i\sigma_2^1\, i\sigma_2^2 E. \end{array} \tag{9.14}$$

This procedure extends simply to higher multiplicities. All that is required is to find the 'quantum correlator' E_n satisfying

$$E_n i\sigma_3^j = E_n i\sigma_3^k = J_n \qquad \text{for all } j,\, k. \tag{9.15}$$

E_n can be constructed by picking out the $j = 1$ space, say, and correlating all the

other spaces to this, so that

$$E_n = \prod_{j=2}^{n} \tfrac{1}{2}(1 - i\sigma_3^1\, i\sigma_3^j). \tag{9.16}$$

The value of E_n is independent of which of the n spaces is singled out and correlated to. The complex structure is defined by

$$J_n = E_n i\sigma_3^j, \tag{9.17}$$

where $i\sigma_3^j$ can be chosen from any of the n spaces. To illustrate this consider the case of $n = 3$, where

$$\begin{aligned} E_3 &= \tfrac{1}{4}(1 - i\sigma_3^1\, i\sigma_3^2)(1 - i\sigma_3^1\, i\sigma_3^3) && (9.18)\\ &= \tfrac{1}{4}(1 - i\sigma_3^1\, i\sigma_3^2 - i\sigma_3^1\, i\sigma_3^3 - i\sigma_3^2\, i\sigma_3^3) && (9.19) \end{aligned}$$

and

$$J_3 = \tfrac{1}{4}(i\sigma_3^1 + i\sigma_3^2 + i\sigma_3^3 - i\sigma_3^1\, i\sigma_3^2\, i\sigma_3^3). \tag{9.20}$$

Both E_3 and J_3 are symmetric under permutations of their indices.

A significant feature of this approach is that all the operations defined for the single-particle STA extend naturally to the multiparticle algebra. The reversion operation, for example, still has precisely the same definition — it simply reverses the order of vectors in any given multivector. The spinor inner product (3.12) also generalises immediately, to

$$(\psi, \phi)_S = \langle E_n \rangle^{-1} [\langle \psi^\dagger \phi \rangle - \langle \psi^\dagger \phi J_n \rangle i\sigma_3], \tag{9.21}$$

where the right-hand side is projected onto a single copy of the STA. The factor of $\langle E_n \rangle^{-1}$ is included so that the state '1' always has unit norm, which matches with the inner product used in the matrix formulation.

The Non-Relativistic Singlet State

As an application of the formalism outlined above, consider the 2-particle singlet state $|\epsilon\rangle$, defined by

$$|\epsilon\rangle = \tfrac{1}{\sqrt{2}} \left\{ \begin{pmatrix} 1 \\ 0 \end{pmatrix} \otimes \begin{pmatrix} 0 \\ 1 \end{pmatrix} - \begin{pmatrix} 0 \\ 1 \end{pmatrix} \otimes \begin{pmatrix} 1 \\ 0 \end{pmatrix} \right\}. \tag{9.22}$$

This is represented in the 2-particle STA by the multivector

$$\epsilon = \tfrac{1}{\sqrt{2}}(i\sigma_2^1 - i\sigma_2^2)\tfrac{1}{2}(1 - i\sigma_3^1\, i\sigma_3^2). \tag{9.23}$$

The properties of ϵ are more easily seen by writing

$$\epsilon = \tfrac{1}{2}(1 + i\sigma_2^1\, i\sigma_2^2)\tfrac{1}{2}(1 + i\sigma_3^1\, i\sigma_3^2)\sqrt{2}\, i\sigma_2^1, \tag{9.24}$$

which shows how ϵ contains the commuting idempotents $\frac{1}{2}(1 + i\sigma_2^1\, i\sigma_2^2)$ and $\frac{1}{2}(1 + i\sigma_3^1\, i\sigma_3^2)$. The normalisation ensures that

$$\begin{aligned}(\epsilon, \epsilon)_S &= 2\langle \epsilon^\dagger \epsilon \rangle \\ &= 4\langle \tfrac{1}{2}(1 + i\sigma_2^1 i\sigma_2^2)\tfrac{1}{2}(1 + i\sigma_3^1 i\sigma_3^2)\rangle \\ &= 1. \end{aligned} \tag{9.25}$$

The identification of the idempotents in ϵ leads immediately to the results that

$$i\sigma_2^1\epsilon = \tfrac{1}{2}(i\sigma_2^1 - i\sigma_2^2)\tfrac{1}{2}(1 + i\sigma_3^1\, i\sigma_3^2)\sqrt{2} i\sigma_2^1 = -i\sigma_2^2\epsilon \tag{9.26}$$

and

$$i\sigma_3^1\epsilon = -i\sigma_3^2\epsilon, \tag{9.27}$$

and hence that

$$i\sigma_1^1\epsilon = i\sigma_3^1\, i\sigma_2^1\epsilon = -i\sigma_2^2\, i\sigma_3^1\epsilon = i\sigma_2^2\, i\sigma_3^2\epsilon = -i\sigma_1^2\epsilon. \tag{9.28}$$

If M^1 is an arbitrary even element in the Pauli algebra ($M = M^0 + M^k i\sigma_k^1$), it follows that ϵ satisfies

$$M^1\epsilon = M^{2\dagger}\epsilon. \tag{9.29}$$

This now provides a novel demonstration of the rotational invariance of ϵ. Under a joint rotation in 2-particle space, a spinor ψ transforms to $R^1R^2\psi$, where R^1 and R^2 are copies of the same rotor but acting in the two different spaces. From equation (9.29) it follows that, under such a rotation, ϵ transforms as

$$\epsilon \mapsto R^1R^2\epsilon = R^1{R^1}^\dagger\epsilon = \epsilon, \tag{9.30}$$

so that ϵ is a genuine 2-particle scalar.

Non-Relativistic Multiparticle Observables

Multiparticle observables are formed in the same way as for single-particle states. Some combination of elements from the fixed $\{\sigma_k^j\}$ frames is sandwiched between a multiparticle wavefunction ψ and its spatial reverse $\psi^\dagger$. An important example of this construction is provided by the multiparticle spin-vector. In the matrix formulation, the kth component of the particle-1 spin vector is given by

$$S_{1k} = \langle\psi|\hat{\sigma}_k^1|\psi\rangle \tag{9.31}$$

which has the STA equivalent

$$\begin{aligned} S_{1k} &= 2^{n-1}\left(\langle\psi^\dagger\sigma_k^1\psi\sigma_3^1\rangle - \langle\psi^\dagger i\sigma_k^1\psi\rangle i\sigma_3\right) \\ &= -2^{n-1}\langle i\sigma_k^1\psi i\sigma_3^1\psi^\dagger\rangle \\ &= -2^{n-1}(i\sigma_k^1)\cdot(\psi J\psi^\dagger). \end{aligned} \tag{9.32}$$

Clearly, the essential quantity is the bivector part of $\psi J\psi^\dagger$, which neatly generalises the single-particle formula. If we denote the result of projecting out from a multivector M the components contained entirely in the ith-particle space by $\langle M\rangle^i$, we can then write

$$\boldsymbol{S}_a^a = 2^{n-1}\langle\psi J\psi^\dagger\rangle_2^a. \tag{9.33}$$

The various subscripts and superscripts deserve some explanation. On both sides of equation (9.33) the superscript a labels the copy of the STA of interest. The subscript on the right-hand side as usual labels the fact that we are projecting out the grade-2 components of some multivector. The subscript a on the left-hand side is necessary to distinguish the separate projections of $\psi J\psi^\dagger$. Had we not included the subscript, then $\boldsymbol{S}^1$ and $\boldsymbol{S}^2$ would refer to two copies of the *same* bivector, whereas $\boldsymbol{S}_1^1$ and $\boldsymbol{S}_2^2$ are different bivectors with different components. The reason for including both the subscript and the superscript on $\boldsymbol{S}_a^a$ is that we often want to copy the individual bivectors from one space to another, without changing the components.

We can hold all of the individual $\boldsymbol{S}_a^a$ bivectors in a single multiparticle bivector defined by

$$\boldsymbol{S} = 2^{n-1}\langle\psi J\psi^\dagger\rangle_2. \tag{9.34}$$

Under a joint rotation in n-particle space, ψ transforms to $R_1\ldots R_n\psi$ and $\boldsymbol{S}$

Pauli State	Multivector Form	Spin Current
$\vert\uparrow\uparrow\rangle$	E_2	$i\sigma_3^1 + i\sigma_3^2$
$\vert\uparrow\downarrow\rangle$	$-i\sigma_2^2 E_2$	$i\sigma_3^1 - i\sigma_3^2$
$\vert\downarrow\uparrow\rangle$	$-i\sigma_2^1 E_2$	$-i\sigma_3^1 + i\sigma_3^2$
$\vert\downarrow\downarrow\rangle$	$i\sigma_2^1\, i\sigma_2^2 E_2$	$-i\sigma_3^1 - i\sigma_3^2$

Table 7: *Spin Currents for 2-Particle Pauli States*

therefore transforms to

$$R^1 \dots R^n \boldsymbol{S} R^{n\dagger} \dots R^{1\dagger} = R^1 \boldsymbol{S}_1^1 R^{1\dagger} + \dots + R^n \boldsymbol{S}_n^n R^{n\dagger}. \tag{9.35}$$

Each of the separate projections of the spin current is therefore rotated by the same amount, in its own space. That the definition (9.34) is sensible can be checked with the four basis states (9.14). The form of $\boldsymbol{S}$ for each of these is contained in Table 7. Multiparticle observables for the 2-particle case are discussed further below.

Other observables can be formed using different fixed multivectors. For example, a 2-particle invariant is generated by sandwiching a constant multivector Σ between the singlet state ϵ,

$$M = \epsilon \Sigma \epsilon^\dagger. \tag{9.36}$$

Taking $\Sigma = 1$ yields

$$M = \epsilon\epsilon^\dagger = 2\tfrac{1}{2}(1 + i\sigma_2^1\, i\sigma_2^2)\tfrac{1}{2}(1 + i\sigma_3^1\, i\sigma_3^2) = \tfrac{1}{2}(1 + i\sigma_1^1\, i\sigma_1^2 + i\sigma_2^1\, i\sigma_2^2 + i\sigma_3^1\, i\sigma_3^2), \tag{9.37}$$

which rearranges to give

$$i\sigma_k^1\, i\sigma_k^2 = 2\epsilon\epsilon^\dagger - 1. \tag{9.38}$$

This equation contains the essence of the matrix result

$$\hat{\sigma}^a_{k\,a'}\, \hat{\sigma}^b_{k\,b'} = 2\delta^a_{b'}\, \delta^b_{a'} - \delta^a_{a'}\, \delta^b_{b'} \tag{9.39}$$

where a, b, a', b' label the matrix components. This matrix equation is now seen to express a relationship between 2-particle invariants. Further invariants are obtained by taking $\Sigma = i^1 i^2$, yielding

$$M = \epsilon i^1 i^2 \epsilon^\dagger = \tfrac{1}{2}(i^1 i^2 + \sigma_1^1\, \sigma_1^2 + \sigma_2^1\, \sigma_2^2 + \sigma_3^1\, \sigma_3^2). \tag{9.40}$$

This shows that both $i\sigma_k^1\, i\sigma_k^2$ and $\sigma_k^1\, \sigma_k^2$ are invariants under 2-particle rotations. In standard quantum mechanics these invariants would be thought of as arising from the "inner product" of the spin vectors $\hat{\sigma}_i^1$ and $\hat{\sigma}_i^2$. Here, we have seen that the invariants arise in a completely different way by looking at the full multivector $\epsilon\epsilon^\dagger$.

The contents of this section should have demonstrated that the multiparticle STA approach is capable of reproducing most (if not all) of standard multiparticle quantum mechanics. One important result that follows is that the unit scalar imaginary j can be completely eliminated from quantum mechanics and replaced by geometrically meaningful quantities. This should have significant implications for the interpretation of quantum mechanics.

9.2 Comparison with the 'Causal' Approach to Non-Relativistic Spin States

As an application of the techniques outlined above, we look at the work of Holland on the 'Causal interpretation of a system of two spin-1/2 particles' [60]. This work attempts to give a non-relativistic definition of local observables in the higher-dimensional space of a 2-particle wavefunction. As we have seen, such a construction appears naturally in our approach. Holland's main application is to a Bell inequality type experiment, with spin measurements carried out on a system of two correlated spin-1/2 particles by Stern-Gerlach experiments at spatially separated positions. Such an analysis, though interesting, will only be convincing if carried out in the fully relativistic domain, where issues of causality and superluminal propagation can be coherently addressed. We intend to carry out such an analysis in the future, using the STA multiparticle methods, and the work below on the observables of a 2-particle system can be seen as part of this aim.

The aspect of Holland's work that concerns us here (his Section 3 and Appendix A) deals with the joint spin-space of a system of two non-relativistic spin-1/2 particles. The aim is to show that 'all 8 real degrees of freedom in the two body spinor wavefunction may be interpreted (up to a sign) in terms of the properties of algebraically interconnected Euclidean tensors' [60]. Holland's working is complex and requires a number of index manipulations and algebraic identities. Furthermore, the meaning of the expressions derived is far from transparent. Using the above techniques, however, the significant results can be derived more efficiently and in such a way that their geometric meaning is made much clearer. Rather than give a line-by-line translation of Holland's work, we simply state the key results in our notation and prove them.

Let $\psi = \psi E$ be a 2-particle spinor in the correlated product space of the one-particle spin-spaces (the even subalgebra of the Pauli algebra). The observables of this 2-particle system are formed from projections of bilinear products of the form $\psi\Gamma\tilde{\psi}$, where Γ is an element of the 2-particle Pauli spinor algebra. For example, the two 3-dimensional spin-vectors, $\boldsymbol{s}_1^1$, $\boldsymbol{s}_2^2$, are defined by

$$i\boldsymbol{s}_1^1 + i\boldsymbol{s}_2^2 = 2\psi J\tilde{\psi} \tag{9.41}$$

where the right-hand side can be written in the equivalent forms

$$\psi J\tilde{\psi} = \psi i\sigma_3^1\tilde{\psi} = \psi i\sigma_3^2\tilde{\psi}. \tag{9.42}$$

The formula (9.41) is a special case of equation (9.34) where, as we are working in a 2-particle system, the projection onto bivector parts is not required. The vectors $\boldsymbol{s}_1^1$ and $\boldsymbol{s}_2^2$ correspond to the two spin vectors defined by Holland, with the explicit correspondence to his S_{1k} and S_{2k} given by

$$S_{1k} = -(i\boldsymbol{s}_1^1)\cdot(i\sigma_k^1), \qquad S_{2k} = -(i\boldsymbol{s}_2^2)\cdot(i\sigma_k^2). \tag{9.43}$$

An important relation proved by Holland is that the vectors $\boldsymbol{s}_1^1$ and $\boldsymbol{s}_2^2$ are of equal magnitude,

$$(\boldsymbol{s}_1^1)^2 = (\boldsymbol{s}_2^2)^2 = 2\Omega - \rho^2, \tag{9.44}$$

where

$$\rho \equiv 2\langle\psi\psi^\dagger\rangle \tag{9.45}$$

and an explicit form for Ω is to be determined. To prove this result, we write the formulae for the components of $\boldsymbol{s}_1^1$ and $\boldsymbol{s}_2^2$ (9.43) in the equivalent forms

$$S_{1k} = -2(\psi^\dagger i\sigma_k^1\psi)\cdot(i\sigma_3^1), \qquad S_{2k} = -2(\psi^\dagger i\sigma_k^2\psi)\cdot(i\sigma_3^2). \tag{9.46}$$

But, in both cases, the term $\psi^\dagger i\sigma_k^a\psi$ contains a bivector sandwiched between two idempotents, so is of the form $E\ldots E$. This sandwiching projects out the $i\sigma_3^1$ and $i\sigma_3^2$ components of the full bivector, and ensures that that the terms have equal magnitude. The inner products in (9.46) can therefore be dropped and we are left with

$$\psi^\dagger i\sigma_k^a\psi = S_{ak}J \tag{9.47}$$

where the $a = 1, 2$ labels the two separate spin-vectors. It follows immediately from

equation (9.47) that

$$(\boldsymbol{s}_a^a)^2 = -2\langle\psi^\dagger i\sigma_k^a\psi\psi^\dagger i\sigma_k^a\psi\rangle, \tag{9.48}$$

where the a's are not summed. But the quantity $\psi\psi^\dagger$ contains only scalar and 4-vector components, so we find that

$$i\sigma_k^1\psi\psi^\dagger i\sigma_k^1 = i\sigma_k^2\psi\psi^\dagger i\sigma_k^2 = -3\langle\psi\psi^\dagger\rangle + \langle\psi\psi^\dagger\rangle_4 = \psi\psi^\dagger - 2\rho. \tag{9.49}$$

(This result follows immediately from $\sigma_k i\boldsymbol{a}\sigma_k = -i\boldsymbol{a}$, which is valid for any vector $\boldsymbol{a}$ in the single-particle Pauli algebra.) Inserting equation (9.49) back into (9.48) we can now write

$$(\boldsymbol{s}_1^1)^2 = (\boldsymbol{s}_2^2)^2 = 2\rho^2 - 2\langle\psi\psi^\dagger\psi\psi^\dagger\rangle, \tag{9.50}$$

which shows that $\boldsymbol{s}_1^1$ and $\boldsymbol{s}_2^2$ are indeed of equal magnitude, and enables us to identify Ω as

$$\Omega = \tfrac{1}{2}(3\rho^2 - 2\langle\psi\psi^\dagger\psi\psi^\dagger\rangle). \tag{9.51}$$

In addition to ρ, $\boldsymbol{s}_1^1$ and $\boldsymbol{s}_2^2$, Holland defines a tensor S_{jk} whose components are given by

$$S_{jk} = -2\langle\psi^\dagger i\sigma_j^1\, i\sigma_k^2\psi\rangle. \tag{9.52}$$

This object has the simple frame-free form

$$T \equiv \langle\psi\psi^\dagger\rangle_4. \tag{9.53}$$

Between them, ρ, $\boldsymbol{s}_1^1$, $\boldsymbol{s}_2^2$ and T pick up 7 of the possible 8 degrees of freedom in ψ. The remaining freedom lies in the phase, since all of the observables defined above are phase-invariant. Encoding this information caused Holland some difficulty, but in the STA the answer is straightforward, and is actually already contained in the above working. The crucial observation is that as well as containing only scalar and 4-vector terms, the quantity $\psi^\dagger\psi$ is invariant under rotations. So, in addition to the scalar ρ, the 4-vector components of $\psi^\dagger\psi$ must pick up important rotationally-invariant information. Furthermore, since $\psi^\dagger\psi$ is of the form $E\ldots E$, the four-vector component of $\psi^\dagger\psi$ contains only two independent terms, which can be taken as a complex combination of the $i\sigma_2^1\, i\sigma_2^2$ term. This is seen most clearly using an explicit realisation of ψ. Suppose that we write

$$\psi = (p - i\sigma_2^1 q - i\sigma_2^2 r + i\sigma_2^1\, i\sigma_2^2 s)E \tag{9.54}$$

where p, q, r, and s are complex combinations of 1 and J, we then find that

$$\psi^\dagger\psi = [\rho + 2i\sigma_2^1\, i\sigma_2^2(ps - qr)]E. \tag{9.55}$$

This shows explicitly that the additional complex invariant is given by $ps - qr$. It is this term that picks up the phase of ψ, and we therefore define the complex quantity

$$\alpha \equiv \langle\psi i\sigma_2^1\, i\sigma_2^2\psi^\dagger\rangle - \langle\psi i\sigma_1^1\, i\sigma_2^2\psi^\dagger\rangle i\sigma_3, \tag{9.56}$$

which is the STA equivalent of the complex scalar $\bar{\rho}$ defined by Holland. The complex scalar α is invariant under rotations, and under the phase change

$$\psi \mapsto \psi e^{J\phi} \tag{9.57}$$

α transforms as

$$\alpha \mapsto \alpha e^{2\phi i\sigma_3}. \tag{9.58}$$

The set $\{\rho, \alpha, \boldsymbol{s}_1^1, \boldsymbol{s}_2^2, T\}$ encode all the information contained in the 2-particle spinor ψ, up to an overall sign. They reproduce the quantities defined by Holland, but their STA derivation makes their properties and geometric origin much clearer.

9.3 Relativistic 2-Particle States

The ideas developed for the multi-particle Pauli algebra extend immediately to the relativistic domain. The direct product of the two single-particle spinor spaces (the even subalgebras) now results in a space of $8 \times 8 = 64$ real dimensions. Unlike the single-particle case, this space is not equivalent to the even subalgebra of the full 8-dimensional algebra. The full algebra is 256-dimensional, and its even subalgebra is therefore 128-dimensional. It is not yet clear whether the remaining 64-dimensional space which is not picked up by sums of direct-product states could be of use in constructing 2-particle wavefunctions, and for the remainder of this section we work only with the space obtained from sums of direct-product states. Post-multiplying the direct-product space by the quantum correlator E reduces it to 32 real dimensions, which are equivalent to the 16 complex dimensions employed in standard 2-particle relativistic quantum theory. All the single-particle observables discussed in Section 3.3 extend simply. In particular, we define the vectors

$$\mathcal{J} \equiv \langle\psi(\gamma_0^1 + \gamma_0^2)\tilde{\psi}\rangle_1 \tag{9.59}$$

$$s \equiv \langle\psi(\gamma_3^1 + \gamma_3^2)\tilde{\psi}\rangle_1 \tag{9.60}$$

which are respectively the 2-particle current and spin-vector. (The calligraphic symbol $\mathcal{J}$ is used to avoid confusion with the correlated bivector J.) We also define the spin bivector S by

$$S \equiv \langle \psi J \tilde{\psi} \rangle_2. \tag{9.61}$$

Of particular interest are the new Lorentz-invariant quantities that arise in this approach. From the work of the preceding section, we form the quantity $\tilde{\psi}\psi$, which decomposes into

$$\tilde{\psi}\psi = \langle \tilde{\psi}\psi \rangle_{0,8} + \langle \tilde{\psi}\psi \rangle_4. \tag{9.62}$$

The grade-0 and grade-8 terms are the 2-particle generalisation of the scalar + pseudoscalar combination $\psi\tilde{\psi} = \rho \exp(i\beta)$ found at the single-particle level. Of greater interest are the 4-vector terms. These offer a wealth of Lorentz-invariant 2-particle observables, the meaning of which we are only beginning to appreciate. Such invariants are rarely seen in the traditional matrix approach.

The Relativistic Singlet State and Relativistic Invariants

Our task here is to find a relativistic analogue of the Pauli singlet state discussed in Section 9.1. Recalling the definition of ϵ (9.23), the property that ensured that ϵ was a singlet state was that

$$i\sigma_k^1 \epsilon = -i\sigma_k^2 \epsilon, \qquad k = 1 \ldots 3. \tag{9.63}$$

In addition to (9.63) a relativistic singlet state, which we will denote as η, must satisfy

$$\sigma_k^1 \eta = -\sigma_k^2 \eta, \qquad k = 1 \ldots 3. \tag{9.64}$$

It follows that η satisfies

$$i^1\eta = \sigma_1^1\sigma_2^1\sigma_3^1\eta = -\sigma_3^2\sigma_2^2\sigma_1^2\eta = i^2\eta \tag{9.65}$$

so that

$$\eta = -i^1 i^2 \eta \tag{9.66}$$

$$\implies \eta = \tfrac{1}{2}(1 - i^1 i^2)\eta. \tag{9.67}$$

The state η can therefore be constructed by multiplying ϵ by the idempotent $\frac{1}{2}(1 - i^1 i^2)$. We therefore define

$$\eta \equiv \epsilon \tfrac{1}{\sqrt{2}}(1 - i^1 i^2) = (i\sigma_2^1 - i\sigma_2^2)\tfrac{1}{2}(1 - i\sigma_3^1\, i\sigma_3^2)\tfrac{1}{2}(1 - i^1 i^2), \tag{9.68}$$

which is normalised such that $(\eta, \eta)_S = 1$. The invariant η satisfies

$$i\sigma_k^1 \eta = i\sigma_k^1\, \epsilon \tfrac{1}{2}(1 - i^1 i^2) = -i\sigma_k^2 \eta \qquad k = 1 \ldots 3 \tag{9.69}$$

and

$$\sigma_k^1 \eta = -\sigma_k^1 i^1 i^2 \eta = i^2\, i\sigma_k^2 \eta = -\sigma_k^2 \eta \qquad k = 1 \ldots 3. \tag{9.70}$$

These results are summarised by

$$M^1 \eta = \tilde{M}^2 \eta, \tag{9.71}$$

where M is an even multivector in either the particle-1 or particle-2 STA. The proof that η is a relativistic invariant now reduces to the simple identity

$$R^1 R^2 \eta = R^1 \tilde{R}^1 \eta = \eta, \tag{9.72}$$

where R is a single-particle relativistic rotor.

Equation (9.71) can be seen as arising from a more primitive relation between vectors in the separate spaces. Using the result that $\gamma_0^1 \gamma_0^2$ commutes with η, we can derive

$$\begin{aligned} \gamma_\mu^1 \eta \gamma_0^1 &= \gamma_\mu^1 \gamma_0^1 \gamma_0^2 \eta \gamma_0^2 \gamma_0^1 \gamma_0^1 \\ &= \gamma_0^2 (\gamma_\mu \gamma_0)^1 \eta \gamma_0^2 \\ &= \gamma_0^2 \gamma_0^2 \gamma_\mu^2 \eta \gamma_0^2 \\ &= \gamma_\mu^2 \eta \gamma_0^2, \end{aligned} \tag{9.73}$$

and hence we find that, for an arbitrary vector a,

$$a^1 \eta \gamma_0^1 = a^2 \eta \gamma_0^2. \tag{9.74}$$

Equation (9.71) now follows immediately from (9.74) by writing

$$\begin{aligned}(ab)^1\eta &= a^1b^1\eta\gamma_0^1\gamma_0^1\\ &= a^1b^2\eta\gamma_0^2\gamma_0^1\\ &= b^2a^1\eta\gamma_0^1\gamma_0^2\\ &= b^2a^2\eta\gamma_0^2\gamma_0^2\\ &= (ba)^2\eta. \end{aligned} \tag{9.75}$$

Equation (9.74) can therefore be viewed as the fundamental property of the relativistic invariant η.

From η a number of Lorentz-invariant 2-particle multivectors can be constructed by sandwiching arbitrary multivectors between η and $\tilde{\eta}$. The simplest such object is

$$\begin{aligned}\eta\tilde{\eta} &= \epsilon\tfrac{1}{2}(1-i^1i^2)\tilde{\epsilon}\\ &= \tfrac{1}{2}(1+i\sigma_1^1\,i\sigma_1^2+i\sigma_2^1\,i\sigma_2^2+i\sigma_3^1\,i\sigma_3^2)\tfrac{1}{2}(1-i^1i^2)\\ &= \tfrac{1}{4}(1-i^1i^2)-\tfrac{1}{4}(\sigma_k^1\,\sigma_k^2-i\sigma_k^1\,i\sigma_k^2). \end{aligned} \tag{9.76}$$

This contains a scalar + pseudoscalar (grade-8) term, which is obviously invariant, together with the invariant grade-4 multivector $(\sigma_k^1\,\sigma_k^2-i\sigma_k^1\,i\sigma_k^2)$. The next simplest object is

$$\begin{aligned}\eta\gamma_0^1\gamma_0^2\tilde{\eta} &= \tfrac{1}{2}(1+i\sigma_1^1\,i\sigma_1^2+i\sigma_2^1\,i\sigma_2^2+i\sigma_3^1\,i\sigma_3^2)\tfrac{1}{2}(1-i^1i^2)\gamma_0^1\gamma_0^2\\ &= \tfrac{1}{4}(\gamma_0^1\gamma_0^2+i^1i^2\gamma_k^1\gamma_k^2-i^1i^2\gamma_0^1\gamma_0^2-\gamma_k^1\gamma_k^2)\\ &= \tfrac{1}{4}(\gamma_0^1\gamma_0^2-\gamma_k^1\gamma_k^2)(1-i^1i^2). \end{aligned} \tag{9.77}$$

On defining the bivector

$$K \equiv \gamma_\mu^1\gamma^{\mu 2} \tag{9.78}$$

and the 2-particle pseudoscalar

$$W \equiv i^1i^2 = i^2i^1 \tag{9.79}$$

the invariants from (9.77) are simply K and WK. That W is invariant under rotations is obvious, and the invariance of K under joint rotations in the two particle spaces follows from equation (9.77). The bivector K is of the form of a 'doubling' bivector discussed in [61], where such bivectors are shown to play an

Invariant	Type of Interaction	Grade
1	Scalar	0
K	Vector	2
$K \wedge K$	Bivector	4
WK	Pseudovector	6
W	Pseudoscalar	8

Table 8: *2-Particle Relativistic Invariants*

important role in the bivector realisation of many Lie algebras.

From the definition of K (9.78), we find that

$$\begin{aligned} K \wedge K &= -2\gamma_0^1\gamma_0^2\gamma_k^1\gamma_k^2 + (\gamma_k^1\gamma_k^2)\wedge(\gamma_j^1\gamma_j^2) \\ &= 2(\sigma_k^1\,\sigma_k^2 - i\sigma_k^1\,i\sigma_k^2), \end{aligned} \tag{9.80}$$

which recovers the grade-4 invariant from (9.76). The full set of 2-particle invariants constructed from K are summarised in Table 8. These invariants are well-known and have been used in constructing phenomenological models of interacting particles [62, 63]. The STA derivation of the invariants is quite new, however, and the fundamental role played by the bivector K is hidden in the matrix formalism.

9.4 Multiparticle Wave Equations

In order to extend the local-observables approach to quantum theory to the multiparticle domain, we need to construct a relativistic wave equation satisfied by an n-particle wavefunction. This is a subject that is given little attention in the literature, with most textbooks dealing solely with the field-quantised description of an n-particle system. An n-particle wave equation is essential, however, if one aims to give a relativistic description of a bound system (where field quantisation and perturbation theory on their own are insufficient). A description of this approach is given in Chapter 10 of Itzykson & Zuber [36], who deal mainly with the Bethe-Salpeter equation for a relativistic 2-particle system. Written in the STA, this equation becomes

$$(j\nabla^1 - m_1)(j\nabla^2 - m_2)\psi(r,s) = I(r,s)\psi(r,s) \tag{9.81}$$

where j represents right-sided multiplication by J, $I(r,s)$ is an integral operator representing the inter-particle interaction, and

$$\nabla^1 \equiv \gamma^1_\mu \frac{\partial}{\partial r^\mu}, \qquad \nabla^2 \equiv \gamma^2_\mu \frac{\partial}{\partial s^\mu}, \tag{9.82}$$

with r and s the 4-D positions of the two particles. Strictly, we should have written ∇^1_r and ∇^2_s instead of simply ∇^1 and ∇^2. In this case, however, the subscripts can safely be ignored.

The problem with equation (9.81) is that it is not first-order in the 8-dimensional vector derivative $\nabla = \nabla^1 + \nabla^2$. We are therefore unable to generalise many of the simple first-order propagation techniques discussed in Section 5. Clearly, we would like to find an alternative to (9.81) which retains the first-order nature of the single-particle Dirac equation. Here we will simply assert what we believe to be a good candidate for such an equation, and then work out its consequences. The equation we shall study, for two free spin-1/2 particles of masses m_1 and m_2 respectively, is

$$\left(\frac{\nabla^1}{m_1} + \frac{\nabla^2}{m_2}\right) \psi(x) \left(i\gamma^1_3 + i\gamma^2_3\right) = 2\psi(x). \tag{9.83}$$

We can assume, *a priori*, that ψ is not in the correlated subspace of the the direct-product space. But, since E commutes with $i\gamma^1_3 + i\gamma^2_3$, any solution to (9.83) can be reduced to a solution in the correlated space simply by right-multiplying by E. Written out explicitly, the vector x in equation (9.83) is

$$x = r^1 + s^2 = \gamma^1_\mu r^\mu + \gamma^2_\mu s^\mu \tag{9.84}$$

where $\{r^\mu, s^\mu\}$ are a set of 8 independent components for ψ. Of course, all particle motions ultimately occur in a single space, in which the vectors r and s label two independent position vectors. We stress that in this approach there are two time-like coordinates, r^0 and s^0, which is necessary if our 2-particle equation is to be Lorentz covariant. The derivatives ∇^1 and ∇^2 are as defined by equation (9.82), and the 8-dimensional vector derivative $\nabla = \nabla_x$ is given by

$$\nabla = \nabla^1 + \nabla^2. \tag{9.85}$$

Equation (9.83) can be derived from a Lorentz-invariant action integral in 8-dimensional configuration space in which the $1/m_1$ and $1/m_2$ factors enter via a

linear distortion of the vector derivative ∇. We write this as

$$\left(\frac{\nabla^1}{m_1}+\frac{\nabla^2}{m_2}\right)=\overline{h}\left(\nabla\right), \tag{9.86}$$

where $\overline{h}$ is the linear mapping of vectors to vectors defined by

$$\overline{h}(a)=\frac{1}{m_1}\left(a\cdot\gamma^{\mu\,1}\right)\gamma^1_\mu+\frac{1}{m_2}\left(a\cdot\gamma^{\mu\,2}\right)\gamma^2_\mu. \tag{9.87}$$

This distortion is of the type used in the gauge theory approach to gravity developed in [48, 64, 65, 66], and it is extremely suggestive that mass enters equation (9.83) via this route.

Any candidate 2-particle wave equation must be satisfied by factored states of the form

$$\psi=\phi^1(r^1)\chi^2(s^2)E, \tag{9.88}$$

where ϕ^1 and χ^2 are solutions of the separate single-particle Dirac equations,

$$\nabla\phi=-m_1\phi i\gamma_3, \qquad \nabla\chi=-m_2\chi i\gamma_3. \tag{9.89}$$

To verify that our equation (9.83) meets this requirement, we substitute in the direct-product state (9.88) and use (9.89) to obtain

$$\left(\frac{\nabla^1}{m_1}+\frac{\nabla^2}{m_2}\right)\phi^1\chi^2E\left(i\gamma^1_3+i\gamma^2_3\right)=-\phi^1\chi^2E\left(i\gamma^1_3+i\gamma^2_3\right)\left(i\gamma^1_3+i\gamma^2_3\right), \tag{9.90}$$

where we have used the result that ∇^2 commutes with ϕ^1. Now, since $i\gamma^1_3$ and $i\gamma^2_3$ anticommute, we have

$$\left(i\gamma^1_3+i\gamma^2_3\right)\left(i\gamma^1_3+i\gamma^2_3\right)=-2 \tag{9.91}$$

so that

$$\left(\frac{\nabla^1}{m_1}+\frac{\nabla^2}{m_2}\right)\phi^1\chi^2E\left(i\gamma^1_3+i\gamma^2_3\right)=2\phi^1\chi^2E, \tag{9.92}$$

and (9.83) is satisfied. Equation (9.83) is only satisfied by direct-product states as a result of the fact that vectors from separate particle spaces anticommute. Hence equation (9.83) does not have an equivalent expression in terms of the direct-product matrix formulation, which can only form *commuting* operators from different spaces.

9.5 The Pauli Principle

In quantum theory, indistinguishable particles must obey either Fermi-Dirac or Bose-Einstein statistics. For fermions this requirement results in the Pauli exclusion principle that no two particles can occupy a state in which their properties are identical. At the relativistic multiparticle level, the Pauli principle is usually encoded in the anticommutation of the creation and annihilation operators of fermionic field theory. Here we show that the principle can be successfully encoded in a simple geometrical manner at the level of the relativistic wavefunction, without requiring the apparatus of quantum field theory.

We start by introducing the grade-4 multivector

$$I \equiv \Gamma_0\Gamma_1\Gamma_2\Gamma_3, \tag{9.93}$$

where

$$\Gamma_\mu \equiv \frac{1}{\sqrt{2}}\left(\gamma_\mu^1 + \gamma_\mu^2\right). \tag{9.94}$$

It is a simple matter to verify that I has the properties

$$I^2 = -1, \tag{9.95}$$

and

$$I\gamma_\mu^1 I = \gamma_\mu^2, \qquad I\gamma_\mu^2 I = \gamma_\mu^1. \tag{9.96}$$

It follows that I functions as a geometrical version of the particle exchange operator. In particular, acting on the 8-dimensional position vector $x = r^1 + s^2$ we find that

$$IxI = r^2 + s^1 \tag{9.97}$$

where

$$r^2 = \gamma_\mu^2 r^\mu, \qquad s^1 = \gamma_\mu^1 s^\mu. \tag{9.98}$$

So I can certainly be used to interchange the coordinates of particles 1 and 2. But, if I is to play a fundamental role in our version of the Pauli principle, we must first confirm that it is independent of our choice of initial frame. To see that it is, suppose that we start with a rotated frame $\{R\gamma_\mu\tilde{R}\}$ and define

$$\Gamma'_\mu = \frac{1}{\sqrt{2}}\left(R^1\gamma_\mu^1\tilde{R}^1 + R^2\gamma_\mu^2\tilde{R}^2\right) = R^1R^2\Gamma_\mu\tilde{R}^2\tilde{R}^1. \tag{9.99}$$

The new Γ'_μ give rise to the rotated 4-vector

$$I' = R^1 R^2 I \tilde{R}^2 \tilde{R}^1. \tag{9.100}$$

But, acting on a bivector in particle space 1, we find that

$$Ia^1 \wedge b^1 I = -(Ia^1 I) \wedge (Ib^1 I) = -a^2 \wedge b^2, \tag{9.101}$$

and the same is true of an arbitrary even element in either space. More generally, $I \ldots I$ applied to an even element in one particle space flips it to the other particle space and changes sign, while applied to an odd element it just flips the particle space. It follows that

$$I\tilde{R}^2\tilde{R}^1 = \tilde{R}^1 I \tilde{R}^1 = \tilde{R}^1 \tilde{R}^2 I, \tag{9.102}$$

and substituting this into (9.100) we find that $I' = I$, so I is indeed independent of the chosen orthonormal frame.

We can now use the 4-vector I to encode the Pauli exchange principle geometrically. Let $\psi(x)$ be a wavefunction for two electrons. Our suggested relativistic generalization of the Pauli principle is that $\psi(x)$ should be invariant under the operation

$$\psi(x) \mapsto I\psi(IxI)I. \tag{9.103}$$

For n-particle systems the extension is straightforward: the wavefunction must be invariant under the interchange enforced by the I's constructed from each pair of particles.

We must first check that (9.103) is an allowed symmetry of the 2-particle Dirac equation. With x' defined as IxI it is simple to verify that

$$\nabla_{x'} = \nabla^2_r + \nabla^1_s = I\nabla I, \tag{9.104}$$

and hence that

$$\nabla = I\nabla_{x'} I. \tag{9.105}$$

So, assuming that $\psi(x)$ satisfies the 2-particle equation (9.83) with equal masses m, we find that

$$\begin{aligned} \nabla[I\psi(IxI)I]\left(i\gamma^1_3 + i\gamma^2_3\right) &= -I\nabla_{x'}\psi(x')I\left(i\gamma^1_3 + i\gamma^2_3\right) \\ &= mI\psi(x')\left(i\gamma^1_3 + i\gamma^2_3\right)I\left(i\gamma^1_3 + i\gamma^2_3\right). \end{aligned} \tag{9.106}$$

But $i\gamma_3^1 + i\gamma_3^2$ is odd and symmetric under interchange of its particle labels. It follows that

$$I\left(i\gamma_3^1 + i\gamma_3^2\right) I = \left(i\gamma_3^1 + i\gamma_3^2\right) \tag{9.107}$$

and hence that

$$\nabla[I\psi(IxI)I]\left(i\gamma_3^1 + i\gamma_3^2\right) = 2mI\psi(IxI)I. \tag{9.108}$$

So, if $\psi(x)$ is a solution of the 2-particle equal-mass Dirac equation, then so to is $I\psi(IxI)I$.

Next we must check that the proposed relativistic Pauli principle deals correctly with well-known elementary cases. Suppose that two electrons are in the same spatial state. Then we should expect our principle to enforce the condition that they are in an antisymmetric spin state. For example, consider $i\sigma_2^1 - i\sigma_2^2$, the spin singlet state. We find that

$$I(i\sigma_2^1 - i\sigma_2^2)I = -i\sigma_2^2 + i\sigma_2^1, \tag{9.109}$$

recovering the original state, which is therefore compatible with our principle. On the other hand

$$I(i\sigma_2^1 + i\sigma_2^2)I = -(i\sigma_2^1 + i\sigma_2^2), \tag{9.110}$$

so no part of this state can be added in to the wavefunction, which again is correct. In conclusion, given some 2-particle solution $\psi(x)$, the corresponding state

$$\psi_I \equiv \psi(x) + I\psi(IxI)I \tag{9.111}$$

still satisfies the Dirac equation and is invariant under $\psi(x) \mapsto I\psi(IxI)I$. We therefore claim that the state ψ_I is the correct relativistic generalisation of a state satisfying the Pauli principle. In deference to standard quantum theory, we refer to equation (9.111) as an antisymmetrisation procedure.

The final issue to address is the Lorentz covariance of the antisymmetrisation procedure (9.111). Suppose that we start with an arbitrary wavefunction $\psi(x)$ satisfying the 2-particle equal-mass equation (9.83). If we boost this state via

$$\psi(x) \mapsto \psi'(x) \equiv R^1R^2\psi(\tilde{R}^2\tilde{R}^1xR^1R^2) \tag{9.112}$$

then $\psi'(x)$ also satisfies the same equation (9.83). The boosted wavefunction $\psi'(x)$ can be thought of as corresponding to a different observer in relative motion. The boosted state $\psi'(x)$ can also be antisymmetrised to yield a solution satisfying our relativistic Pauli principle. But, for this procedure to be covariant, the same state

must be obtained if we first antisymmetrise the original $\psi(x)$, and then boost the result. Thus we require that

$$S\psi(\tilde{S}xS) + IS\psi(I\tilde{S}xSI)I = S[\psi(\tilde{S}xS) + I\psi(\tilde{S}IxIS)I] \tag{9.113}$$

where $S \equiv R^1R^2$. Equation (9.113) reduces to the requirement that

$$IS\psi(I\tilde{S}xSI) = SI\psi(\tilde{S}IxIS) \tag{9.114}$$

which is satisfied provided that

$$IS = SI \tag{9.115}$$

or

$$R^1R^2I = IR^1R^2. \tag{9.116}$$

But we proved precisely this equation in demonstrating the frame-invariance of I, so our relativistic version of the Pauli principle is Lorentz invariant. This is important as, rather like the inclusion of the quantum correlator, the Pauli procedure discussed here looks highly non-local in character.

9.6 8-Dimensional Streamlines and Pauli Exclusion

For a single Dirac particle, a characteristic feature of the STA approach is that the probability current is a rotated/dilated version of the γ_0 vector, $J = \psi\gamma_0\tilde{\psi}$. This current has zero divergence and can therefore be used to define streamlines, as discussed in Section 7. Here we demonstrate how the same idea extends to the 2-particle case. We find that the conserved current is now formed from ψ acting on the $\gamma_0^1 + \gamma_0^2$ vector, and therefore exists in 8-dimensional configuration space. This current can be used to derive streamlines for two particles in correlated motion. This approach should ultimately enable us to gain a better insight into what happens in experiments of the Bell type, where spin measurements on pairs of particles are performed over spacelike separations. We saw in Section 8 how the local observables viewpoint leads to a radical re-interpretation of what happens in a single spin-measurement, and we can expect an equally radical shift to occur in the analysis of spin measurements of correlated particles. As a preliminary step in this direction, here we construct the current for two free particles approaching each other head-on. The streamlines for this current are evaluated and used to study both the effects of the Pauli antisymmetrisation and the spin-dependence of the trajectories. This work generalises that of Dewdney *et al.* [67, 26] to the

relativistic domain.

We start with the 2-particle Dirac equation (9.83), and multiply on the right by E to ensure the total wavefunction is in the correlated subspace. Also, since we want to work with the indistinguishable case, we assume that both masses are m. In this case our basic equation is

$$\nabla\psi E\left(i\gamma_3^1 + i\gamma_3^2\right) = 2m\psi E \tag{9.117}$$

and, since

$$E\left(i\gamma_3^1 + i\gamma_3^2\right) = J(\gamma_0^1 + \gamma_0^2), \tag{9.118}$$

equation (9.117) can be written in the equivalent form

$$\nabla\psi E\left(\gamma_0^1 + \gamma_0^2\right) = -2m\psi J. \tag{9.119}$$

Now, assuming that ψ satisfies $\psi = \psi E$, we obtain

$$\nabla\psi(\gamma_0^1 + \gamma_0^2)\tilde{\psi} = -2m\psi J\tilde{\psi}, \tag{9.120}$$

and adding this equation to its reverse yields

$$\nabla\psi(\gamma_0^1 + \gamma_0^2)\tilde{\psi} + \psi(\gamma_0^1 + \gamma_0^2)\dot{\tilde{\psi}}\dot{\nabla} = 0. \tag{9.121}$$

The scalar part of this equation gives

$$\nabla\cdot\langle\psi(\gamma_0^1 + \gamma_0^2)\tilde{\psi}\rangle_1 = 0, \tag{9.122}$$

which shows that the current we seek is

$$\mathcal{J} = \langle\psi(\gamma_0^1 + \gamma_0^2)\tilde{\psi}\rangle_1, \tag{9.123}$$

as defined in equation (9.59). The vector $\mathcal{J}$ has components in both particle-1 and particle-2 spaces, which we write as

$$\mathcal{J} = \mathcal{J}_1^1 + \mathcal{J}_2^2. \tag{9.124}$$

The current $\mathcal{J}$ is conserved in *eight*-dimensional space, so its streamlines never cross there. The streamlines of the individual particles, however, are obtained by integrating $\mathcal{J}_1$ and $\mathcal{J}_2$ in ordinary 4-d space, and these can of course cross. An example of this is illustrated in Figure 9.6, which shows the streamlines corresponding

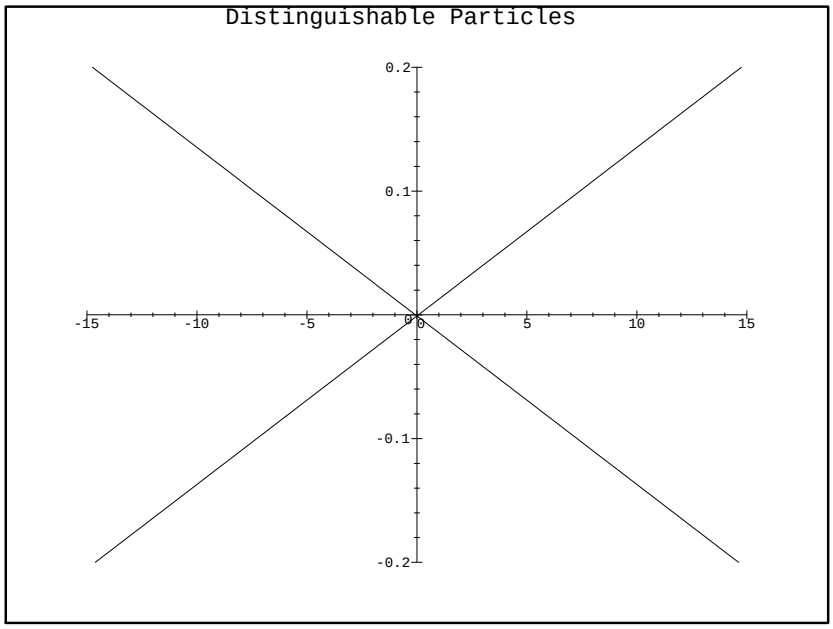

Figure 11: Streamlines generated by the unsymmetrised 2-particle wavefunction $\psi = \phi^1(r^1)\chi^2(s^2)E$. Time is shown on the vertical axis. ϕ and χ are Gaussian wavepackets moving in opposite directions and the 'collision' is arranged to take place at $t = 0$. The lack of any antisymmetrisation applied to the wavefunction means that the streamlines pass straight through each other.

to distinguishable particles in two Gaussian wavepackets approaching each other head-on. The wavefunction used to produce this figure is just

$$\psi = \phi^1(r^1)\chi^2(s^2)E, \tag{9.125}$$

with ϕ and χ being Gaussian wavepackets, moving in opposite directions. Since the distinguishable case is assumed, no Pauli antisymmetrisation is used. The individual currents for each particle are given by

$$\mathcal{J}_1(r,s) = \phi(r)\gamma_0\tilde{\phi}(r)\,\langle\chi(s)\tilde{\chi}(s)\rangle, \qquad \mathcal{J}_2(r,s) = \chi(s)\gamma_0\tilde{\chi}(s)\,\langle\phi(r)\tilde{\phi}(r)\rangle \tag{9.126}$$

and, as can be seen, the streamlines (and the wavepackets) simply pass straight through each other.

An interesting feature emerges in the individual currents in (9.126). One

of the main problems with single-particle Dirac theory is that the current is always positive-definite so, if we wish to interpret it as a charge current, it fails to represent antiparticles correctly. The switch of sign of the current necessary to represent positrons is put into conventional theory essentially 'by hand', via the anticommutation and normal ordering rules of fermionic field theory. In equation (9.126), however, the norm $\langle\chi\tilde{\chi}\rangle$ of the second state multiplies the current for the first, and vice versa. Since $\langle\chi\tilde{\chi}\rangle$ can be negative, it is possible to obtain currents which flow backwards in time. This suggests that the required switch of signs can be accomplished whilst remaining wholly within a wavefunction-based approach. An apparent problem is that, if only one particle has a negative norm state — say for example χ has $\langle\chi\tilde{\chi}\rangle < 0$ — then it is the ϕ current which is reversed, and not the χ current. However, it is easy to see that this objection is not relevant to indistinguishable particles, and it is to these we now turn.

We now apply the Pauli symmetrization procedure of the previous subsection to the wavefunction of equation (9.125), so as to obtain a wavefunction applicable to indistinguishable particles. This yields

$$\psi = \left(\phi^1(r^1)\chi^2(s^2) - \chi^1(r^2)\phi^2(s^1)\right) E, \tag{9.127}$$

from which we form $\mathcal{J}_1$ and $\mathcal{J}_2$, as before. We must next decide which spin states to use for the two particles. We first take both particles to have their spin vectors pointing in the positive z-direction, with all motion in the $\pm z$-direction. The resulting streamlines are shown in Figure 9.6(a). The streamlines now 'repel' one another, rather than being able to pass straight through. The corrugated appearance of the lines near the origin is the result of the streamlines having to pass through a region of highly-oscillatory destructive interference, since the probability of both particles occupying the same position (the origin) with the same spin state is zero. If instead the particles are put in *different* spin states then the streamlines shown in Figure 9.6(b) result. In this case there is no destructive interference near the origin, and the streamlines are smooth there. However, they still repel! The explanation for this lies in the symmetry properties of the 2-particle current. Given that the wavefunction ψ has been antisymmetrised according to our version of the Pauli principle, then it is straightforward to show that

$$I\mathcal{J}(IxI)I = \mathcal{J}(x). \tag{9.128}$$

It follows that at the same spacetime position, encoded by $IxI = x$ in the 2-particle algebra, the two currents $\mathcal{J}_1$ and $\mathcal{J}_2$ are equal. Hence, if two streamlines ever met,

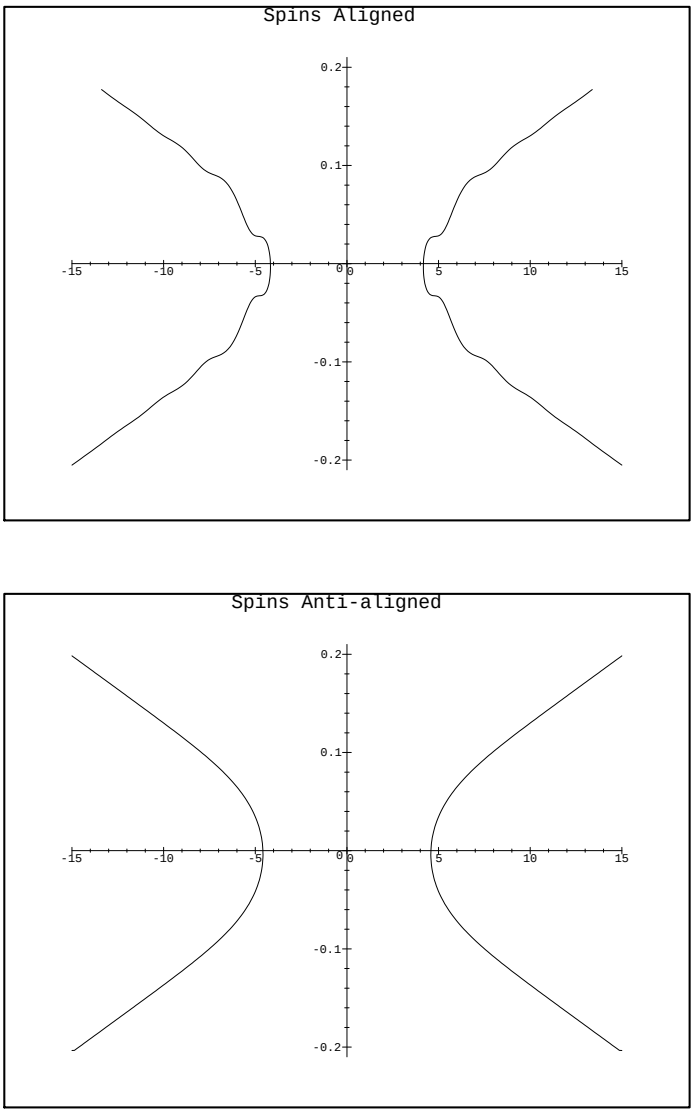

Figure 12: Streamlines generated by the antisymmetrised 2-particle wavefunction $\psi = [\phi^1(r^1)\chi^2(s^2) - \chi^1(r^2)\phi^2(s^1)]E$. The individual wavepackets pass through each other, but the streamlines from separate particles do not cross. The upper figure has both particles with spins aligned in the $+z$-direction, and the lower figure shows particles with opposite spins, with ϕ in the $+z$ direction, and χ in the $-z$ direction. Both wavepackets have energy 527KeV and a spatial spread of $\sim$ 20pm. The spatial units are 10^{-12}m and the units of time are 10^{-18}s. The effects of the antisymmetrisation are only important where there is significant wavepacket overlap.

they could never separate again. For the simulations presented here, it follows from the symmetry of the set-up that the spatial currents at the origin are both zero and so, as the particles approach the origin, they are forced to slow up. The delay means that they are then swept back in the direction they have just come from by the wavepacket travelling through from the other side. We therefore see that 'repulsion' as measured by streamlines has its origin in indistinguishability, and that the spin of the states exerts only a marginal effect.

10 Further Applications

In this section we briefly review two further applications of spacetime algebra to important areas of electron physics. The first of these is classical and semiclassical mechanics. As well as simplifying many calculations in quantum mechanics, spacetime algebra is well suited to handling problems in classical mechanics where electrons are treated as point charges following a single trajectory. In recent years there has been considerable interest in finding modifications to the simple classical equations to include the effects of spin, without losing the idea of a definite trajectory [30, 68]. One of the aims behind this work is to find a suitable classical model which can be quantised via the path-integral route [69]. One of the more promising candidates is discussed here, and we outline some improvements that could repair some immediate defects.

The second application discussed here is to Grassmann algebra and the associated 'calculus' introduced by Berezin [70]. Grassmann quantities are employed widely in quantum field theory, and the Berezin calculus plays a crucial role in the path-integral quantisation of fermionic systems. Here we outline how many of the calculations can be performed within geometric algebra, and draw attention to some work in the literature. We do not attempt a more detailed analysis of path-integral quantisation here.

10.1 Classical and Semiclassical Mechanics

The Lorentz force law for a point-particle with velocity v, mass m and charge q is

$$\dot{v} = \frac{q}{m} F \cdot v \tag{10.1}$$

where $\dot{v}$ denotes differentiation with respect to the affine parameter and F is the external electromagnetic field bivector. Any future-pointing unit timelike vector

can be written in terms of a rotor acting on a fixed vector γ_0,

$$v(\tau) = R(\tau)\gamma_0\tilde{R}(\tau) \tag{10.2}$$

from which we find

$$\dot{v} = (2\dot{R}\tilde{R})\cdot v. \tag{10.3}$$

The quantity $\dot{R}\tilde{R}$ is a bivector, so we can recover equation (10.1) by setting

$$2\dot{R}\tilde{R} = \frac{q}{m}F \tag{10.4}$$

$$\Longrightarrow \quad \dot{R} = \frac{q}{2m}FR. \tag{10.5}$$

This is not the only equation for R that is consistent with (10.1), since any bivector that commutes with v could be added to F. However, (10.5) is without doubt the simplest equation available.

It turns out that equation (10.5) is often easier to analyse than (10.1), as was first shown by Hestenes [13]. Furthermore, we can extend this approach to include a classical notion of spin. Let us suppose that, as well as describing the tangent vector v, the rotor R determines how a frame of vectors is transported along the curve. We can then define the spin vector as the unit spatial vector

$$s \equiv R\gamma_3\tilde{R}, \tag{10.6}$$

which matches the definition given for the quantum observable. If we now assume that equation (10.5) is valid, we find that the spin-vector satisfies the equation

$$\dot{s} = \frac{q}{m}F\cdot s, \tag{10.7}$$

which gives the correct precession equation for a particle of gyromagnetic ratio 2 [13]. It follows that $g = 2$ can be viewed as the natural value from the viewpoint of the relativistic classical mechanics of a rotating frame — a striking fact that deserves to be more widely known. We can use the same approach to analyse the motion of a particle with a g-factor other than 2 by replacing (10.5) with

$$\dot{R} = \frac{q}{2m}[FR + (g/2 - 1)R\boldsymbol{B}], \tag{10.8}$$

which reproduces the Bargmann-Michel-Telegdi equation employed in the analysis of spin-precession measurements [47].

A remarkable aspect of the Dirac theory is that the current $\psi\gamma_0\tilde{\psi}$ and the momentum (which is defined in terms of the momentum operator) are not necessarily colinear. This suggests that a more realistic classical model for an electron should employ an independent quantity for the momentum which is not necessarily related to the tangent vector to the spacetime trajectory. Such a model was proposed by Barut & Zanghi [68], who did not employ the STA, and was analysed further in [5] (see also [71]). Written in the STA, the action proposed by Barut & Zanghi takes the form

$$S = \int d\lambda \, \langle \dot{\psi} i\sigma_3 \tilde{\psi} + p(\dot{x} - \psi\gamma_0\tilde{\psi}) + qA(x)\psi\gamma_0\tilde{\psi} \rangle \tag{10.9}$$

where the dynamical variables are $x(\lambda)$, $p(\lambda)$ and $\psi(\lambda)$. Variation with respect to these variables yields the equations [5]

$$\begin{aligned} \dot{x} &= \psi\gamma_0\tilde{\psi} && (10.10)\\ \dot{P} &= qF\cdot\dot{x} && (10.11)\\ \dot{\psi} i\sigma_3 &= P\psi\gamma_0 && (10.12) \end{aligned}$$

where

$$P \equiv p - qA. \tag{10.13}$$

These constitute a set of first-order equations so, with x, p and ψ given for some initial value of λ, the future evolution is uniquely determined. Equations (10.10)–(10.12) contain a number of unsatisfactory features. One does not expect to see P entering the Lorentz force law (10.12), but rather the dynamical variable p. This problem is simply addressed by replacing (10.9) with

$$S_1 = \int d\lambda \, \langle \dot{\psi} i\sigma_3 \tilde{\psi} + p(\dot{x} - \psi\gamma_0\tilde{\psi}) + q\dot{x}A(x) \rangle \tag{10.14}$$

so that the $\dot{p}$ and $\dot{\psi}$ equations become

$$\begin{aligned} \dot{p} &= qF\cdot\dot{x} && (10.15)\\ \dot{\psi} i\sigma_3 &= p\psi\gamma_0. && (10.16) \end{aligned}$$

The quantity $p\cdot\dot{x}$ is a constant of the motion, and can be viewed as defining the mass.

A more serious problem remains, however. If we form the spin bivector $S = \psi i\sigma_3\tilde{\psi}$ we find that

$$\dot{S} = 2p\wedge\dot{x} \tag{10.17}$$

so, if p and $\dot{x}$ are initially colinear, the spin bivector does not precess, even in the presence of an external $\boldsymbol{B}$-field [35]. To solve this problem an extra term must be introduced into the action. The simplest modification is

$$S_2 = \int d\lambda \, \langle \dot{\psi} i\sigma_3 \tilde{\psi} + p(\dot{x} - \psi\gamma_0\tilde{\psi}) + q\dot{x}A(x) - \frac{q}{2m} F\psi i\sigma_3\tilde{\psi} \rangle \tag{10.18}$$

which now yields the equations

$$\begin{aligned} \dot{x} &= \psi\gamma_0\tilde{\psi} && (10.19)\\ \dot{p} &= qF\cdot\dot{x} - \frac{q}{2m}\nabla F(x)\cdot S && (10.20)\\ \dot{\psi} i\sigma_3 &= p\psi\gamma_0 - \frac{q}{2m}F\psi. && (10.21) \end{aligned}$$

The problem with this system of equations is that m has to be introduced explicitly, and there is nothing to identify this quantity with $p\cdot\dot{x}$. If we assume that $p = m\dot{x}$ we can recover the pair of equations

$$\begin{aligned} \dot{S} &= \frac{q}{m}F\times S && (10.22)\\ \dot{v} &= \frac{q}{m}F\cdot v - \frac{q}{2m^2}\nabla F(x)\cdot S, && (10.23) \end{aligned}$$

which were studied in [72].

Whilst a satisfactory semiclassical mechanics for an electron still eludes us, it should be clear that the STA is a very useful tool in constructing and analysing candidate models.

10.2 Grassmann Algebra

Grassmann algebras play an essential role in many areas of modern quantum theory. However, nearly all calculations with Grassmann algebra can be performed more efficiently with geometric algebra. A set of quantities $\{\zeta_i\}$ form a Grassmann algebra if their product is totally antisymmetric

$$\zeta_i\zeta_j = -\zeta_j\zeta_i. \tag{10.24}$$

Examples include fermion creation operators, the fermionic generators of a supersymmetry algebra, and ghost fields in the path integral quantisation of non-abelian gauge theories. Any expression involving the Grassmann variables $\{\zeta_i\}$ has a geometric algebra equivalent in which the $\{\zeta_i\}$ are replaced by a frame of inde-

pendent vectors $\{e_i\}$ and the Grassmann product is replaced by the outer (wedge) product [73, 74]. For example, we can make the replacement

$$\zeta_i\zeta_j \;\leftrightarrow\; e_i \wedge e_j. \tag{10.25}$$

This translation on its own clearly does not achieve a great deal, but the geometric algebra form becomes more powerful when we consider the 'calculus' defined by Berezin [70]. This calculus is defined by the rules

$$\frac{\partial \zeta_j}{\partial \zeta_i} = \delta_{ij}, \tag{10.26}$$

$$\zeta_j \frac{\overleftarrow{\partial}}{\partial \zeta_i} = \delta_{ij}, \tag{10.27}$$

together with the 'graded Leibniz' rule',

$$\frac{\partial}{\partial \zeta_i}(f_1 f_2) = \frac{\partial f_1}{\partial \zeta_i} f_2 + (-1)^{[f_1]} f_1 \frac{\partial f_2}{\partial \zeta_i}, \tag{10.28}$$

where $[f_1]$ is the parity (even/odd) of f_1. In geometric algebra, the operation of the Grassmann derivatives can be replaced by inner products of the reciprocal frame vectors

$$\frac{\partial}{\partial \zeta_i}(\;\leftrightarrow\; e^i \cdot (\tag{10.29}$$

so that

$$\frac{\partial \zeta_j}{\partial \zeta_i} \;\leftrightarrow\; e^i \cdot e_j = \delta^i_j. \tag{10.30}$$

Some consequences of this translation procedure were discussed in [73], where it was shown that the geometric product made available by the geometric algebra formulation simplifies many computations. Applications discussed in [73] included 'Grauss' integrals, pseudoclassical mechanics, path integrals and Grassmann-Fourier transforms. It was also shown that super-Lie algebras have a very simple representation within geometric algebra. There seems little doubt that the systematic replacement of Grassmann variables with geometric multivectors would considerably enhance our understanding of quantum field theory.

11 Conclusions

There is a growing realisation that geometric algebra provides a unified and powerful tool for the study of many areas of mathematics, physics and engineering. The underlying algebraic structure (Clifford algebra) appears in many key areas of physics and geometry [75], and the geometric techniques are finding increasing application in areas as diverse as gravitation theory [64] and robotics [76, 77]. The only impediment to the wider adoption of geometric algebra appears to be physicists' understandable reluctance to adopt new techniques. We hope that the applications discussed in this paper make a convincing case for the use of geometric algebra, and in particular the STA, in electron physics. Unfortunately, in concentrating on a single area of physics, the unifying potential of geometric algebra does not necessarily come across. However, a brief look at other applications should convince one of the wider utility of many of the techniques developed here.

Further work in this field will centre on the multiparticle STA. At various points we have discussed using the multiparticle STA to analyse the non-locality revealed by EPR-type experiments. This is just one of many potential applications of the approach outlined here. Others include following the streamlines for two particles through a scattering event, or using the 3-particle algebra to model pair creation. It will also be of considerable interest to develop simplified techniques for handling more complicated many-body problems. Behind these goals lies the desire to construct an alternative to the current technique of fermionic field quantisation. The canonical anticommutation relations imposed there remain mysterious, despite forty years of discussion of the spin-statistics theorem. Elsewhere, there is still a clear need to develop the wavepacket approach to tunnelling. This is true not only of fermions, but also of photons, on which most of the present experiments are performed.

Looking further afield, the approach to the Dirac equation described in Section 4 extends simply to the case of a gravitational background [48]. The wavepacket and multiparticle techniques developed here are essentially all that is required to address issues such as superradiance and pair creation by black holes. Closer to home, the STA is a powerful tool for classical relativistic physics. We dealt briefly with the construction of classical models for the electron in Section 10. Elsewhere, similar techniques have been applied to the study of radiation reaction and the Lorentz-Dirac equation [35]. The range of applicability of geometric algebra is truly vast. We believe that all physicists should be exposed to its benefits and insights.

A The Spherical Monogenic Functions

We begin by assuming that the spherical monogenic is an eigenstate of the $\boldsymbol{x}\wedge\boldsymbol{\nabla}$ and J_3 operators, where all operators follow the conventions of Section 4.2. We label this state as $\psi(l,\mu)$, so

$$-\boldsymbol{x}\wedge\boldsymbol{\nabla}\psi(l,\mu) = l\psi(l,\mu), \qquad J_3\psi(l,\mu) = \mu\psi(l,\mu). \tag{A.1}$$

The J_i operators satisfy

$$\begin{aligned} J_iJ_i &= -[(i\sigma_i)\cdot(\boldsymbol{x}\wedge\vec{\boldsymbol{\nabla}}) - \tfrac{1}{2}i\sigma_i][(i\sigma_i)\cdot(\boldsymbol{x}\wedge\boldsymbol{\nabla}) - \tfrac{1}{2}i\sigma_i] \\ &= 3/4 - \boldsymbol{x}\wedge\boldsymbol{\nabla} + \langle\boldsymbol{x}\wedge\vec{\boldsymbol{\nabla}}\boldsymbol{x}\wedge\boldsymbol{\nabla}\rangle \end{aligned} \tag{A.2}$$

where the $\vec{\boldsymbol{\nabla}}$ indicates that the derivative acts on everything to its right. Since

$$\langle\boldsymbol{x}\wedge\vec{\boldsymbol{\nabla}}\boldsymbol{x}\wedge\boldsymbol{\nabla}\rangle\psi = \boldsymbol{x}\wedge\boldsymbol{\nabla}(\boldsymbol{x}\wedge\boldsymbol{\nabla}\psi) - \boldsymbol{x}\wedge\boldsymbol{\nabla}\psi \tag{A.3}$$

we find that

$$\begin{aligned} J_iJ_i\psi(l,\mu) &= (3/4 + 2l + l^2)\psi(l,\mu) \\ &= (l+1/2)(l+3/2)\psi(l,\mu). \end{aligned} \tag{A.4}$$

With the ladder operators J_+ and J_- defined by

$$\begin{aligned} J_+ &\equiv J_1 + jJ_2 \\ J_- &\equiv J_1 - jJ_2, \end{aligned} \tag{A.5}$$

it is a simple matter to prove the following results:

$$\begin{aligned} [J_+, J_-] &= 2J_3 & J_iJ_i &= J_-J_+ + J_3 + {J_3}^2 \\ [J_\pm, J_3] &= \mp J_\pm & J_iJ_i &= J_+J_- - J_3 + {J_3}^2. \end{aligned} \tag{A.6}$$

The raising operator J_+ increases the eigenvalue of J_3 by an integer. But, for fixed l, μ must ultimately attain some maximum value. Denoting this value as μ_+, we must reach a state for which

$$J_+\psi(l,\mu_+) = 0. \tag{A.7}$$

Acting on this state with J_iJ_i and using one of the results in (A.6) we find that

$$(l+1/2)(l+3/2) = \mu_+(\mu_+ + 1) \tag{A.8}$$

and, as l is positive and μ_+ represents an upper bound, it follows that

$$\mu_+ = l + 1/2. \tag{A.9}$$

There must similarly be a lowest eigenvalue of J_3 and a corresponding state with

$$J_-\psi(l,\mu_-) = 0. \tag{A.10}$$

In this case we find that

$$(l+1/2)(l+3/2) = \mu_-(\mu_- - 1) \tag{A.11}$$

$$\implies \mu_- = -(l+1/2). \tag{A.12}$$

The spectrum of eigenvalues of J_3 therefore ranges from $(l+1/2)$ to $-(l+1/2)$, a total of $2(l+1)$ states. Since the J_3 eigenvalues are always of the form (integer $+1/2$), it is simpler to label the spherical monogenics with a pair of integers. We therefore write the spherical monogenics as ψ_l^m, where

$$-\boldsymbol{x}\wedge\boldsymbol{\nabla}\psi_l^m = l\psi_l^m \qquad l \geq 0 \tag{A.13}$$

$$J_3\psi_l^m = (m+\tfrac{1}{2})\psi_l^m \qquad -1-l \leq m \leq l. \tag{A.14}$$

To find an explicit form for the ψ_l^m we first construct the highest-m case. This satisfies

$$J_+\psi_l^l = 0 \tag{A.15}$$

and it is not hard to see that this equation is solved by

$$\psi_l^l \propto \sin^l\theta\, e^{-l\phi i\sigma_3}. \tag{A.16}$$

Introducing a convenient factor, we write

$$\psi_l^l = (2l+1)P_l^l(\cos\theta)\, e^{l\phi i\sigma_3}. \tag{A.17}$$

Our convention for the associated Legendre polynomials follows Gradshteyn &

Ryzhik [43], so

$$P_l^m(x) = \frac{(-1)^m}{2^l l!}(1-x^2)^{m/2}\frac{d^{l+m}}{dx^{l+m}}(x^2-1)^l \tag{A.18}$$

and we have the following recursion relations:

$$(1-x^2)\frac{dP_l^m(x)}{dx} + mxP_l^m(x) = -(1-x^2)^{1/2}P_l^{m+1}(x) \tag{A.19}$$

$$(1-x^2)\frac{dP_l^m(x)}{dx} - mxP_l^m(x) = (1-x^2)^{1/2}(l+m)(l-m+1)P_l^{m-1}(x). \tag{A.20}$$

The lowering operator J_- has the following effect on ψ:

$$J_-\psi = [-\partial_\theta\psi + \cot\theta\,\partial_\phi\psi i\sigma_3]e^{-\phi i\sigma_3} - i\sigma_2\,\tfrac{1}{2}(\psi + \sigma_3\psi\sigma_3). \tag{A.21}$$

The latter term just projects out the $\{1, i\sigma_3\}$ terms and multiplies them by $-i\sigma_2$. This is the analog of the lowering matrix in the standard formalism. The derivatives acting on ψ_l^l form

$$\begin{aligned}
&[-\partial_\theta\psi_l^l + \cot\theta\,\partial_\phi\psi_l^l i\sigma_3]e^{-\phi i\sigma_3} \\
&\qquad = (2l+1)[-\partial_\theta P_l^l(\cos\theta) - l\cot\theta\,P_l^l(\cos\theta)]e^{(l-1)\phi i\sigma_3} \\
&\qquad = (2l+1)2lP_l^{l-1}(\cos\theta)e^{(l-1)\phi i\sigma_3},
\end{aligned} \tag{A.22}$$

and, if we use the result that

$$\sigma_\phi = \sigma_2 e^{\phi i\sigma_3}, \tag{A.23}$$

we find that

$$\psi_l^{l-1} \propto [2lP_l^{l-1}(\cos\theta) - P_l^l(\cos\theta)i\sigma_\phi]e^{(l-1)\phi i\sigma_3}. \tag{A.24}$$

Proceeding in this manner, we are led to the following formula for the spherical monogenics:

$$\psi_l^m = [(l+m+1)P_l^m(\cos\theta) - P_l^{m+1}(\cos\theta)i\sigma_\phi]e^{m\phi i\sigma_3}, \tag{A.25}$$

in which l is a positive integer or zero, m ranges from $-(l+1)$ to l and the P_l^m are taken to be zero if $|m| > l$. The positive- and negative-m states can be related using the result that

$$P_l^{-m}(x) = (-1)^m\frac{(l-m)!}{(l+m)!}P_l^m(x), \tag{A.26}$$

from which it can be shown that

$$\psi_l^m(-i\sigma_2) = (-1)^m \frac{(l+m+1)!}{(l-m)!}\psi_l^{-(m+1)}. \tag{A.27}$$

The spherical monogenics presented here are unnormalised. Normalisation factors are not hard to compute, and we find that

$$\int_0^\pi d\theta \int_0^{2\pi} d\phi \, \sin\theta \, \psi_l^m \psi_l^{m\dagger} = 4\pi \frac{(l+m+1)!}{(l-m)!}. \tag{A.28}$$

References

[1] W.K. Clifford. Applications of Grassmann's extensive algebra. *Am. J. Math.*, 1:350, 1878.

[2] H. Grassmann. *Die Ausdehnungslehre*. Enslin, Berlin, 1862.

[3] S.F. Gull, A.N. Lasenby, and C.J.L. Doran. Imaginary numbers are not real — the geometric algebra of spacetime. *Found. Phys.*, 23(9):1175, 1993.

[4] C.J.L. Doran, A.N. Lasenby, and S.F. Gull. States and operators in the spacetime algebra. *Found. Phys.*, 23(9):1239, 1993.

[5] A.N. Lasenby, C.J.L. Doran, and S.F. Gull. A multivector derivative approach to Lagrangian field theory. *Found. Phys.*, 23(10):1295, 1993.

[6] S.F. Gull, A.N. Lasenby, and C.J.L. Doran. Electron paths, tunnelling and diffraction in the spacetime algebra. *Found. Phys.*, 23(10):1329, 1993.

[7] D. Hestenes. A unified language for mathematics and physics. In J.S.R. Chisholm and A.K. Common, editors, *Clifford Algebras and their Applications in Mathematical Physics (1985)*, page 1. Reidel, Dordrecht, 1986.

[8] D. Hestenes. *Space–Time Algebra*. Gordon and Breach, New York, 1966.

[9] D. Hestenes. Clifford algebra and the interpretation of quantum mechanics. In J.S.R. Chisholm and A.K. Common, editors, *Clifford Algebras and their Applications in Mathematical Physics (1985)*, page 321. Reidel, Dordrecht, 1986.

[10] D. Hestenes. *New Foundations for Classical Mechanics (Second Edition).* Kluwer Academic Publishers, Dordrecht, 1999.

[11] D. Hestenes. Proper particle mechanics. *J. Math. Phys.*, 15(10):1768, 1974.

[12] D. Hestenes and G. Sobczyk. *Clifford Algebra to Geometric Calculus.* Reidel, Dordrecht, 1984.

[13] D. Hestenes. Proper dynamics of a rigid point particle. *J. Math. Phys.*, 15(10):1778, 1974.

[14] W.E. Baylis, J. Huschilt, and Jiansu Wei. Why i? *Am. J. Phys.*, 60(9):788, 1992.

[15] T.G. Vold. An introduction to geometric algebra with an application to rigid body mechanics. *Am. J. Phys.*, 61(6):491, 1993.

[16] T.G. Vold. An introduction to geometric calculus and its application to electrodynamics. *Am. J. Phys.*, 61(6):505, 1993.

[17] B. Jancewicz. *Multivectors and Clifford Algebras in Electrodynamics.* World Scientific, Singapore, 1989.

[18] J.S.R. Chisholm and A.K. Common, eds. *Clifford Algebras and their Applications in Mathematical Physics (1985).* Reidel, Dordrecht, 1986.

[19] A. Micali, R. Boudet and J. Helmstetter, eds. *Clifford Algebras and their Applications in Mathematical Physics (1989).* Kluwer Academic, Dordrecht, 1991.

[20] F. Brackx and R. Delanghe and H. Serras, eds. *Clifford Algebras and their Applications in Mathematical Physics (1993).* Kluwer Academic, Dordrecht, 1993.

[21] D. Hestenes and A. Weingartshofer, eds. *The Electron. New Theory and Experiment.* Kluwer Academic, Dordrecht, 1991.

[22] D. Hestenes. Real spinor fields. *J. Math. Phys.*, 8(4):798, 1967.

[23] D. Hestenes. Vectors, spinors, and complex numbers in classical and quantum physics. *Am. J. Phys.*, 39:1013, 1971.

[24] A.N. Lasenby, C.J.L. Doran, and S.F. Gull. 2-spinors, twistors and supersymmetry in the spacetime algebra. In Z. Oziewicz, B. Jancewicz, and A. Borowiec, editors, *Spinors, Twistors, Clifford Algebras and Quantum Deformations*, page 233. Kluwer Academic, Dordrecht, 1993.

[25] D. Bohm, R. Schiller, and J. Tiomno. A causal interpretation of the Pauli equation. *Nuovo Cim. Suppl.*, 1:48, 1955.

[26] J.P. Vigier, C. Dewdney, P.R. Holland, and A. Kyprianidis. Causal particle trajectories and the interpretation of quantum mechanics. In B.J. Hiley and F.D. Peat, editors, *Quantum Implications*, page 169. Routledge, London, 1987.

[27] C. Dewdney, P.R. Holland, A. Kyprianidis, and J.P. Vigier. Spin and non-locality in quantum mechanics. *Nature*, 336:536, 1988.

[28] D. Hestenes and R. Gurtler. Consistency in the formulation of the Dirac, Pauli and Schrödinger theories. *J. Math. Phys.*, 16(3):573, 1975.

[29] D. Hestenes. Spin and uncertainty in the interpretation of quantum mechanics. *Am. J. Phys.*, 47(5):399, 1979.

[30] D. Hestenes. The zitterbewegung interpretation of quantum mechanics. *Found. Phys.*, 20(10):1213, 1990.

[31] C. Dewdney, P.R. Holland, and A. Kyprianidis. What happens in a spin measurement? *Phys. Lett. A.*, 119(6):259, 1986.

[32] P.R. Holland. *The Quantum Theory of Motion.* Cambridge University Press, 1993.

[33] D. Hestenes. Observables, operators, and complex numbers in the Dirac theory. *J. Math. Phys.*, 16(3):556, 1975.

[34] J.D. Bjorken and S.D. Drell. *Relativistic Quantum Mechanics, vol 1.* McGraw-Hill, New York, 1964.

[35] S.F. Gull. Charged particles at potential steps. In A. Weingartshofer and D. Hestenes, editors, *The Electron*, page 37. Kluwer Academic, Dordrecht, 1991.

[36] C. Itzykson and J-B. Zuber. *Quantum Field Theory.* McGraw–Hill, New York, 1980.

[37] J. D. Hamilton. The Dirac equation and Hestenes' geometric algebra. *J. Math. Phys.*, 25(6):1823, 1984.

[38] R. Boudet. The role of the duality rotation in the Dirac theory. In A. Weingartshofer and D. Hestenes, editors, *The Electron*, page 83. Kluwer Academic, Dordrecht, 1991.

[39] H. Krüger. New solutions of the Dirac equation for central fields. In A. Weingartshofer and D. Hestenes, editors, *The Electron*, page 49. Kluwer Academic, Dordrecht, 1991.

[40] C. Daviau and G. Lochak. Sur un modèle d' équation spinorielle non linéaire. *Ann. de la fond. L. de Broglie*, 16(1):43, 1991.

[41] R.P. Feynman. *Quantum Electrodynamics.* Addison–Wesley, Reading MA, 1961.

[42] J.J. Sakurai. *Advanced Quantum Mechanics.* Addison–Wesley, Reading MA, 1967.

[43] I.S. Gradshteyn and I.M. Ryzhik. *Table of Integrals, Series and Products. Fifth Edition.* Academic Press Ltd., London, 1994.

[44] M. Moshinsky and A. Szczepaniak. The Dirac oscillator. *J. Phys. A: Math. Gen.*, 22:L817, 1989.

[45] W.T. Grandy, Jr. *Relativistic Quantum Mechanics of Leptons and Fields.* Kluwer Academic, Dordrecht, 1991.

[46] R.P. Martinez Romero and A.L. Salas-Brito. Conformal invariance in a Dirac oscillator. *J. Math. Phys.*, 33(5):1831, 1992.

[47] D. Hestenes. Geometry of the Dirac theory. In J. Keller, editor, *The Mathematics of Physical Spacetime*, page 67. UNAM, Mexico, 1982.

[48] A.N. Lasenby, C.J.L. Doran, and S.F. Gull. Gravity, gauge theories and geometric algebra. To appear in *Phil. Trans. R. Soc. Lond. A*, 1997.

[49] D.M. Fradkin and R.J. Kashuba. Spatial displacement of electrons due to multiple total reflections. *Phys. Rev. D*, 9(10):2775, 1974.

[50] M.E. Rose. *Relativistic Electron Theory.* Wiley, New York, 1961.

[51] C.A. Manogue. The Klein paradox and superradiance. *Ann. Phys.*, 181:261, 1988.

[52] W. Greiner, B. Müller, and J. Rafelski. *Quantum Electrodynamics of Strong Fields*. Springer–Verlag, Berlin, 1985.

[53] R.Y. Chiao, P.G. Kwiat, and A.M. Steinberg. Faster than light? *Sci. Am.*, 269(2):38, 1993.

[54] A.M. Steinberg, P.G. Kwiat, and R.Y. Chiao. Measurement of a single-photon tunneling time. *Phys. Rev. Lett.*, 71(5):708, 1993.

[55] R. Landauer. Light faster than light? *Nature*, 365:692, 1993.

[56] E.H. Hauge and J.A. Støvneng. Tunnelling times: a critical review. *Rev. Mod. Phys.*, 61(4):917, 1989.

[57] R. Landauer and Th. Martin. Barrier interaction time in tunneling. *Rev. Mod. Phys.*, 66(1):217, 1994.

[58] J.O. Hirschfelder, A.C. Christoph, and W.E. Palke. Quantum mechanical streamlines. I. Square potential barrier. *J. Chem. Phys.*, 61(12):5435, 1974.

[59] B.J. Hiley and F.D. Peat, eds. *Quantum Implications*. Routledge, London, 1987.

[60] P.R. Holland. Causal interpretation of a system of two spin-1/2 particles. *Phys. Rep.*, 169(5):294, 1988.

[61] C.J.L. Doran, D. Hestenes, F. Sommen, and N. van Acker. Lie groups as spin groups. *J. Math. Phys.*, 34(8):3642, 1993.

[62] A.P. Galeao and P. Leal Ferreira. General method for reducing the two-body Dirac equation. *J. Math. Phys.*, 33(7):2618, 1992.

[63] Y. Koide. Exactly solvable model of relativistic wave equations and meson spectra. *Il Nuovo Cim.*, 70A(4):411, 1982.

[64] A.N. Lasenby, C.J.L. Doran, and S.F. Gull. Astrophysical and cosmological consequences of a gauge theory of gravity. In N. Sánchez and A. Zichichi, editors, *Advances in Astrofundamental Physics, Erice 1994*, page 359. World Scientific, Singapore, 1995.

[65] C.J.L. Doran, A.N. Lasenby, and S.F. Gull. Gravity as a gauge theory in the spacetime algebra. In F. Brackx, R. Delanghe, and H. Serras, editors, *Clifford Algebras and their Applications in Mathematical Physics (1993)*, page 375. Kluwer Academic, Dordrecht, 1993.

[66] A.N. Lasenby, C.J.L. Doran, and S.F. Gull. Cosmological consequences of a flat-space theory of gravity. In F. Brackx, R. Delanghe, and H. Serras, editors, *Clifford Algebras and their Applications in Mathematical Physics (1993)*, page 387. Kluwer Academic, Dordrecht, 1993.

[67] C. Dewdney, A. Kyprianidis, and J.P. Vigier. Illustration of the causal model of quantum statistics. *J. Phys. A*, 17:L741, 1984.

[68] A.O. Barut and N. Zanghi. Classical models of the Dirac electron. *Phys. Rev. Lett.*, 52(23):2009, 1984.

[69] A.O. Barut and I.H. Duru. Path integral formulation of quantum electrodynamics from classical particle trajectories. *Phys. Rep.*, 172(1):1, 1989.

[70] F.A. Berezin. *The Method of Second Quantization.* Academic Press Ltd., London, 1966.

[71] W.A. Rodrigues, Jr., J. Vaz, Jr., E. Recami, and G. Salesi. About zitterbewegung and electron structure. *Phys. Lett. B*, 318:623, 1993.

[72] J.W. van Holten. On the electrodynamics of spinning particles. *Nucl. Phys.*, B356(3):3, 1991.

[73] A.N. Lasenby, C.J.L. Doran, and S.F. Gull. Grassmann calculus, pseudoclassical mechanics and geometric algebra. *J. Math. Phys.*, 34(8):3683, 1993.

[74] C.J.L. Doran, A.N. Lasenby, and S.F. Gull. Grassmann mechanics, multivector derivatives and geometric algebra. In Z. Oziewicz, B. Jancewicz, and A. Borowiec, editors, *Spinors, Twistors, Clifford Algebras and Quantum Deformations*, page 215. Kluwer Academic, Dordrecht, 1993.

[75] H.B. Lawson and M.-L. Michelsohn. *Spin Geometry.* Princeton University Press, Princeton NJ, 1989.

[76] D. Hestenes. Invariant body kinematics: I. Saccadic and compensatory eye movements. *Neural Networks*, 7(1):65, 1994.

[77] D. Hestenes. Invariant body kinematics: II. Reaching and neurogeometry. *Neural Networks*, 7(1):79, 1994.